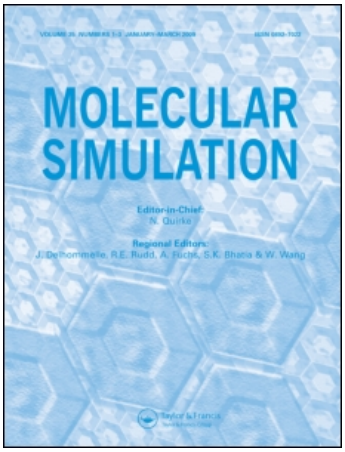

Molecular Simulation

Publication details, including instructions for authors and subscription information:
http://www.informaworld.com/smpp/title~content=t713644482

Multi-scale Molecular Modeling of Chemical Reactivity

Erik E. Santiso[a]; Keith E. Gubbins[a]
[a] Department of Chemical Engineering, North Carolina State University, Raleigh, NC, USA

Online publication date: 26 October 2010

To cite this Article Santiso, Erik E. and Gubbins, Keith E.(2004) 'Multi-scale Molecular Modeling of Chemical Reactivity', Molecular Simulation, 30: 11, 699 — 748
To link to this Article: DOI: 10.1080/08927020412331294878
URL: http://dx.doi.org/10.1080/08927020412331294878

Molecular Simulation, Vol. 30 (11–12), 15 September–15 October 2004, pp. 699–748

Multi-scale Molecular Modeling of Chemical Reactivity

ERIK E. SANTISO and KEITH E. GUBBINS*

Department of Chemical Engineering, North Carolina State University, Raleigh, NC 27695-7905, USA

(Received March 2004; In final form June 2004)

We present a review of the most widely used methods to model chemical reactions, at both the electronic and atomistic levels. While, in principle, *ab initio* methods alone should provide the required prediction of reaction mechanisms, yields and rates, in practice this can rarely be achieved due to the intensive nature of the computations and the poor scaling of the computational burden with the number of electrons. In many applications a combination of *ab initio* and semi-classical atomistic simulations will be needed. Specialized atomistic simulation methods are necessary, since the reactions are themselves rare events, and the free energy landscape for the reaction is often rugged with many possible reaction paths. We provide a survey of these methods, with comments on their applicability and a description of their strengths and weaknesses.

Keywords: Multi-scale molecular modeling; Chemical reactivity; Quantum chemistry; Statistical mechanics

INTRODUCTION

The newcomers to the arcane field of modeling of chemical reactions will usually find themselves bewildered by the profusion of proposed methods, both *ab initio* and classical atomistic. In the case of the *ab initio* approaches, we find a plethora of mathematical formulations of the electronic problem, approximations, basis sets. Such methods include Hartree–Fock theory, Configuration Interaction, Møller–Plesset perturbation methods, Coupled–Cluster methods, Multireference Self-Consistent Field methods, various Semi-Empirical Methods, Density Functional Theory and Car-Parrinello Molecular Dynamics, and within each of these there are, on average, four or five different variations. The atomistic methods include various forms of Transition State Theory, "Blue Moon" Molecular Dynamics, the Reactive Flux Method, Transition Path Sampling, Kinetic Monte Carlo, Quantum Mechanics/Molecular Mechanics, and others. The multitude of acronyms used, particularly for the quantum mechanical methods, further strengthens the apparent impenetrability of the field. We find ourselves confronted with sentences such as: "Geometries were optimized at the B3LYP/6-31G(*d*) level and single-point energies were obtained from CASSCF and CASPT2 calculations".

This wide range of methods reflects both the difficulty and importance of this area. While surveys exist of some of the *ab initio* [1–9] and classical atomistic [9–11] methods, there does not appear to be a general overview of the important methods of both types. However, many applications require a multi-scale approach in which *ab initio* and atomistic methods are combined; due to computer limitations, *ab initio* methods alone are often insufficient to deal with adequate system sizes or time scales. This is particularly the case when strong intermolecular interactions are involved, as in reactions in solution, in supercritical fluids, and in nanostructured environments (reactions in porous media, composites, reverse micelles, etc.). In this paper, we present a review of some of the most important *ab initio* and classical atomistic methods, at a level that is appropriate for a newcomer to the area. While space does not permit us to review all of the methods that have been proposed, we have tried to select those that we believe are most widely useful, and endeavor to make this area accessible to those researchers who, while being familiar with some simulation or *ab initio* methods, may be approaching reacting systems for the first time. Examples of recent

*Corresponding author. E-mail: keg@ncsu.edu

ISSN 0892-7022 print/ISSN 1029-0435 online © 2004 Taylor & Francis Ltd
DOI: 10.1080/08927020412331294878

applications of each of the methods are mentioned at the end of each section.

We begin by introducing the basic concepts common to chemical reactions (second section), such as potential energy surfaces, transition states and reaction coordinates. Empirical force field methods to describe the potential energy surface (PES) are described in the third section. The basis of the *ab initio* methods, and the various approximate methods available for their solution, are covered in the fourth section. In the fifth section, we discuss the atomistic simulation methods, and in the sixth section we present some concluding remarks.

CHEMICAL REACTIONS [1–5,12–14]

Before we start discussing methods for dealing with chemical reactions, it is convenient to talk about the kind of problems we want to consider and define some terms. From a practical point of view, what we usually want to obtain about a chemical reaction is either an equilibrium constant or a kinetic rate. Equilibrium constants are in this sense the easiest to obtain because they depend only on the thermodynamic properties of the reactants and the products. One may not know how a reaction proceeds from reactants to products and still get the equilibrium constant for the reaction. The complications that may arise are those associated with the estimation of thermodynamic properties: non-ideality, effects due to external imposed fields, etc. In the "Classical Simulation Methods for Equilibrium and Rate Constants" section, we will describe the Reactive Monte Carlo method, which can deal with this kind of situation.

The estimation of rate constants is an entirely different matter, however, because they are dynamic properties and hence depend on *how* the system evolves from reactants to products. Even for very simple systems, e.g. a reacting mixture of ideal gases, it is not a trivial task to solve this problem. Since chemical reactions usually involve breaking and formating chemical bonds, finding out exactly how a reaction proceeds is inherently a quantum mechanical problem. In the Sections "Force Field Methods" and "*Ab Initio* Methods", we will discuss some of the methods that can be used to describe these processes.

One of the things that we will discuss in "*Ab Initio* Methods" is the *Born–Oppenheimer approximation*. Within this approximation, one assumes that the only relevant parameters necessary to describe the reaction mechanism are the positions of the atomic nuclei in space. Thus a *PES* which gives the potential energy of the system $E(\{\mathbf{R}_I\})$ as a function of the nuclear configuration, is used to describe a chemical reaction.

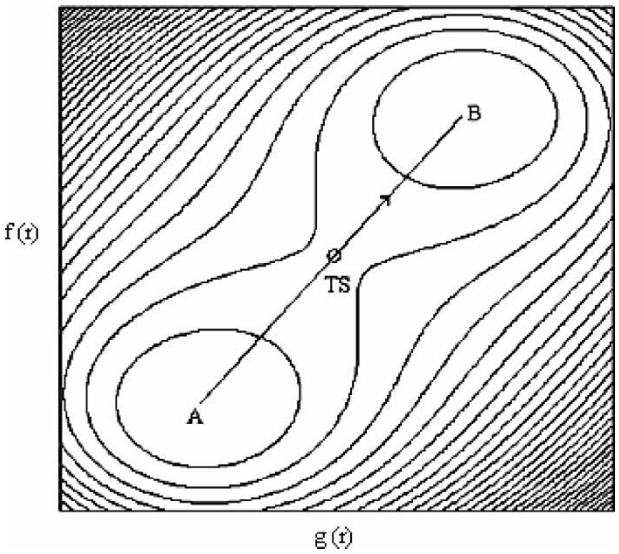

FIGURE 1 A simple potential energy surface; contours are lines of constant energy. The variables $f(r)$ and $g(r)$ represent functions of the configuration. A and B are the reactant and product states, and TS is the transition state.

Figure 1 is a sketch of a PES. This plot corresponds to a simple case where the PES depends only on two coordinates [15]. The variables f and g represent functions of the configurational variables and could be, for example, distances between two atoms, angles formed by three atoms or dihedral angles formed by four atoms. The labels A and B indicate the reactant and product states. The maximum along the minimum energy path, labeled as TS, is the *transition state* (also known as the *activated state* or *activated complex*). This point is a first-order saddle point, i.e. the energy increases in all directions but one.

The PES for a given reaction can be found using a quantum mechanical method. Its description, however, can be very complicated. In principle, the nuclear configuration space $\{\mathbf{R}_I\}$ contains the coordinates of all the nuclei that may have an effect on the reaction, i.e. not only the reactants and the products but also all the neighboring atoms. In some cases, for example, reactions happening in solution or in confinement, there may be collective effects involving large numbers of molecules that affect the reaction [16–19]. Thus the PES may exist in a highly multidimensional space, and just describing it could be impossible. It is often necessary to simplify the system by considering only some of the coordinates. Even then there may still be several possible pathways through which the reaction can proceed.

At finite temperature, the reaction path is really defined on a *free* energy surface, and this must be taken into account when calculating reaction rates. However, the way to define reaction paths is usually to do *ab initio* calculations, and these are done at zero temperature (i.e. the atoms are taken as stationary), so temperature effects have to be

included afterwards. It is possible to directly explore the free energy surface (FES) using, for example, modified *ab initio* molecular dynamics methods, but these approaches are relatively new and have not yet had widespread application [20].

Many methods for estimating reaction rates require defining one or more *reaction coordinates* that serve as a measure of the extent of the reaction. A reaction coordinate is a function of the configurational variables $\{\mathbf{R}_I\}$ that measures how far along the reaction path the system is in a given configuration. In principle the way to find this function is to search mathematically for the path(s) of minimum energy on the PES that connects the reactants to the products (such as the one indicated in Fig. 1). The reaction coordinate(s) can then be defined by parameterizing this path. When this procedure is followed one speaks of an *intrinsic reaction coordinate*, a term due to Fukui [21–23].

A way to obtain minimum energy paths and hence define intrinsic reaction coordinates is to follow the softest vibrational mode of the reacting molecule [21–23]. This requires numerically calculating the Hessian [24] of the PES as one advances along the path, and finding its lowest eigenvalue and corresponding eigenvector, and is usually a very expensive calculation [25]. In some cases there are also several possible pathways, and it would be necessary to move along all of them, which multiplies the computational cost.

In principle, intrinsic reaction coordinates are the correct ones. Nevertheless, obtaining a reaction coordinate in this way is costly, and frequently the parameterized path obtained from a numerical method is difficult to interpret. For this reason, it is often preferable to choose a reaction coordinate beforehand based on an intuition of how the reaction should proceed, or on available data. By choosing a reaction coordinate in this way, however, one is artificially imposing a reaction path. If this path turns out to be very different from the true minimum energy path, the results obtained from it (e.g. reaction rates) may be in significant error, and even physically inconsistent. There are several ways to check whether one has chosen a good reaction coordinate besides, of course, doing the full search for the minimum energy path. Some of these will be discussed in the "Classical Simulation Methods for Equilibrium and Rate Constants" section. Choosing the right reaction coordinate(s) for complex systems such as reactions occurring in solvents or involving macromolecules is one of the major problems in the simulation of chemical reactions. In many cases it is a trial-and-error procedure, and one of the standing problems in the field is to find a systematic and practical way to deal with this.

The ideas above are best illustrated with an example. Figure 2 shows a contour plot of the collinear PES for the reaction $O + H_2 \rightarrow H + OH$ as obtained by Schinke and Lester [26]. The points labeled "$O + H_2$" and "$H + OH$" correspond to reactants and products states. The line joining them is the minimum energy path, i.e. the most probable reaction path, and the point labeled "TS" is the transition state, the first-order saddle point along the reaction path. A 3D plot showing the corresponding values of the energy is in Fig. 3.

The reaction path shown in Fig. 2 was obtained by following the softest eigenmode of the Hessian, *i.e.* it corresponds to an intrinsic reaction coordinate. Since the computational cost of calculating the Hessian does not always permit using this definition, one may need to rely on intuition about the reaction mechanism to define the reaction coordinate.

Let us imagine that, for the reaction above, we choose to define our reaction coordinate as the distance between the two hydrogen atoms. With this definition, the lines of constant reaction coordinate will be horizontal lines on the contour plot. The points on the reaction path will then be the minima of the energy along these lines, as shown in Fig. 4. From this figure, we see that the reaction path obtained using this definition of the reaction coordinate is very different from the minimum energy path. Furthermore, starting from the products side and moving back we get a different path, with a large hysteresis loop. As discussed in the "Constrained Reaction Dynamics: 'Blue Moon' Method" section, this is one way to identify an inadequate choice of reaction coordinate.

If we choose instead to use the difference between the H–H and the O–H distance, $r_{HH} - r_{OH}$, as our reaction coordinate, the results are quite different. The lines of constant reaction coordinate are now inclined 45° with respect to the horizontal, and minimizing the energy along these lines gives the path shown in Fig. 5. This path is much closer to the minimum energy path than the one shown in Fig. 4. Furthermore, the reaction path is the same going forwards and backwards, i.e. there is no hysteresis as in Fig. 4. All of this indicates that this is a good choice of reaction coordinate.

Even when using a simple method, like transition state theory (TST), which does not require determining the full minimum energy path, estimating a reaction rate requires at least finding the minima and the transition state(s) in the PES [27]. There are standard optimization methods for dealing with this (see for example, Refs. [28–30]). Quasi-Newton methods, particularly the Broyden–Fletcher–Goldfarb–Shanno (BFGS) method [31–35] are generally considered the best for this kind of problem. The BFGS method works only for a minimization problem, i.e. for the location of the reactant and product states.

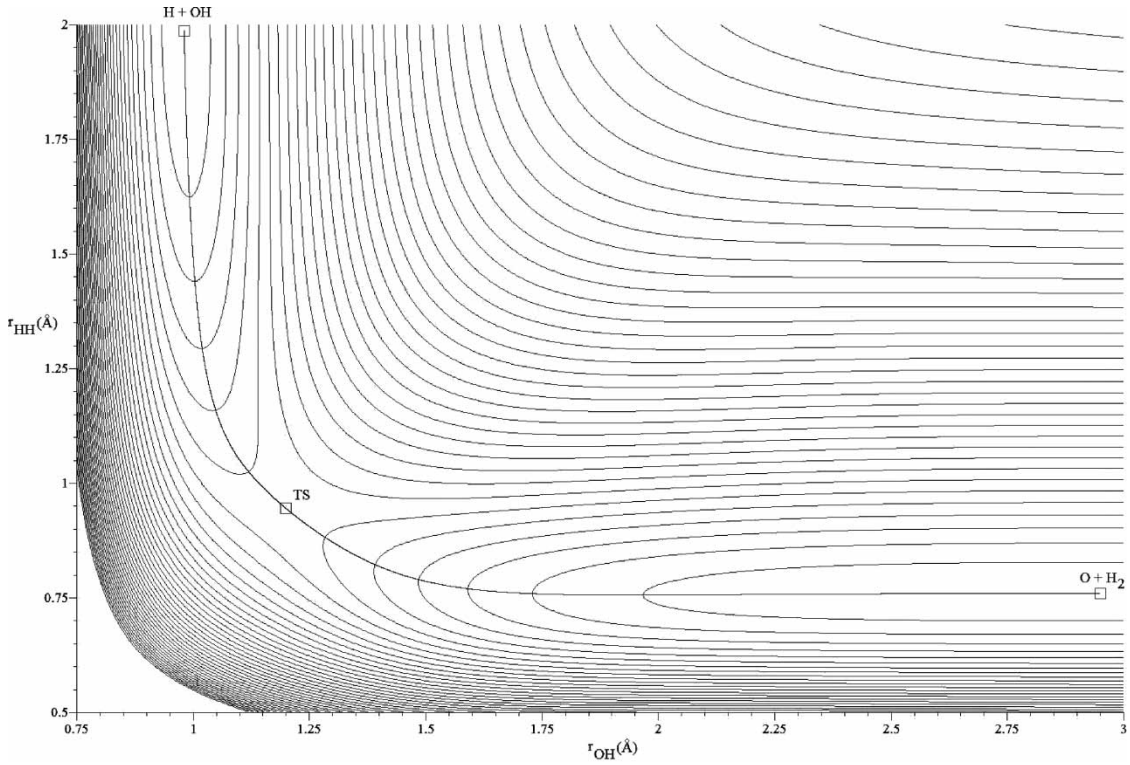

FIGURE 2 Contour plot of the potential energy surface for the reaction $O + H_2 \rightarrow H + OH$ as obtained with the data in Ref. [26]. The line connecting the $O + H_2$, transition state, and $H + OH$ points is the minimum energy path.

There are also quasi-Newton methods that can be used to find first order saddle points, such as the Rational Function Optimization (RFO) and Partitioned Rational Function Optimization (PRFO) methods [36]. For large systems, a limited-memory BFGS method [37,38] that does not require storing the full Hessian is available. We will not describe these methods in detail in this work. Schlegel [30] has recently published a review of the methods used for exploring PESs, and a good introduction can also be found in Ref. [3]. There are also methods available to efficiently construct a PES by interpolating the results from a subset of points, either by assuming a pre-specified functional form [39], or using numerical interpolation techniques [40–42], including iterative improvement of the PES by using results from rate calculations [43–49] or optimization of discretized reaction paths [50–52]. Once an interpolated PES is known, it is much easier to determine its main features. Finally, there are newer methods that can be used to obtain the minimum energy path on the PES for given initial and final states without computing second derivatives of the energy, like the *nudged elastic band* method of Jónsson *et al.* [53]. Since these methods do not require obtaining the Hessian, they can be used to treat more complex systems.

The description of chemical reactions in terms of reactants, products and a transition state, although simple, is very useful. But it is necessary to keep in mind that for many reactions there is not just a single transition state or reaction path. In many cases there are intermediate stable complexes, and multiple energy barriers, connecting the reactant and product sides. Choosing a suitable method for predicting reaction rates usually requires a previous understanding of the reaction mechanism. It is also important to know the size of the energy barrier(s) that the system has to overcome for the reaction to occur. For most reactions, energy barriers are large and reactions happen on a time scale much longer than that characteristic of the molecular motion. If such reactions proceed in a way such that there is good thermal coupling between the transition state molecules and the remaining molecules, and there are only one or a few simple mechanisms for the reaction to proceed, it is possible to use multi-scale classical trajectory methods such as the reactive flux method or blue-moon molecular dynamics (discussed in the "Classical Simulation Methods for Equilibrium and Rate Constants" section). If this is not the case, as for example in photochemical reactions, a fully quantum mechanical description of the dynamics is necessary, as in the wave packet propagation methods. A classical trajectory description is also possible for systems with complex PES's, where there is not a simple reaction

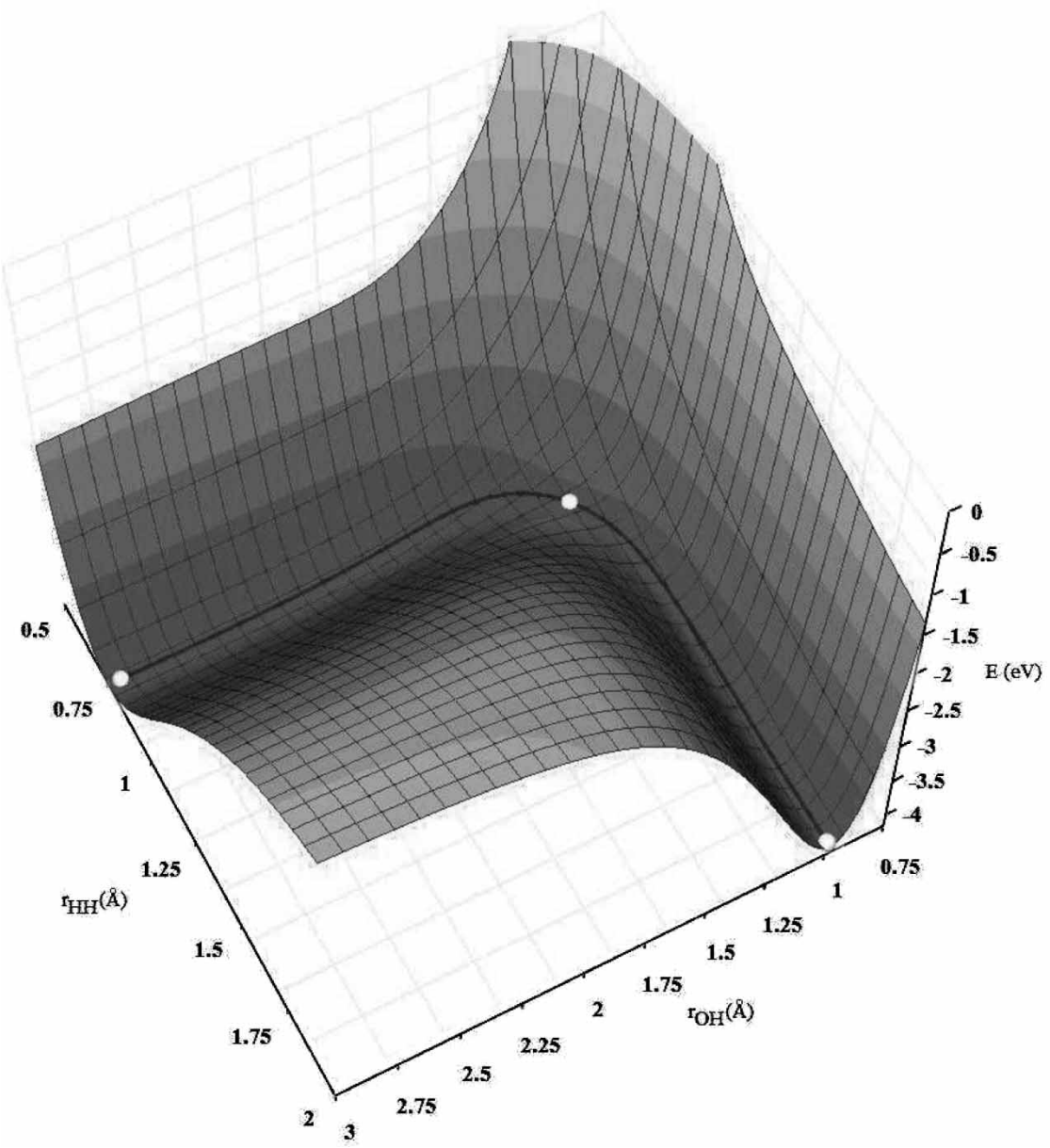

FIGURE 3 Potential energy surface for $O + H_2 \rightarrow H + OH$. The thick line is the minimum energy path.

mechanism, at a higher computational cost. This is the case for the transition path sampling method, also discussed in the "Classical Simulation Methods for Equilibrium and Rate Constants" section.

FORCE FIELD METHODS

Chemical reactions involve the breaking and formation of bonds, which can in principle only be described correctly using quantum mechanics. For the description of many complex systems, however, it is not practical to perform quantum mechanical calculations at each configuration to determine the potential energies. An alternative to this is to construct empirical equations, based on quantum mechanical calculations or experimental results (or both) that describe the PES approximately. These methods are usually called *empirical force field* (FF) methods. The exploration of PESs using empirical force fields is often referred to as *molecular mechanics*. In this section, we describe the main ideas behind the FF approach, and also briefly discuss the combination of FF and electronic structure methods at the end of the "*Ab Initio* Methods" section.

Semiempirical Force Fields [3,4,54–57]

A feature common to FF methods is the decomposition of the total potential energy into several

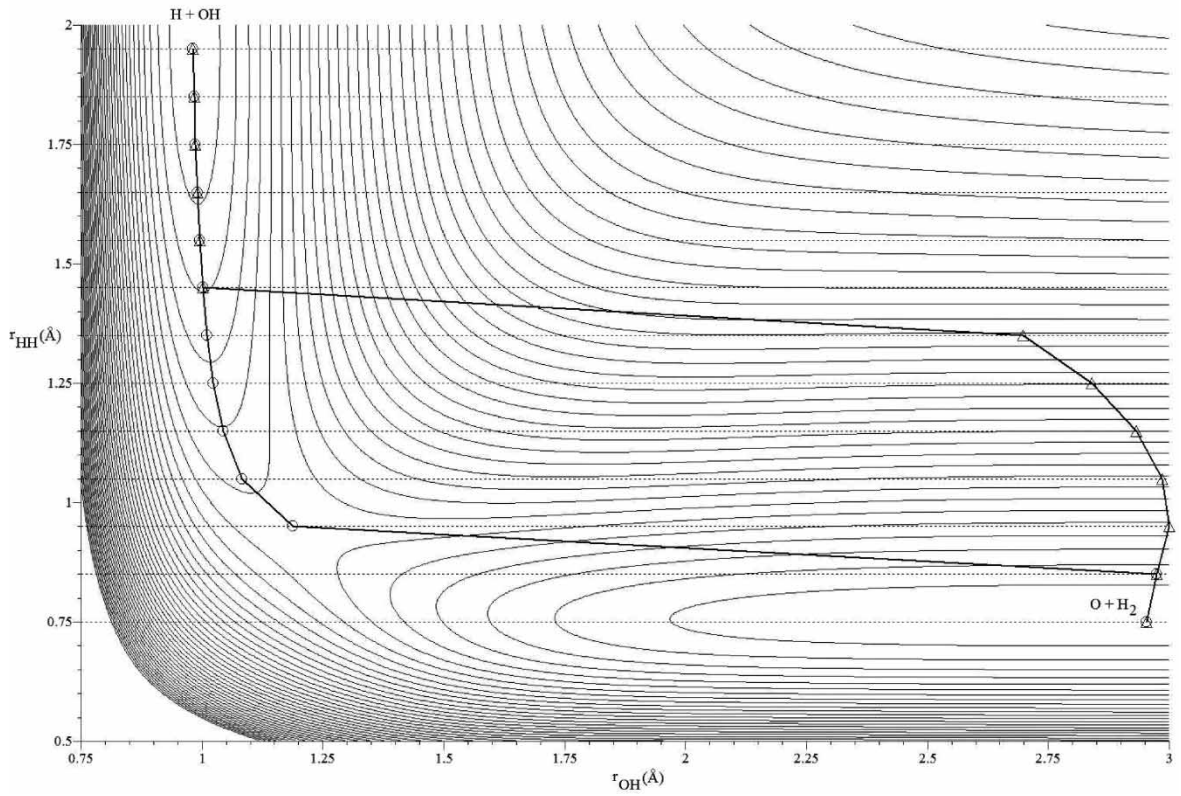

FIGURE 4 The reaction path using the distance H–H as a reaction coordinate. The dashed horizontal lines correspond to a constant reaction coordinate. The triangles are the minimum energy points obtained in the forward direction, and the circles are the points obtained in the backwards direction.

components. A typical FF expansion of the energy is of the form:

$$E_{\text{total}}(\{\mathbf{R}_I\}) = E_{\text{bond}} + E_{\text{val}} + E_{\text{tors}} + E_{\text{vdW}} + E_{\text{coul}} + E_{\text{corr}} \tag{3.1}$$

In Eq. (3.1), $E_{\text{total}}(\{\mathbf{R}_I\})$ represents the total energy as a function of the nuclear configuration, i.e. the PES. Each of the terms is also dependent on the nuclear configuration, but this dependence is not written explicitly for the sake of brevity. The first three and the last term are associated with intramolecular interactions: E_{bond} is the energy associated with stretching/compressing bonds between two atoms, E_{val} is the energy associated with the bending of valence angles, E_{tors} is the torsional energy for rotations around bonds. E_{corr} is a correction term that can include contributions due to conjugation, cross interactions, out-of-plane bending, over/under coordination, etc. The fourth and fifth terms in Eq. (3.1) represent the intermolecular interactions: E_{vdW} is the van der Waals contribution and E_{coul} is the electrostatic contribution. Figure 6 shows a schematic of what each of the terms accounts for. In some FFs the nuclear configuration is simplified by using the *united atom* approach, which models groups of atoms (e.g. CH_3, CH_2, etc.) as a single atom to reduce the computational cost.

There are different ways to represent each of the energy contributions in Eq. (3.1), depending on the particular FF method used. The simplest way to represent the energies E_{bond} and E_{val}, for example, is the harmonic approximation:

$$E_{\text{bond},IJ} = k_{\text{bond},IJ}\left(R_{IJ} - R_{IJ}^0\right)^2 \tag{3.2}$$

$$E_{\text{val},IJK} = k_{\text{val},IJK}\left(\theta_{IJK} - \theta_{IJK}^0\right)^2 \tag{3.3}$$

In Eqs. (3.2) and (3.3), $E_{\text{bond},IJ}$ and $E_{\text{val},IJK}$ are the stretching energy associated with the bond between the nuclei I and J and the bending energy associated with the valence angle between the nuclei I, J and K. R_{IJ} and θ_{IJK} are the distance between I and J and the valence angle between I, J and K; R_{IJ}^0 and θ_{IJK}^0 are the corresponding equilibrium values of these quantities. The force constants $k_{\text{bond},IJ}$ and $k_{\text{val},IJK}$ are empirical parameters that must be fitted to available data. The $E_{\text{bond},IJ}$ and $E_{\text{val},IJK}$ values would have to be summed over all bonds and valence angles to give the E_{bond} and E_{val} terms in Eq. (3.1) [58]. The harmonic approximation has the advantage of its very low computational cost, but it will only work

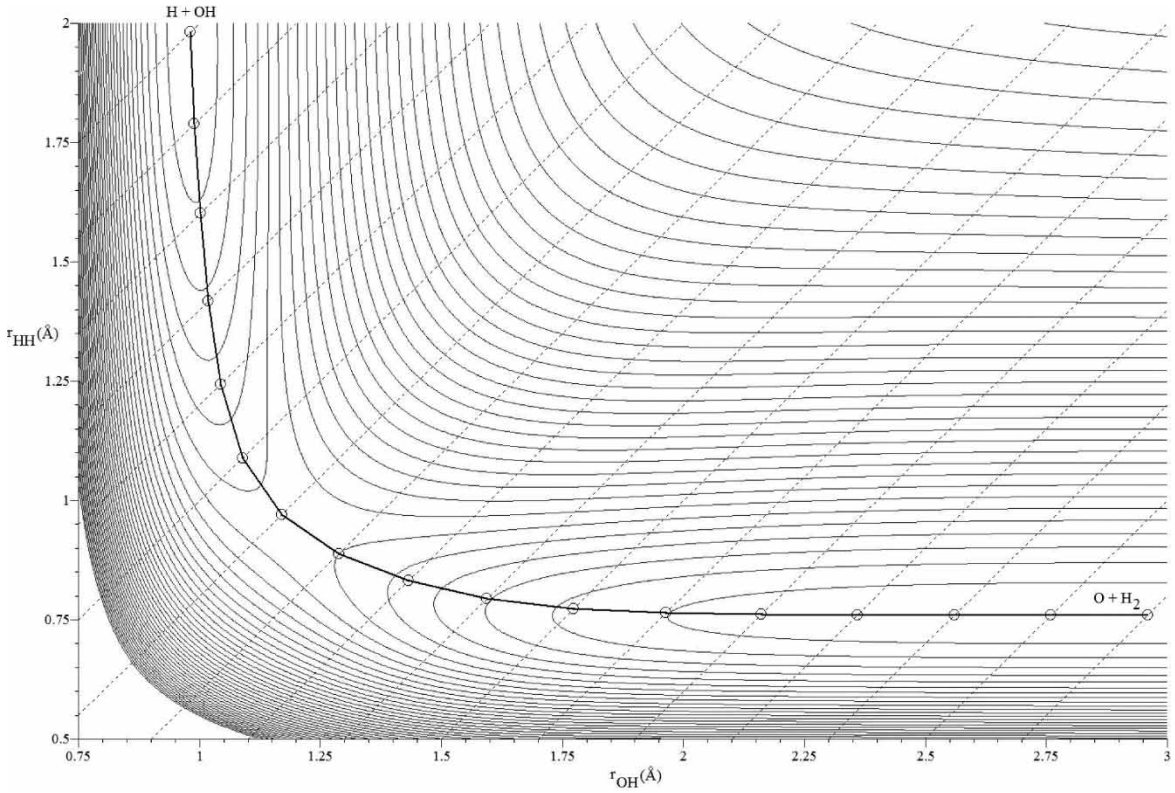

FIGURE 5 The reaction path using the difference between the H–H and O–H distances as a reaction coordinate. The dashed lines correspond to a constant reaction coordinate. The circles are the minimum energy points found on the lines of constant reaction coordinate.

well for small deviations from the equilibrium values. It is possible to add higher-order corrections (typically up to fourth order) to Eqs. (3.2) and (3.3) to get more accurate results at low separations, but this requires additional parameters. These Taylor expansions will also not work when the FF is used to describe a dissociation, since the energy will diverge as the separation grows. In order to describe the dissociation limit correctly different functional forms must be used. A typical choice is the Morse [59] potential:

$$E_{\text{bond},IJ} = D\left[1 - \exp\left(aR_{IJ}\right)\right]^2 \tag{3.4}$$

In Eq. (3.4), D is the dissociation energy and a is a parameter related to the classical vibrational

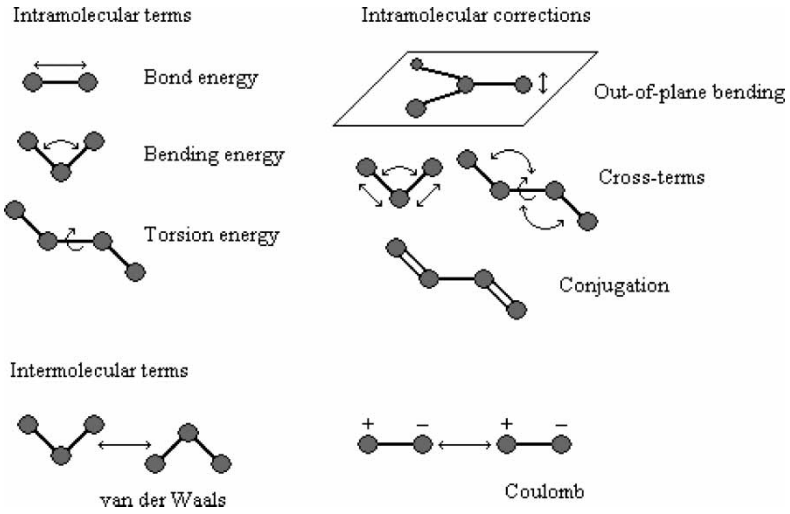

FIGURE 6 Energy contributions in a typical force field.

frequency of the bond. This function describes the stretching energy much more realistically than a Taylor expansion, but has a larger computational cost due to the exponential function. More complicated expressions can be used to fit the intramolecular contribution (for an example see Ref. [60]).

Torsional contributions to the potential energy are typically represented by Fourier cosine expansions:

$$E_{\text{tors},IJKL} = \sum_{n=0}^{N_F} a_{n,IJKL} \cos\left(n\omega_{IJKL}\right) \tag{3.5}$$

In Eq. (3.5), $E_{\text{tors},IJKL}$ is the torsional energy associated with the nuclei I, J, K and L, $N_F + 1$ is the number of terms in the Fourier expansion, and the $a_{n,IJKL}$ are coefficients that must be fitted to available data. These coefficients depend not only on the nature of the atoms, but also on the nature of the bond: a double bond, for example, will have a much higher penalty for rotation than a single bond [61]. The torsional angle ω_{IJKL} is defined as the angle between the plane containing the nuclei I, J, K and the plane containing the nuclei J, K, L.

The correction term E_{corr} is the one that varies the most between different empirical FFs. It can contain contributions due to conjugation, out-of-plane bending, over/under coordination, coupling between stretching, bending and torsional modes, etc. The particular form of the corrections depends on the kinds of systems that the FF should be able to represent accurately, and the degree of approximation required.

The terms E_{vdW} and E_{coul} account for the nonbonded interactions between the atoms. The van der Waals energy (E_{vdW}) is often represented as a sum of two contributions: a repulsive part accounting for the overlap energy when the nuclei are close to each other, and an attractive part due to the mutually induced multipole interactions:

$$E_{\text{vdW},IJ} = E_{\text{ov}}(R_{IJ}) - E_{\text{att}}(R_{IJ}) \tag{3.6}$$

The attractive energy E_{att} in Eq. (3.6) can in general be expressed as:

$$E_{\text{att}}(R_{IJ}) = \frac{C_{6,IJ}}{R_{IJ}^6} + \frac{C_{8,IJ}}{R_{IJ}^8} + \frac{C_{10,IJ}}{R_{IJ}^{10}} + \cdots \tag{3.7}$$

The first term in Eq. (3.7) accounts for the mutually induced dipole interaction, the second for the induced dipole-induced quadrupole interaction, and so on. The expansion is typically truncated at the first term.

The overlap energy E_{ov} is more difficult to represent than the attractive part. Although the expansion (3.7) can be formally derived using quantum mechanics [62–65], there is no equivalent formal result for the overlap energy. The form for E_{ov} that has the best theoretical justification is an exponential function. Combining this with the expansion (3.7) truncated to the first term we have the *Buckingham potential*:

$$E_{\text{vdW},IJ} = A_{IJ} \exp\left(-\frac{R_{IJ}}{\sigma_{IJ}}\right) - C_{IJ}\left(\frac{\sigma_{IJ}}{r_{IJ}}\right)^6 \tag{3.8}$$

The energy parameters A_{IJ} and C_{IJ}, as well as the distance parameter σ_{IJ} in Eq. (3.8) are empirical constants. This functional form has the disadvantage of requiring an exponential evaluation. An option is to represent the overlap term by a simpler function of the form kR_{IJ}^{-n}, where k and $n > 6$ are also empirical parameters. The most popular choice of this type is the *Lennard–Jones* (LJ) *potential*:

$$E_{\text{vdW},IJ} = 4\varepsilon_{IJ}\left[\left(\frac{\sigma_{IJ}}{R_{IJ}}\right)^{12} - \left(\frac{\sigma_{IJ}}{R_{IJ}}\right)^6\right] \tag{3.9}$$

The energy parameter ε_{IJ} and the distance parameter σ_{IJ} in Eq. (3.9) are empirical constants. An advantage of the particular form of the LJ potential is that the first term in the square bracket can be computed by multiplying the second one by itself, adding only one multiplication to the computational cost instead of an exponential evaluation. The LJ and Buckingham potentials are the most commonly used for the van der Waals energy. Variations of the LJ equation with different exponents are also common. A Morse or Morse-like potential has also been used to describe the van der Waals energy, as in the COSMIC [66] and ReaxFF [60,67] force fields.

The electrostatic contribution E_{coul} to the potential energy can be obtained by assigning charges to atoms and/or bonds in the molecule, or by using a multipole expansion. The latter option requires knowledge of the dipole moment of each molecule (and higher moments if more terms in the multipole expansion are included). The atomic charges used to calculate E_{coul} can be treated as fitting parameters or obtained using an estimation method. Examples of such methods are the Q_{eq} method [68] and the *electronegativity equalization method* (EEM) [69,70]. Sometimes charges are assigned to positions in the molecule that do not correspond to atoms or bonds to improve the fitting, as in some of the potentials used to simulate liquid water. For a description of these see Ref. [3].

The main advantage of FF methods in general is their much lower computational cost compared to quantum mechanical calculations. For many complex systems, such as biomolecules and many reactions in solution, FF methods are the only viable alternative to describe the PES. There are many different FFs in the literature. In most cases, the FF is developed to treat a particular class of systems, although there are several FFs that are general

(i.e. parameters are available for all atoms). Some commonly used FFs are [71] the molecular mechanics force fields of Allinger *et al.*, MM2 [72,73], MM3 [73–76], and MM4 [77–81], the Merck molecular force field (MMFF) [82–86], Assisted Model Building with Energy Refinement (AMBER) [87–89], Optimized Potentials for Liquid Simulation (OPLS) [89–91], Chemistry at HARvard Macromolecular Mechanics (CHARMM) [89,92,93], GROningen MOlecular Simulation (GROMOS) [94–96], Empirical Conformational Energy Program for Peptides (ECEPP) [97–99], and DREIDING [100]. Most of these methods were originally developed for the study of biomolecules such as proteins, nucleic acids and carbohydrates, or hydrocarbons, but some have been extended to handle any atom types. There are also force fields, such as MOMEC [101] and SHAPES [102] that were developed for the study of inorganic compounds, particularly transition metal complexes; and force fields specifically developed for hydrocarbon compounds, such as Empirical Force Field (EFF) [103,104], the Brenner potential [105], Adaptive Intermolecular Reactive Empirical Bond Order (AIREBO) [106] and ReaxFF [60]. Other more specialized force fields have been reviewed by Leach [3].

Many force fields, as mentioned in the previous paragraph, have been extended to include practically all kinds of atoms. There are also force fields developed from the beginning with the purpose of spanning the full periodic table, such as Universal Force Field (UFF) [107] and Reaction Force Field (RFF) [108]. The problem with the more general FFs is that they are in general less accurate than FFs developed specifically for a particular family of compounds, but they have also been around for a shorter time, so it is quite possible that further refinements can make them competitive. The main problem in fitting a general force field is to ensure its transferability while using a reasonable number of parameters; in order to be useful the FF has to be able to predict correctly properties for compounds that fall outside the set used to fit the parameters.

There are several techniques for exploring PESs, and particularly for finding transition states, using FF methods [4,109–113]. These methods are useful for situations where a more accurate description of the system is not possible, and also for finding initial estimates of transition state structures to be further refined with, e.g. an *ab initio* method. There are also methods that use a combination of a FF with quantum mechanical calculations for efficient exploration of reactive PESs, like the multiconfigurational molecular mechanics (MCMM) method [114,115] and the QM-guided molecular mechanics (Q2 MM) method [116], among others [117–120]. Some of these methods are related to the approach discussed at the end of the "*Ab Initio* Methods" section.

The main disadvantage of the FF approach is that there is no way to systematically improve the results within the method. In the case of *ab initio* methods, for example, one can improve the results by increasing the basis set size, or by using a higher level of theory. In FF this is not possible. The only way to assess the results is to compare to either experimental data or to results obtained with an *ab initio* method, but this comparison is not always possible. Nevertheless, since for many systems a FF approach is practically the only viable option, they remain a very useful tool in computational chemistry.

Another problem with FF methods is that there seem to be too many of them. It is difficult to decide *a priori* which FF is the best for the particular system that one wants to study. Many comparisons and evaluations of FFs for different applications, however, have been published that can serve as a guide in making such a decision. Some of them can be found in Refs. [121–135].

Applications of FF methods are numerous, particularly in the study of complex systems like biomolecules, polymers and reactions in solution. Some recent representative works that show the applicability of the FF approach include:

- A molecular dynamics study of seven different oligosaccharide complexes of the galectin-1 protein [136] using the AMBER FF, that sheds light on the mechanism of carbohydrate binding in this protein.
- A study of the side-chain conformations in the gramicidin-A channel [137] through molecular dynamics simulations using the CHARMM FF, showing the different states and the frequency of the transitions between states for this system.
- A conformational study of the O-specific polysaccharide of the bacteria *Shigella flexneri* [138], a molecule that plays an important role on the immune response against this microorganism. The study used the MM3 force field, and the models obtained were in good agreement with NMR measurements.
- A study of the dynamical effects of mutations on an RNA hairpin [139] using constrained molecular dynamics and the free energy perturbation method. The simulations were performed using the CHARMM27 FF. The results obtained show good agreement with experimental measurements.

AB INITIO METHODS [2–9,140,141]

Although one may use a previously fitted force field to describe the PES, determining it from first principles is the purpose of *ab initio* methods. In these methods the potential energy is obtained

using the principles of quantum mechanics, using only as input the nature of the atoms comprising the system.

Since we are restricting ourselves to the calculation of chemical reaction rates using classical trajectory methods, we will not discuss here time-dependent *ab initio* methods or quantum scattering methods. An introduction to time-dependent *ab initio* methods can be found in Ref. [2], and a recent review in Ref. [142]. A recent review of the quantum scattering methods is in Ref. [143]. The *quantum Monte Carlo* method, which uses the analogy between the time-dependent Schrödinger equation in imaginary time and the classical diffusion equation for electronic structure calculations, will also not be discussed here. Good introductions to this subject can be found in Refs. [144,145].

The *ab initio* methods that we will discuss attempt to find approximate solutions to the time-independent Schrödinger equation for a given many-atom system:

$$\hat{H}\Phi = E\Phi \tag{4.1}$$

In Eq. (4.1), Φ represents the wave function of the many-atom system, E is the total energy and $\hat{H}$ is the Hamiltonian operator. For the general case of a system of N electrons and M nuclei, the Hamiltonian operator is:

$$\hat{H} = -\sum_{i=1}^{N}\frac{1}{2}\nabla_i^2 - \sum_{I=1}^{M}\frac{1}{2M_I}\nabla_I^2 - \sum_{i=1}^{N}\sum_{I=1}^{M}\frac{Z_I}{r_{iI}} + \sum_{i=1}^{N-1}\sum_{j=i+1}^{N}\frac{1}{r_{ij}} + \sum_{I=1}^{M-1}\sum_{J=I+1}^{M}\frac{Z_I Z_J}{R_{IJ}} \tag{4.2}$$

In writing Eq. (4.2), and in what follows, we use the indices $i, j, \ldots$ for the electrons and the indices $I, J, \ldots$ for the nuclei. The symbol ∇_i^2 is a Laplacian operator with respect to the coordinates of electron i, and ∇_I^2 is a Laplacian operator with respect to the coordinates of the nucleus I. The first term in Eq. (4.2) represents the electronic kinetic energy; the second term is the nuclear kinetic energy. The remaining three terms are the Coulomb interactions between the nuclei and the electrons, between electron pairs and between nucleus pairs, respectively. All the equations we will write in the "*Ab initio* Methods Section" will be in atomic units.

In the second and third sections, we will introduce some of the basic elements that are common to most *ab initio* methods: the Born–Oppenheimer approximation, the variational principle and the concept of orbitals and the basis sets used to construct them. In the remaining sections, we will explore some of the most common approaches to finding approximate solutions to Eq. (4.1), and discuss their advantages and limitations.

The Born–Oppenheimer Approximation

Most *ab initio* methods make use of the Born–Oppenheimer (BO) approximation, proposed by Born and Oppenheimer in 1927 [146,147]. The idea behind this approximation is that, since the nuclei are much heavier than the electrons, their motion will be much slower, i.e. the characteristic time scales of processes involving the electrons are much smaller. If this is true, the electronic wave functions can be found by assuming that the nuclei are static. This means that the PES will only depend on configurational variables, i.e. on the way the nuclei are arranged in space, and not on their momenta. The BO approximation is good for many quantum chemistry problems [148], but it fails if two different solutions to the electronic Schrödinger equation are very close in energy. If non-BO effects (also called *non-adiabatic* [149] effects) may be important, it is possible to include them as corrections after a BO calculation has been made [148], e.g. with a perturbation approach. It is also possible to do simulations where there is more than one adiabatic [149] PES, and the system is permitted to "hop" from one to the other in order to allow for electronic transitions. These methods are called *surface-hopping* methods [150–152]. For a review on these methods see Ref. [153]. A review on non-BO reaction dynamics is given in Ref. [154].

Within the BO approximation, only the terms in the Hamiltonian (4.2) involving the electrons have to be taken into account. The second term—the kinetic energy of the nuclei—is neglected because the nuclei are assumed to be static. The last term—the Coulomb repulsion between the nuclei—is assumed to be constant, and thus can be added to the energy after solving the electronic problem. The Hamiltonian for the electronic problem is hence:

$$\hat{H}_{\mathrm{e}} = -\sum_{i=1}^{N}\frac{1}{2}\nabla_i^2 - \sum_{i=1}^{N}\sum_{I=1}^{M}\frac{Z_I}{r_{iI}} + \sum_{i=1}^{N-1}\sum_{j=i+1}^{N}\frac{1}{r_{ij}} \tag{4.3}$$

where the subscript "e" refers to the electrons. The corresponding Schrödinger equation for the electronic problem is:

$$\hat{H}_{\mathrm{e}}\Phi_{\mathrm{e}} = E_{\mathrm{e}}(\{\mathbf{R}_I\})\Phi_{\mathrm{e}} \tag{4.4}$$

The electronic energy E_{e} obtained by solving Eq. (4.4) depends parametrically on the positions of the nuclei, and it does not include the Coulomb repulsion between them. In order to obtain the total energy of the system it is necessary to add this contribution separately:

$$E_{\mathrm{total}}(\{\mathbf{R}_I\}) = E_{\mathrm{e}}(\{\mathbf{R}_I\}) + \sum_{I=1}^{M-1}\sum_{j=I+1}^{M}\frac{Z_I Z_J}{R_{IJ}} \tag{4.5}$$

The quantity $E_{\mathrm{total}}(\{\mathbf{R}_I\})$ is the PES that is required to study chemical reactions. Within the BO

approximation we need to find solutions to the electronic problem (4.4), and then use Eq. (4.5) to get the PES. Note that solving Eq. (4.4) is an eigenvalue problem that will have an infinite number of solutions. In many cases one is interested in the solution with the lowest energy, which corresponds to the *ground state* of the electronic system.

The Variational Principle

Many *ab initio* methods are based on the *variational principle*, sometimes called the *Rayleigh–Ritz variational principle*. This principle states that, given *any* normalized electronic wave function $\tilde{\Phi}_e(\mathbf{r})$, which need not be the true solution to the Schrödinger equation (4.4), the expectation value of the Hamiltonian:

$$E[\tilde{\Phi}_e] = \int d\mathbf{r} \tilde{\Phi}_e^* \hat{H} \Phi_e \tag{4.6}$$

corresponding to $\tilde{\Phi}_e$ will always be greater than or equal to the ground state energy E_0, *i.e.*:

$$E[\tilde{\Phi}_e] \geq E_0 \quad \text{for all } \tilde{\Phi}_e \tag{4.7}$$

The proof of this principle is simple. Since the Hamiltonian is a Hermitian operator [155], all of its eigenfunctions are orthogonal:

$$\int d\mathbf{r} \Phi_\alpha^* \Phi_\beta = \delta_{\alpha\beta} \tag{4.8}$$

In Eq. (4.8), Φ_α and Φ_β are two normalized eigenfunctions of the Hamiltonian and $\delta_{\alpha\beta}$ is the Kronecker delta. The eigenfunctions also form a complete basis for the space of all functions $\Phi(\mathbf{r})$, so any electronic wave function $\tilde{\Phi}_e(\mathbf{r})$ can be expanded in terms of the eigenfunctions as:

$$\tilde{\Phi}_e(\mathbf{r}) = \sum_\alpha c_\alpha \Phi_\alpha(\mathbf{r}) \tag{4.9}$$

where the c_α are constants. If we substitute Eq. (4.9) into Eq. (4.6) and use Eq. (4.8) together with the fact that the functions Φ_α satisfy the Schrödinger equation (4.4), we obtain:

$$E[\tilde{\Phi}_e] = \sum_\alpha |c_\alpha|^2 E_\alpha \tag{4.10}$$

Now, since the ground state energy is the smallest of the E_α, this means that:

$$E[\tilde{\Phi}_e] = \sum_\alpha |c_\alpha|^2 E_\alpha \geq E_0 \sum_\alpha |c_\alpha|^2 = E_0 \tag{4.11}$$

The last equality follows from the fact that the Φ_α are normalized. The variational principle provides a very good test of the quality of an approximation to the electronic wave function. Since the true ground state energy is a lower bound for the expectation energy, one always knows that, among different calculations with the same Hamiltonian, the one giving the lowest energy is the best. Note that this argument is good only if we are interested in the ground-state wave function. For an *excited* wave function (i.e. one corresponding to a higher energy), the true energy eigenvalue will be a lower bound only if the approximate wave function happens to be orthogonal to all the *exact* wave functions corresponding to the lower energies. Since in general we do not know these exact wave functions, the variational principle is not as useful in this case. Nevertheless, in many quantum chemistry applications we are interested only in finding the ground state wave function, and hence the variational principle remains very useful.

The variational principle actually provides a way to reformulate the problem of finding the ground state wave function. From Eq. (4.11) it is clear that the expectation value of the energy will be *equal* to E_0 only if $\tilde{\Phi}_e$ is the true ground state wave function (that is, if all the coefficients c_α for $\alpha \neq 0$ are zero). Hence finding the ground state wave function can be formulated as a variational minimization problem:

$$\delta E[\Phi_0] = 0 \tag{4.12}$$

This is the basis for many *ab initio* methods, some of which will be discussed in the following sections.

Orbitals and Basis Functions [156,157]

The wave function appearing in the electronic problem (4.4) depends on the coordinates of all the electrons. For ease of both visualization and computation, it is convenient to express the electronic problem in terms of functions that depend only on the coordinates of a single electron. These functions are called *orbitals*. In the following sections, we will see several ways to relate the many-electron wave function appearing in Eq. (4.4) to these orbitals. In this section, we will discuss some common ways to represent these orbitals in *ab initio* calculations.

A *spatial orbital* $\psi_i(\mathbf{r})$ is a function of the position of a single electron i defined such that the probability density of finding the electron in a position $\mathbf{r}$ is $|\psi_i(\mathbf{r})|^2$. The description of an electron also requires assigning a *spin* to it. When the spatial orbitals are combined with functions that specify the spin of the electron, σ, we obtain the *spin orbitals* $\chi_i(\mathbf{r}, \sigma)$. Since the spin of an electron can have two values ("spin up" and "spin down"), any given spatial orbital gives rise to two spin orbitals. Any single electron can be described by a single spin orbital.

In order to find approximate solutions to the electronic problem, it is necessary to assume a mathematical form for the spatial orbitals. This is

usually done by expanding these orbitals in terms of a set of *basis functions* $\phi_\mu(\mathbf{r})$:

$$\psi_i(\mathbf{r}) = \sum_{\mu=1}^{K} C_{\mu i}\phi_\mu(\mathbf{r}) \tag{4.13}$$

These basis functions are often, but not always, centered at the nuclei. When functions centered at different nuclei in a molecule are combined linearly as in Eq. (4.13), we have the Linear Combination of Atomic Orbitals Molecular Orbitals (*LCAO-MO*) representation. This is the most common way to represent molecular wave functions. Once a set of basis functions is chosen, the problem of finding the orbitals reduces to finding the expansion coefficients $C_{\mu i}$. In general, a larger basis set leads to a more accurate solution, but the computational cost typically increases as $O(K^4)$ or more, so it is imperative to choose basis functions that give good results with the lowest possible number of terms.

One set of basis functions that can be used for the spatial orbitals is inspired by the form of the analytical solution of the Schrödinger equation for the hydrogen atom. These functions are called *Slater Type Orbitals* (STOs) [158]. The normalized STO for a 1*s* orbital centered at $\mathbf{R}_A$ is given by:

$$\phi_{1s}^{STO} = \left(\frac{\zeta^3}{\pi}\right)^{1/2} \exp\left(-\zeta|\mathbf{r}-\mathbf{R}_A|\right) \tag{4.14}$$

where ζ, the *Slater orbital exponent*, is a parameter. In principle, this parameter should be adjusted together with the expansion coefficients $C_{\mu i}$ in Eq. (4.14). This however, makes the problem non-linear and much more difficult to solve. There are published values of the best Slater exponents for each atomic species (see, for example, Ref. [156]), and these are normally used to avoid the non-linearity. For orbitals other than the 1*s*, the STOs are multiplied by polynomials in the components of $\mathbf{r}-\mathbf{R}_A$.

STOs usually give very good results, but they have a major drawback. In most *ab initio* methods, it is necessary to calculate integrals involving the orbitals in order to obtain the expectation values of all the terms in the Hamiltonian (4.3). These integrals do not have an analytical solution for STOs, and their numerical calculation adds a lot of computational cost. An alternative is to use *Gaussian type orbitals* (GTOs) [159]. For a 1*s* orbital, the normalized GTO centered at $\mathbf{R}_A$ is:

$$\phi_{1s}^{GTO} = \left(\frac{2\alpha}{\pi}\right)^{3/4} \exp\left(-\alpha|\mathbf{r}-\mathbf{R}_A|^2\right) \tag{4.15}$$

where α is a parameter. It is possible to obtain analytical expressions for the expectation values of all terms in the Hamiltonian (4.3) when GTOs are used, hence reducing the computational cost considerably with respect to STO calculations. As with STOs, the orbitals other than 1*s* are obtained by multiplying by polynomials in the components of $\mathbf{r}-\mathbf{R}_A$.

One major difference between STOs and GTOs is that the slope at $\mathbf{r}=\mathbf{R}_A$ of a GTO is always zero, which is not the case for the STOs. The GTOs also decay much faster with increasing distance. Since STOs usually give better results, one way to use GTOs but still keep some of the precision of the STOs is to fit the STOs using GTOs. The orbitals obtained in this way are called STO-NG orbitals, where the "NG" indicates the number of Gaussians used to fit the STO. For example, the STO-3G function is given by:

$$\phi_{1s}^{STO-3G} = d_1\phi_{1s}^{GTO}(\alpha_1) + d_2\phi_{1s}^{GTO}(\alpha_2) + d_3\phi_{1s}^{GTO}(\alpha_3) \tag{4.16}$$

where the d_i are *contraction coefficients*. For a given STO, it is possible to find these coefficients and the corresponding Gaussian exponents α_i that provide the best fit. Using this kind of orbital considerably improves the computational speed with respect to an STO calculation, retaining much of its accuracy. Figure 7 shows how an increasingly better approximation is obtained by adding more GTOs to the expansion (4.16).

A way to incorporate more flexibility into the basis set is to allow for more than one Slater function to represent the same orbital. These orbitals are called *multiple-zeta* or *split* basis sets, and the most common are the double-zeta, which use two Slater functions for one orbital. Since in most cases the chemistry is determined by the valence electrons, it is common to use split basis functions only for them, and single STO-NGs for the core electrons. Such a basis set is called a *split valence* basis set. Split valence basis sets are usually labeled by three numbers (in the case of a double-zeta basis for the valence): one is the number of GTOs used to fit the STO for the core electrons, the other two are the numbers of GTOs used to fit the two STOs for the valence electrons. Hence, a 4-31G basis would consist of STO-4G functions for the core electrons, and a STO-3G and a STO-1G (the latter being effectively just one GTO) for the valence electrons. This can be extended to multiple-zeta basis for the valence, for example a 6-311G basis would use STO-6G functions for the core electrons, and one STO-3G and two GTOs for the valence electrons. Among the most common split-valence basis sets are the 3-21G [160–162], 4-31G [163–165], 6-21G [160–162], 6-31G [164,165] and 6-311G [166–169].

Another improvement on the basis set is to include the possibility of *polarization*, that is contributions from higher angular momentum orbitals in the description. For example, a non-polarized basis set for a hydrogen atom would only contain *s*-type

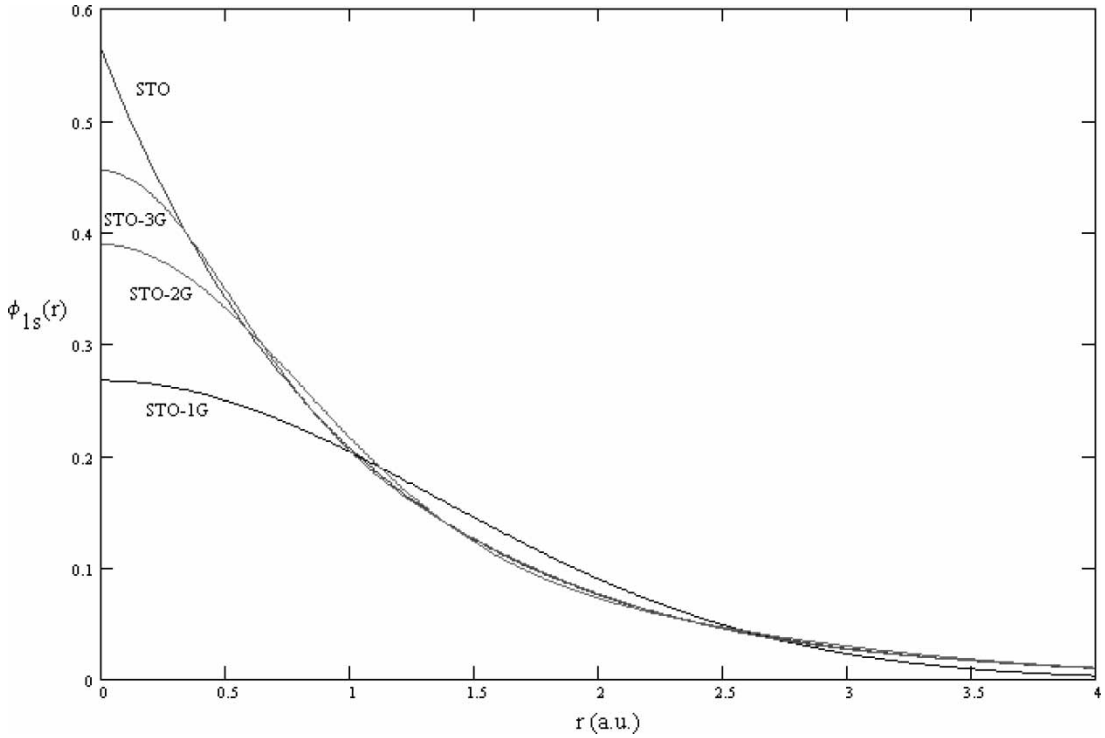

FIGURE 7 Three successive approximations to a hydrogen 1s Slater orbital using Gaussian functions.

functions, but a polarized basis set would also include *p*-type or higher angular momentum functions. Polarized basis sets are usually labeled by adding one or more stars (*) to their name, or by adding a list of the additional polarization functions used. For example, the 6-31G*—or, equivalently, 6-31G(*d*)—basis set [170–173] for the first- and second-row atoms in the periodic table is like the 6-31G but with an additional set of 3*d* GTOs. The 6-31G** basis—or 6-31G(*d*,*p*)—also includes *p*-type GTOs for hydrogen. Including polarization gives more angular freedom so that the basis is able to represent bond angles more accurately, especially in strained ring molecules. Diffuse functions, which are additional GTOs with smaller exponents, can be also added for increased accuracy, and are denoted by adding " + " or "++" to the name. When " + " is used, it indicates the addition of a set of *s*- and *p*-functions for the heavy atoms, whereas "++" indicates that an additional *s*-diffuse GTO for hydrogen. Diffuse functions are especially useful for cases where more radial flexibility is needed, such as the modeling of anions or Rydberg states [174].

The basis sets discussed so far are among the most commonly used. With the increasing computational power available to quantum chemists, some more sophisticated basis sets have been developed. Among the most commonly used are the correlation-consistent basis sets of Dunning [175–177], which include up to quintuple-zeta functions and polarization, and can be augmented with diffuse functions. These sets are usually labeled as (AUG-) cc-pVNZ, where the prefix AUG- is added when diffuse functions are included, and N may be D (for double-zeta), T (triple-), Q (quadruple-) and 5 (quintuple-). A good description of these and other basis sets not discussed here can be found in Ref. [4, chapter 5].

Another approach that is often used in solid-state calculations is to use *plane wave basis sets* (PWs), i.e. to represent the spatial orbitals as 3D Fourier expansions:

$$\psi_i(\mathbf{r}) = \sum_{\mu=1}^{K} C_{\mu i} e^{i\mathbf{k}_\mu \cdot \mathbf{r}} \tag{4.17}$$

Using PW functions has several advantages, especially in the study of periodic solids and in *ab initio* molecular dynamics (discussed in "*Ab initio* Molecular Dynamics Section"). In the latter case, the basis functions that are centered on the nuclei give rise to contributions to the forces on the nuclei due to the fact that the basis functions' centers move in time. These contributions are sometimes called *Pulay forces* [178], and are expensive to calculate [179]. Since PWs do not have a "center", there is no need to calculate these contributions in PW calculations. For a more detailed discussion of this point see Ref. [179]. Another advantage of PWs is that the calculation of forces can be done more easily in Fourier space. Since there are very efficient Fast Fourier Transform algorithms available, this decreases

the computational cost of obtaining forces even further. PW basis sets are also very useful to study electrons that are not tightly bound to a nucleus, as in metals, and this is a reason for their popularity in solid-state calculations. In a sense, PW basis sets are complementary to atom-centered basis sets: a very good description of a material can be obtained by using atomic orbitals in the vicinity of the nuclei and plane waves in the internuclear regions. This is the basis for the *muffin-tin* approximation used in solid-state calculations. For an introduction to this treatment, see Ref. [9]. For a discussion of the relative advantages and disadvantages of PWs see Ref. [179].

The main problem with PWs is that the wave functions tend to oscillate strongly in the core region due to the singularity of the Coulomb potential at $\mathbf{r} = 0$ and the requirement of orthogonality of the one-electron states. This adds very high-frequency components to the wave function, which require a large number of terms in the Fourier expansion (4.17). Since the valence shells are the most important for quantum chemistry, a way around this problem is to replace the core (i.e. nucleus + core electrons) by a potential that does not have a singularity at the origin. This potential is fitted to guarantee that the wave function of the valence electrons beyond a certain radius coincides with the "true" wave function (*i.e.* the one obtained when solving with the real potential and all the electrons). These potential functions are called *atomic pseudopotentials* (also known as *effective core potentials*), and their use permits obtaining good results with fewer terms in the expansion (4.17). The PW pseudopotential approach is very often used in solid-state calculations, and in *ab initio* molecular dynamics (see the "*Ab initio* Molecular Dynamics" section). Another advantage of the pseudopotential approach is that it is not necessary to solve for the core states, which reduces the computational cost significantly. Furthermore, in heavy atoms relativistic effects can be taken care of in the pseudopotential generation.

Self-Consistent Mean-Field Theory—the Hartree–Fock Method

The Hartree–Fock (HF) method is a reference for many other *ab initio* methods [180–182]. Most of the modern picture of atomic and molecular structure in chemistry comes from the HF description. Since HF is the starting point for many other *ab initio* calculations, as well as the simpler semiempirical methods, we will discuss it first.

In the HF method, a many-electron system is treated using a collection of one-electron spin-orbitals. Each electron is assumed to belong to a different spin-orbital according to the exclusion principle, and the electron–electron interactions

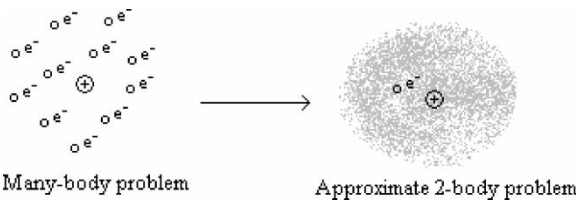

FIGURE 8 The Hartree–Fock picture. The original many-body problem is transformed into a set of two-body problems by replacing all but one of the electrons by a mean field. The equations for each electron are then solved self-consistently.

are replaced by the interaction of each electron with the mean field resulting from the other electrons, as depicted in Fig. 8. Hence the HF method is a mean-field theory. This *ansatz* gives rise to an iterative procedure: each of the electronic wave functions will depend on the mean interaction with the other electrons, which in turn depends on the other electrons' wave functions. Therefore it is necessary to iterate with the set of wave functions until convergence is achieved. The resulting set of solutions after convergence is said to be *self-consistent*, and hence the name *self-consistent mean-field theory.*

In order to carry out this iterative procedure, we need to assume a form of the wave function for the many-electron system that contains some adjustable parameters. Since the many-electron wave function has to be antisymmetric, a possible mathematical form for it is the *Slater determinant* [183]:

$$\Psi = \frac{1}{\sqrt{N!}} \begin{vmatrix} \chi_1(\mathbf{r}_1) & \chi_2(\mathbf{r}_1) & \cdots & \chi_N(\mathbf{r}_1) \\ \chi_1(\mathbf{r}_2) & \chi_2(\mathbf{r}_2) & \cdots & \chi_N(\mathbf{r}_2) \\ \vdots & \vdots & \ddots & \vdots \\ \chi_1(\mathbf{r}_N) & \chi_2(\mathbf{r}_N) & \cdots & \chi_N(\mathbf{r}_N) \end{vmatrix} \tag{4.18}$$

In Eq. (4.18), the χ_i are orthonormal spin-orbitals and the $1/\sqrt{N!}$ is a normalization factor. Note that, since the exchange of two rows in a determinant changes its sign, this function satisfies the requirement of being antisymmetric upon exchange of two electrons. If the system under study is a closed-shell system, *i.e.* a system with equal numbers of electrons of either spin, Eq. (4.18) may be rewritten as:

$$\Psi = \frac{1}{\sqrt{N!}} \times \begin{vmatrix} \psi_1(\mathbf{r}_1)\alpha(\sigma_1) & \psi_2(\mathbf{r}_1)\beta(\sigma_1) & \cdots & \psi_N/2(\mathbf{r}_1)\beta(\sigma_1) \\ \psi_1(\mathbf{r}_2)\alpha(\sigma_2) & \psi_2(\mathbf{r}_2)\beta(\sigma_2) & \cdots & \psi_N/2(\mathbf{r}_2)\beta(\sigma_2) \\ \vdots & \vdots & \ddots & \vdots \\ \psi_1(\mathbf{r}_N)\alpha(\sigma_N) & \psi_2(\mathbf{r}_N)\beta(\sigma_N) & \cdots & \psi_N/2(\mathbf{r}_N)\beta(\sigma_N) \end{vmatrix} \tag{4.19}$$

where the ψ_i are orthonormal spatial orbitals and α, β are functions determining the spin of the electron.

In this case, we have a *restricted Hartree–Fock* (RHF) calculation [184]. When the system under study is not a closed-shell system, it is necessary to perform an *unrestricted Hartree–Fock* calculation (UHF), which treats the electrons with different spins differently. Since the main ideas behind the method are the same in both RHF and UHF, we will describe the simplest one (RHF). For a detailed treatment of UHF see, for example, Refs. [4,6].

Using Eq. (4.19), the expectation value of the Hamiltonian can be written as:

$$E[\Psi] = 2\sum_{i=1}^{N} H_{ii} - \sum_{i=1}^{N}\sum_{j=1}^{N}\left(2J_{ij} - K_{ij}\right) \tag{4.20}$$

where the H_{ii} contain the contributions of the kinetic energy and the potential energy of the electron–nuclei interactions:

$$H_{ii} = \int \mathrm{d}\mathbf{r}\psi_i^*\left[-\frac{1}{2}\nabla^2 - \sum_I \frac{Z_I}{r_{iI}}\right]\psi_i \tag{4.21}$$

The index I in Eq. (4.21) runs over all the nuclei in the molecule. The terms J_{ij} in Eq. (4.20) are called the *Coulomb integrals* and represent the potential energy of the interactions of electrons with orbitals ψ_i and ψ_j:

$$J_{ij} = \int\int \mathrm{d}\mathbf{r}_1\mathrm{d}\mathbf{r}_2\psi_i^*(\mathbf{r}_1)\psi_j^*(\mathbf{r}_2)\frac{1}{r_{12}}\psi_i(\mathbf{r}_1)\psi_j(\mathbf{r}_2) \tag{4.22}$$

Finally, the terms K_{ij} in Eq. (4.20) are the *exchange integrals*, which arise from the requirement that the wave function be antisymmetric, and represent the "exclusion principle" contribution to the energy:

$$K_{ij} = \int\int \mathrm{d}\mathbf{r}_1\mathrm{d}\mathbf{r}_2\psi_i^*(\mathbf{r}_1)\psi_j^*(\mathbf{r}_2)\frac{1}{r_{12}}\psi_i(\mathbf{r}_2)\psi_j(\mathbf{r}_1) \tag{4.23}$$

Now that we have an expression for the energy, we can apply the variational principle. The value that minimizes E in Eq. (4.20), subject to the restriction that the orbitals be orthonormal, is the solution to our problem. Applying the method of Lagrange multipliers to the minimization problem we obtain:

$$\left[\hat{H}_n + \sum_{j=1}^{N/2}(2\hat{J}_j - \hat{K}_j)\right]\psi_i = \hat{F}\psi_i = \varepsilon_i\psi_i \tag{4.24}$$

where we defined the *Fock operator* $\hat{F}$. It is defined in terms of the nuclei–electron Hamiltonian $\hat{H}_n$:

$$\hat{H}_n\psi_i(\mathbf{r}_1) = -\frac{1}{2}\nabla^2 - \sum_I \frac{Z_I}{r_{iI}} \tag{4.25}$$

the Coulomb operators $\hat{J}_j$:

$$\hat{J}_j\psi_i(\mathbf{r}_1) = \int \mathrm{d}\mathbf{r}_2\psi_j^*(\mathbf{r}_2)\frac{1}{r_{12}}\psi_j(\mathbf{r}_2)\psi_i(\mathbf{r}_1) \tag{4.26}$$

and the exchange operators $\hat{K}_j$:

$$\hat{K}_j\psi_i(\mathbf{r}_1) = \int \mathrm{d}\mathbf{r}_2\psi_j^*(\mathbf{r}_2)\frac{1}{r_{12}}\psi_i(\mathbf{r}_2)\psi_j(\mathbf{r}_1) \tag{4.27}$$

The ε_i in Eq. (4.24) are the Lagrange multipliers, called the *orbital energies*, and include the kinetic energy and the energy of the nuclei–electron interactions for each orbital. In order to minimize Eq. (4.24) we need to choose a form for the orbitals, *i.e.* expand them in terms of some basis functions as discussed in the "Orbitals and Basis Functions" section. By substituting the expansion (4.13) into Eq. (4.24), multiplying both sides by ϕ_μ and integrating over all space, we obtain the *Roothaan equations* [185,186] (also known as the *secular equations*, or *Roothaan–Hall equations* [187]):

$$\sum_{\nu=1}^{K} C_{\nu i}(F_{\mu\nu} - \varepsilon_i S_{\mu\nu}) = 0 \tag{4.28}$$

where

$$F_{\mu\nu} = \int \mathrm{d}\mathbf{r}\phi_\mu^*\hat{F}\phi_\nu \tag{4.29}$$

are the matrix elements of the Fock operator in the given basis, and

$$S_{\mu\nu} = \int \mathrm{d}\mathbf{r}\phi_\mu^*\phi_\nu \tag{4.30}$$

are the elements of the *overlap matrix*. There is one secular equation for each value of i, μ from 1 to K. For the solution to be non-trivial, the determinant of this system of equations (the *secular determinant*) has to be zero. Solving this determinant equation for each orbital i gives the values of the orbital energies ε_i, and then the secular equations (4.28) can be solved to obtain the coefficients (except for one, which can be given an arbitrary value).

The general procedure for obtaining a HF wave function is hence as follows:

(1) Choose a set of basis functions ϕ_μ and guess initial values for the coefficients $C_{\mu i}$ for each orbital. Calculate the elements $S_{\mu\nu}$ of the overlap matrix.
(2) Calculate the matrix elements of the Fock operator $F_{\mu\nu}$, find the orbital energies ε_i by setting the secular determinants to zero, and solve Eq. (4.28) in order to obtain improved values of the coefficients $C_{\mu i}$.
(3) With the new $C_{\mu i}$, return to step (2). Repeat until convergence is achieved.
(4) Once the $C_{\mu i}$ are known, Eqs. (4.19) and (4.20) can be used to construct the approximate all-electron wave function and the energy.

The most computationally expensive part of the HF procedure is to evaluate the integrals needed to

build the Fock matrix defined by Eq. (4.29). The reason for this can be seen by substituting the definition of the Fock operator into the expression for its matrix element:

$$\begin{aligned}F_{\mu\nu} &= \int d\mathbf{r}\phi_\mu^* \left[-\frac{1}{2}\nabla^2 - \sum_I \frac{Z_I}{r_{iI}}\right]\phi_\nu + \sum_{j=1}^{N/2}\sum_{\lambda=1}^{K}\sum_{\sigma=1}^{K} C_{\lambda j}C_{\sigma j} \\ &\times \left[2\int\int d\mathbf{r}_1 d\mathbf{r}_2 \phi_\mu^*(\mathbf{r}_1)\phi_\nu^*(\mathbf{r}_1)\frac{1}{r_{12}}\phi_\lambda(\mathbf{r}_2)\phi_\sigma(\mathbf{r}_2)\right. \\ &\left. - \int\int d\mathbf{r}_1 d\mathbf{r}_2 \phi_\mu^*(\mathbf{r}_1)\phi_\lambda^*(\mathbf{r}_1)\frac{1}{r_{12}}\phi_\nu(\mathbf{r}_2)\phi_\sigma(\mathbf{r}_2)\right] \\ &= \int d\mathbf{r}\phi_\mu^* \left[-\frac{1}{2}\nabla^2 - \sum_I \frac{Z_I}{r_{iI}}\right]\phi_\nu \\ &+ \sum_{j=1}^{N/2}\sum_{\lambda=1}^{K}\sum_{\sigma=1}^{K} C_{\lambda j}C_{\sigma j}\left[2(\mu\nu|\lambda\sigma) - (\mu\lambda|\nu\sigma)\right] \quad (4.31)\end{aligned}$$

where we have introduced the shorthand notation [188] $(\mu\nu|\lambda\sigma)$ for the two-electron integrals:

$$(\mu\nu|\lambda\sigma) \equiv \int\int d\mathbf{r}_1 d\mathbf{r}_2 \phi_\mu^*(\mathbf{r}_1)\phi_\nu^*(\mathbf{r}_1)\frac{1}{r_{12}}\phi_\lambda(\mathbf{r}_2)\phi_\sigma(\mathbf{r}_2) \quad (4.32)$$

Note that the number of two-electron integrals needed for a basis set containing K functions grows as $O(K^4)$. This is the reason why it is important to use basis functions that can be integrated analytically, as mentioned in "Orbitals and Basis Functions Section".

One important advantage of the HF method is that it provides a basis to interpret the properties of atoms and molecules in terms of simple orbitals. The HF representation is the basis for most of the modern picture of the electronic structure of atoms. The HF method also has a low computational cost, as compared to most other *ab initio* methods, which makes it able to treat larger systems. Actually, in many cases HF is used to obtain a first approximation to the solution (and a basis for the space of many-electron wave functions, as explained in the next section).

The main disadvantage of HF is that the potential energy of the electron–electron interaction is treated as an average, *i.e.* each electron is assumed to interact with the average force field produced by the other electrons. This neglects the contribution from the instantaneous electron–electron potential energy, which does not average to zero. This energy is called the *correlation energy* and it is an important contribution [189]. Many other *ab initio* methods attempt to correct this by using HF to generate a first approximation and then add terms to account for the correlation energy.

As opposed to force-field methods, in the HF method it is possible to systematically improve on the results by using larger basis sets. In the limit of an infinitely large basis set, the *HF limit*, the only error is the correlation energy. After that point, the only possible improvement is to use a different method that is able to estimate the correlation energy.

Starting with the HF method, there are different pathways that lead to different methods, as depicted in Fig. 9. One option is to develop higher-level

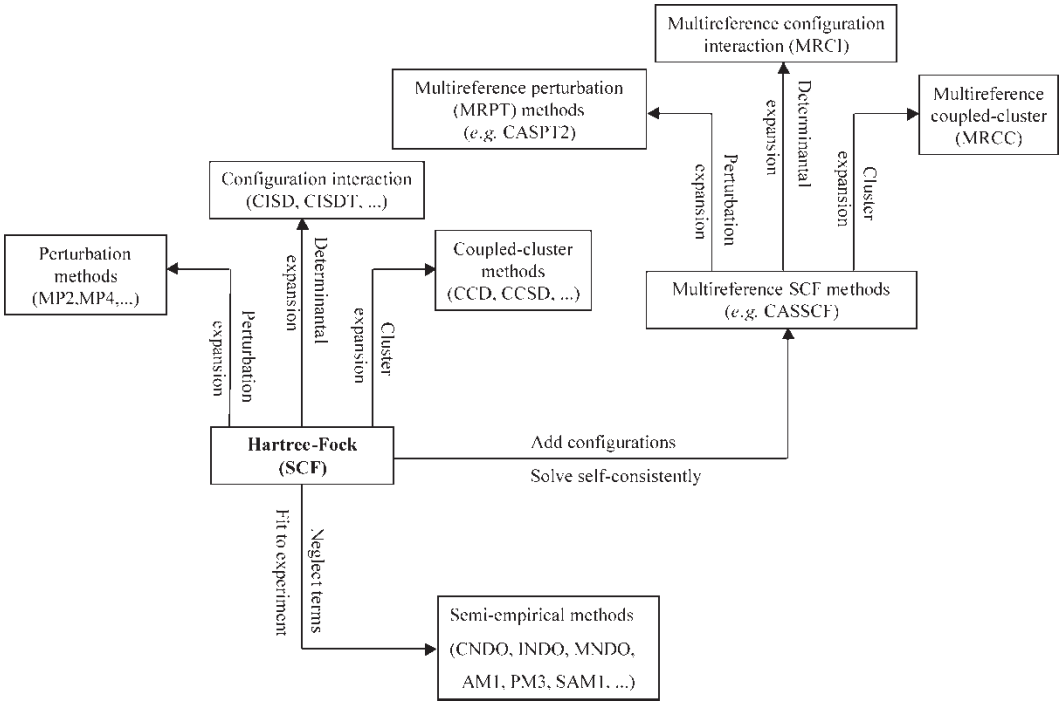

FIGURE 9 Connection between many of the *ab initio* methods. The terms in this schematic are explained in the following sections.

methods to calculate the correlation energy and thus improve the HF results. This gives rise to the families of correlation energy methods discussed in the next three sections. The problem with these approaches, as we will see, is that they increase the computational cost and hence are only applicable to relatively small systems. The other option is to add simplifications to the HF method, and include adjustable parameters that are fitted so that the calculations reproduce experimental data. This gives rise to the family of semi-empirical methods, which have a much lower computational cost and hence can be applied to larger systems. Although these methods are not truly *ab initio* methods, because they rely on experimental data, they also play an important role in the study of chemical reactions and so we will discuss them briefly in the "Semi-empirical Methods" section.

Applications of the HF method, by itself, are nowadays more often in the study of complex systems, such as large molecules, surfaces and solutions. HF calculations are, however, used as a starting point for many other higher-level methods. Some recent studies involving purely HF calculations, showing the kind of systems that can be handled by it with the current computational power, are:

- A study of the charge distribution in spodumene [190], showing the different electron distributions around the non-equivalent oxygen atoms in the mineral's structure. The structural features of spodumene obtained in this work showed a reasonably good agreement with experimental results from X-ray and neutron diffraction studies.
- A conformational analysis of the hormone melatonin [191], which considered all the torsional angles relevant for the description of the conformational PES of the molecule.
- A recent benchmark calculation of the interaction energy of streptavidin and biotin [192], using a system of 1775 atoms. The calculations in this work were made using a new linear-scaling computational method. Several methods that are linear- or almost linear-scaling are currently in development that can make *ab initio* calculations affordable for complex systems in the near future. For examples of these techniques, see Refs. [193,194].

Configuration Interaction and Other Variational Methods

There is an important observation to make about the HF solutions. Since there are K equations in Eq. (4.28), there will be as many spatial orbitals as there are basis functions. If the number of basis functions K were equal to N, *i.e.* half the number of electrons, there would be only one way to build the Slater determinant (4.18) and one set of orbital energies. However, if the basis set is larger (which is usually the case), there are more than N spatial orbitals ψ_i and energies ε_i in the solution. The ground state of the system will be the Slater determinant corresponding to the N lowest-energy eigenvalues. The next higher energy eigenvalues are approximations to the energies of the excited states of the molecule. There is in fact a result, known as *Koopmans' theorem* [195], which relates the energies of the virtual (*i.e.* unoccupied) orbitals to the electron affinities [196]. One may also build additional *excited determinants* by replacing one or more orbitals in the Slater determinant (4.18) with orbitals corresponding to higher energies. Thus one may build singly-excited, doubly-excited, and so on determinants. These determinants are usually not good approximations for the real excited many-electron wave functions of the system, because electronic excitations are often collective effects and neglecting the correlation energy leads to major errors. Excited determinants, however, are important for another reason. Since they are the eigenfunctions of the many-electron Hartree–Fock Hamiltonian, they form a basis for the space of antisymmetric many-electron wave functions. Hence the exact many-electron wave functions may be written as a linear combination of the excited determinants as:

$$\Phi_e = c_0 \Psi_0 + \sum_{a,r} c_a^r \Psi_a^r + \sum_{\substack{a,r \\ b>a \\ s>r}} \sum c_{ab}^{rs} \Psi_{ab}^{rs} + \cdots \quad (4.33)$$

In Eq. (4.33), Ψ_0 is the Hartree–Fock many-electron wave function. The symbol Ψ_a^r indicates a singly excited determinant [184] in which the ath spin orbital has been replaced by the rth excited spin orbital. The symbol Ψ_{ab}^{rs} means that also the bth spin orbital has been replaced by the sth excited spin orbital, and so on. These contributions are depicted in Fig. 10. The second summation is made over $b > a$ and $s > r$ to avoid counting the same doubly excited determinant twice. The expansion (4.33) would be infinite if the basis set were infinite. For the case of a basis set with K functions, there are $\binom{2K}{N}$ excited determinants, and the basis set is not complete. Nevertheless, if all the excited determinants are included in the expansion, the expression (4.33) gives an exact representation of the many-electron wave function within the function space spanned by the chosen orbital basis. The expansion (4.33) is the basis for the *configuration interaction* (CI) methods.

The basic idea of CI is to find the coefficients in the expansion (4.33) by applying the variational principle (4.12) to the all-electron wave function Φ_e. Actually, if the basis set used for the electronic orbitals were infinite, finding all the coefficients

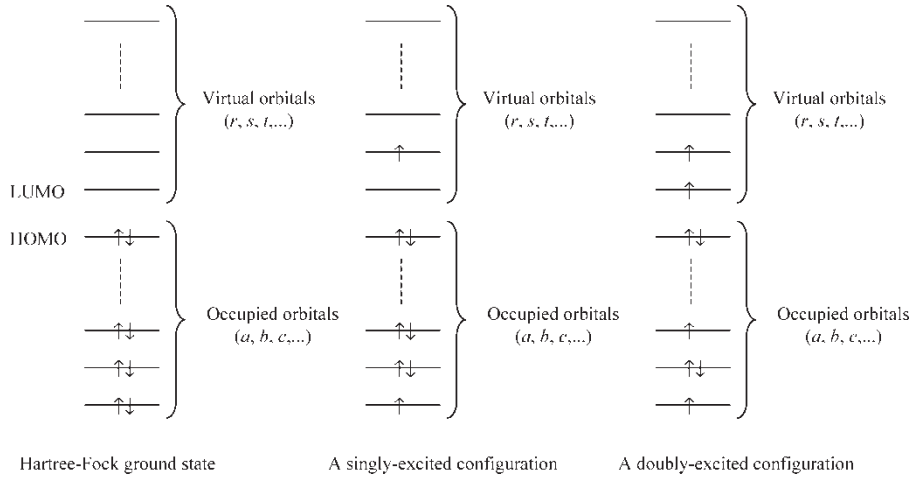

FIGURE 10 Excited configurations. HOMO and LUMO stand for "highest occupied molecular orbital" and "lowest unoccupied molecular orbital".

appearing in Eq. (4.33) would lead to the exact solution to the electronic Schrödinger equation (4.4). Of course, we cannot work with an infinite basis set, so the next step would be using a set with a finite number K of basis functions. If all the terms in the (now finite but large) expansion (4.33) are used, the CI result would be the *exact* solution to the electronic Schrödinger equation within the function space spanned by the chosen basis. This is called a *full CI* calculation. The problem with full CI is that its computational cost grows more than exponentially with the number of electrons, making it impractical for all but the smallest systems. Yet full CI is often used as a reference to benchmark the accuracy of other methods. One of the benchmark requirements usually imposed to modern *ab initio* methods is to be equivalent to full CI when applied to a two-electron system [197,198].

For systems large enough to be impractical for a full CI calculation, it is still possible to do a CI calculation by considering only some of the terms in the expansion (4.33). This gives rise to the CIS (CI with single excitations), CID (CI with double excitations), CISD (CI with single and double excitations), CISDT (CISD plus triple excitations), CISDQ (CISD with quadruple excitations) and CISDTQ (CISD plus triple and quadruple excitations) methods. Very seldom are higher order excitations taken into account because of the computational cost involved.

A CI calculation where the coefficients of the orbitals in Eq. (4.13) are also optimized is an example of a *Multiconfigurational Self-Consistent Field* (MCSCF) method [4]. Besides truncating the full CI expansion, it is possible to select the configurations that make up the all-electron wave function in a different way. One broadly used option is the *Complete Active Space Self-Consistent Field* (CASSCF) method [199]. In this method, the molecular orbitals are divided into inactive orbitals, which are always doubly occupied, and active orbitals. The CASSCF method consists of including all excitations for only the active orbitals, which usually correspond to the valence states [200]. Since the chemistry is determined principally by them, this is usually a very good approximation, and has a much lower computational cost than a full CI calculation, especially for heavy atoms. Another method on the lines of MCSCF is the *Generalized Valence Bond* (GVB) method [201,202], in which two different configurations are used to form the all electron wave function. The GBV method is an extension of the *Valence Bond* (VB) method, originally introduced by Heitler and London to study the hydrogen molecule in 1927 [203,204]. The VB method is an alternative to the molecular orbital description more commonly used in *ab initio* methods. Recent accounts of VB methods including modern VB theory are in Refs. [205–209]. It is also possible to use multireference all-electron wave functions in a determinantal expansion like Eq. (4.13) to obtain a multireference CI (MRCI) method.

An advantage that is common to all variational methods is the very fact that they use the variational principle. Hence, it is easy to compare two different results: the one giving the lowest ground-state energy is the most accurate. On the other hand, many of these methods have what is called the *size-extensivity* problem (exceptions are, for example, full CI and CASSCF if the active space is chosen appropriately). Let us assume that we want to describe the bond between two atoms A and B to form a molecule AB. If we do a CISD calculation to find the energies of both A, B and AB, the results are not consistent. The reason is that a double excitation for A and B atoms would be a quadruple excitation for AB. The result of this is that a CISD calculation for

a system containing an A and a B atom very far from each other would give a different energy than the sum of energies from separate calculations with A and B, which is physically absurd. One way around this problem is to use a perturbation method or a coupled–cluster method; these are described in the next sections.

Unlike the HF method, in the CI methodology there are two different ways to improve on the results: one is to use a larger basis set, and the other is to include more excitations in the CI expansion. Also unlike HF, the CI method can in principle give results arbitrarily close to the exact solution, by letting the basis set and the CI expansion both become large.

Typical applications of CI methods to chemical reactions are usually restricted to simple systems due to their computational cost. Most recent applications employ the more sophisticated methods, like CASSCF and multireference CI. Some recent representative applications of CI and other variational methods are:

- A study of the concerted and stepwise mechanisms of the hetero–Diels–Alder reaction of butadiene with formaldehyde ($C_4H_6 + HCHO \rightarrow C_5H_8O$) and thioformaldehyde ($C_4H_6 + HCHS \rightarrow C_5H_8S$) using the CASSCF method [210]. The Diels–Alder reactions have a notoriously complex reaction mechanism, and have been the subject of many *ab initio* studies.
- A study of the PES for the charge exchange between different cations (H^+, Na^+, C^+ and S^+) and a lithium fluoride surface using several CI approaches and also a coupled–cluster method [211].
- An analysis of the electronic spectrum of the SiSe molecule [212], giving a good agreement with experimentally observed electronic transitions.

Perturbation Methods

Once an approximate solution to the electronic problem (4.4) is known, e.g. from a HF calculation, it is possible to obtain an improved wave function through perturbation theory. In the *Rayleigh–Schrödinger* (RS) approach, we start by assuming that we have a first approximate set of many-electron wave functions $\Psi_i^{(0)}$, which are eigenfunctions of an approximate Hamiltonian $\hat{H}_0$:

$$\hat{H}_0 \Psi_i^{(0)} = E_i^{(0)} \Psi_i^{(0)} \tag{4.34}$$

We can now define a perturbation operator $\hat{V}$ as the difference between the exact electronic Hamiltonian $\hat{H}_e$ and the approximate Hamiltonian $\hat{H}_0$. As is usually done in perturbation theory, we will introduce a perturbation parameter λ, which varies between 0 and 1, and define the functions:

$$\begin{aligned} \Psi_{\lambda,i}(\lambda) &= \Psi_i^{(0)} + \lambda\left(\Phi_i - \Psi_i^{(0)}\right) \\ E_{\lambda,i}(\lambda) &= E_i^{(0)} + \lambda\left(E_i - E_i^{(0)}\right) \end{aligned} \tag{4.35}$$

where Φ_i and E_i are the eigenfunctions and eigenvalues of $\hat{H}_e$. It is clear that these functions give the approximate $\Psi_i^{(0)}$ and $E_i^{(0)}$ for $\lambda = 0$, and approach the exact solutions as $\lambda \rightarrow 1$. If we expand these functions in a Taylor series in λ we get:

$$\Psi_{\lambda,i} = \Psi_i^{(0)} + \lambda \Psi_i^{(1)} + \lambda^2 \Psi_i^{(2)} + O(\lambda^3) \tag{4.36}$$

$$E_{\lambda,i} = E_i^{(0)} + \lambda E_i^{(1)} + \lambda^2 E_i^{(2)} + O(\lambda^3) \tag{4.37}$$

It is possible to take more terms in the series into account; we will just show the procedure for second-order perturbation here. In Eqs. (4.36) and (4.37) we have defined:

$$\Psi_i^{(1)} \equiv \left(\frac{\partial \Psi_{\lambda,i}}{\partial \lambda}\right)_{\lambda=0} \quad \Psi_i^{(2)} = \frac{1}{2}\left(\frac{\partial^2 \Psi_{\lambda,i}}{\partial \lambda^2}\right)_{\lambda=0} \tag{4.38}$$

$$E_i^{(1)} = \left(\frac{\partial E_{\lambda,i}}{\partial \lambda}\right)_{\lambda=0} \quad E_i^{(2)} = \frac{1}{2}\left(\frac{\partial^2 E_{\lambda,i}}{\partial \lambda^2}\right)_{\lambda=0} \tag{4.39}$$

The perturbated Hamiltonian is given by:

$$\hat{H}_e = \hat{H}_0 + \lambda \hat{V} \tag{4.40}$$

This Hamiltonian approaches the exact Hamiltonian as $\lambda \rightarrow 1$. Substituting Eqs. (4.36), (4.37) and (4.40) into the electronic Schrödinger equation (4.4) we get:

$$\begin{aligned} &(\hat{H}_0 + \lambda \hat{V})\left[\Psi_i^{(0)} + \lambda \Psi_i^{(1)} + \lambda^2 \Psi_i^{(2)} + O(\lambda^3)\right] \\ &\quad = \left[E_i^{(0)} + \lambda E_i^{(1)} + \lambda^2 E_i^{(2)} + O(\lambda^3)\right] \\ &\qquad \times \left[\Psi_i^{(0)} + \lambda \Psi_i^{(1)} + \lambda^2 \Psi_i^{(2)} + O(\lambda^3)\right] \end{aligned} \tag{4.41}$$

which can be rewritten as:

$$\begin{aligned} &\left(\hat{H}_0 - E_i^{(0)}\right)\Psi_i^{(0)} + \lambda\left[\hat{H}_0 \Psi_i^{(1)} + \hat{V}\Psi_i^{(0)} - E_i^{(0)}\Psi_i^{(1)} - E_i^{(1)}\Psi_i^{(0)}\right] \\ &+ \lambda^2\left[\hat{H}_0 \Psi_i^{(2)} + \hat{V}\Psi_i^{(1)} - E_i^{(0)}\Psi_i^{(2)} - E_i^{(1)}\Psi_i^{(1)} - E_i^{(2)}\Psi_i^{(0)}\right] \\ &+ O(\lambda^3) = 0 \end{aligned} \tag{4.42}$$

Now, equating like powers of λ on both sides we get:

$$\left(\hat{H}_0 - E_i^{(0)}\right)\Psi_i^{(0)} = 0 \tag{4.43}$$

$$\hat{H}_0 \Psi_i^{(1)} + \hat{V}\Psi_i^{(0)} - E_i^{(0)}\Psi_i^{(1)} - E_i^{(1)}\Psi_i^{(0)} = 0 \tag{4.44}$$

$$\hat{H}_0 \Psi_i^{(2)} + \hat{V}\Psi_i^{(1)} - E_i^{(0)}\Psi_i^{(2)} - E_i^{(1)}\Psi_i^{(1)} - E_i^{(2)}\Psi_i^{(0)} = 0 \tag{4.45}$$

Equation (4.43) tells us something we already knew: that $\Psi_i^{(0)}$ and $E_i^{(0)}$ are the eigenfunctions and

eigenvalues of $\hat{H}_0$. Equation (4.44) gives the first-order corrections and Eq. (4.45) gives the second-order corrections. If more terms are used in expansions (4.36) and (4.37), higher order corrections can be obtained. In order to solve Eq. (4.44), we express the first-order perturbation function $\Psi_i^{(1)}$ as a combination of the $\Psi_i^{(0)}$ orthonormal functions:

$$\Psi_i^{(1)} = \sum_k C_{ik} \Psi_k^{(0)} \tag{4.46}$$

For example, if $\hat{H}_0$ is taken to be the many-electron Hartree–Fock Hamiltonian, this expansion would be equivalent to the expansion (4.33). Substitution of Eq. (4.46) into Eq. (4.44) yields:

$$\left(\hat{H}_0 - E_i^{(0)}\right)\sum_k C_{ik} \Psi_k^{(0)} = -\left(\hat{V} - E_i^{(1)}\right)\Psi_i^{(0)} \tag{4.47}$$

Taking the inner product on both sides with $\Psi_j^{(0)}$ and using Eq. (4.43) and the orthonormality conditions (4.8) we get:

$$\left(E_j^{(0)} - E_i^{(0)}\right)C_{ij} = E_i^{(1)}\delta_{ij} - \int \mathrm{d}\mathbf{r}\, \Psi_j^{(0)*}\hat{V}\Psi_i^{(0)} \tag{4.48}$$

This set of equations allows us to obtain the coefficients in the expansion (4.46) and the energies $E_i^{(1)}$. A similar procedure can be used to obtain the second-order corrections, starting with Eq. (4.45).

What we have described above is the general RS perturbation theory. A more detailed treatment of it can be found, for example, in Ref. [6]. Evidently the details of the solution will depend on the choice of the approximate Hamiltonian $\hat{H}_0$. By far the most common choice is to use the Hartree–Fock Hamiltonian as the reference; in this case we obtain the Møller–Plesset (MP) perturbation theory [213–219]. Usually the MP methods are referred to as MP*N*, where *N* is the order of the corrections used. There is really no such thing as MP1, because the first correction to the Hartree–Fock energies actually arises from the second-order term [6]. The most common implementations are MP2 [216–218] and MP4 [219], but other levels of approximation are available.

It is possible to develop a perturbation theory using different references. In the *complete active space perturbation theory* (CASPT) method [220], for example, the reference is obtained from a CASSCF calculation. CASPT is an example of a *multi-reference perturbation method*, where a MCSCF method is used for the zeroth order approximation.

A major advantage of perturbation approaches is that they do not suffer from size-extensivity problems. They can also handle excited states more easily than most variational methods. Nevertheless, the fact that they are not variational means that one cannot directly assess the relative quality of two different perturbation results. Since different-order perturbations correspond effectively to different Hamiltonians, one cannot invoke the variational principle and say that the lowest ground-state energy is the most accurate one. As is the case with the lower-level CI methods, the simpler perturbation approaches are being displaced by DFT for some applications.

As for the CI methods, perturbation results can be systematically improved in two different ways: by using larger basis sets or by including higher-order corrections. In principle, in the limit of an infinitely large basis set and an infinite expansion, the result should be correct. This, however, is true only if the perturbation expansion converges: if the reference state is too far removed from the actual state, the perturbation may diverge. Unlike CI, in perturbation theory the number of terms in the expansion and the number of basis functions are truly independent.

Some recent applications where perturbation methods are applied, showing typical systems that can be studied with them, are:

- A study of the reaction mechanism of the gas-phase hydrolysis of silicon tetrachloride [221] using MP2, MP4 and DFT methods. In this study, good agreement with experimental reaction rates was obtained at high temperatures, but not for low temperatures.
- A study of the PES for the tautomeric and conformational rearrangements of 2-nitrosophenol and 9,10-phenanthrenequinonemonooxime, using both the MP2 and MP4 methods [222]. The results obtained for both compounds were found to be in good agreement with experimental measurements, including NMR spectroscopy results obtained in the same work.
- A study of the reaction mechanism of the diazetization reactions of several azoalkanes, including one-, two- and three-bond mechanisms [223]. In this work, the CASPT2 method was used to calculate the energetics for this reaction, in conjunction with geometry optimizations using DFT and CASSCF. Figure 11 shows one of the mechanisms obtained.

Coupled–cluster Methods

It is possible to show that the correlation energy in a many-electron system can be obtained from the result of a full CI calculation as [6]:

$$E_c = \sum_{b>a}\sum_{s>r} c_{ab}^{rs} \int \mathrm{d}\mathbf{r}\Psi_0 \hat{H}\Psi_{ab}^{rs} \tag{4.49}$$

where we have used the notation of Eq. (4.33). The integral runs over all the electronic coordinates,

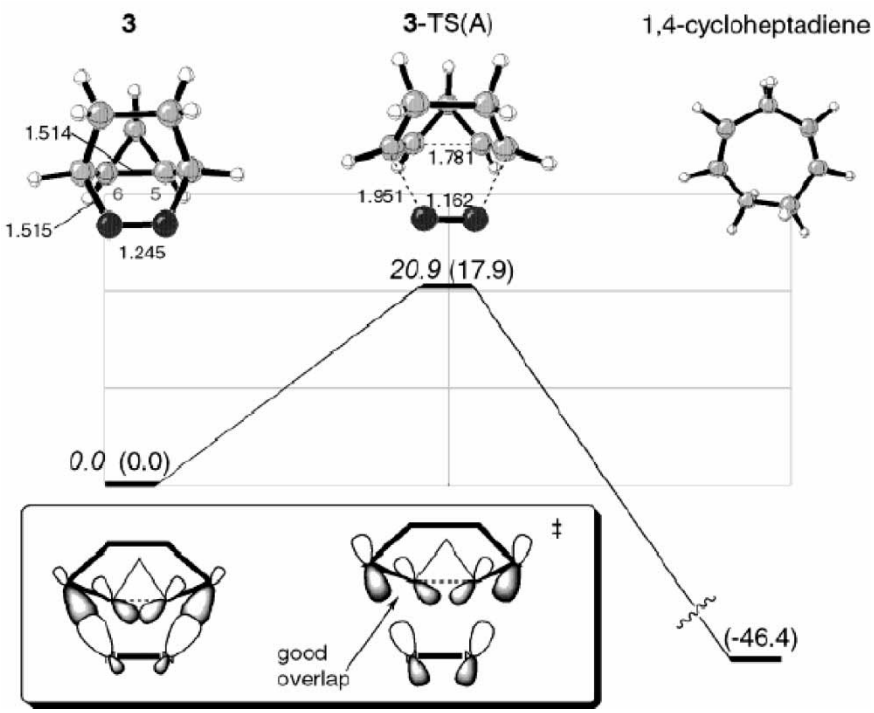

FIGURE 11 Geometries and energies of the reactant, products and transition state for the 1-step diazetization of $C_7H_{10}N_2$. The energies shown were obtained using the CASPT2 method, values in parentheses are from density functional theory calculations. From Ref. [223] (© American Chemical Society, 2003).

and the summations are over pairs of electrons. Equation (4.49) can be interpreted in the following way: if we regard the inner summation as a contribution from the pair of electrons *a* and *b*, then the total correlation energy is just the sum of the contributions from all pairs. Hence a possibility to approximate the correlation energy is to obtain the contribution of each pair independently of the other electrons, and then add the contributions. This is known as the *independent electron pair approximation* (IEPA), originally introduced by Sinanoğlu [224] and Nesbet [225]. In an IEPA calculation, the contribution from each pair of electrons *a* and *b* is obtained separately by applying the variational principle to the *pair function* [226]:

$$\Psi_{ab} = \Psi_0 + \sum_{s>r} c_{ab}^{rs} \Psi_{ab}^{rs} \tag{4.50}$$

which includes the contributions from all the excited determinants in which electrons *a* and *b* have been promoted to excited orbitals. By doing this variational minimization with each pair of electrons, one finds a set of pair energies, and the sum of these pair energies is an approximation to the correlation energy of the system. One important thing to note is that, although the variational principle is used in each of the pair calculations, the method is not truly variational because different contributions to the Hamiltonian are neglected in each of the calculations. The method, however, does not have the size extensivity problem of many variational methods like CISD.

There is a problem with the IEPA, besides the fact that it is not variational. Methods such as HF, CI and perturbation theory yield the same correlation energy when a unitary transformation [227] is applied to the occupied spin orbitals. The IEPA method, however, does not satisfy this condition. There is a way to extend the IEPA in such a way that it is invariant under unitary transformations, however, and that also increases its accuracy significantly. This can be done by including the coupling between different electron pairs in the calculation. A way to do this, of course, would be to perform a CI calculation including the coupling between pairs, quadruples, sextuples [228], etc., but the computational cost would be prohibitive. But applying the idea from the IEPA, one may assume that the coefficients c_{abcd}^{rstu} for the quadruple excitations are not really independent from the coefficients c_{ab}^{rs} (because treating the pairs as independent is not a bad approximation). This is the idea behind the *Coupled–Cluster* (CC) approximation, introduced by Čižek and Paldus [229–231]. In a CC approximation including the double excitations (CCD), the quadruple excitation coefficients would be expressed as combinations of products of the double excitation

coefficients:

$$c^{rstu}_{abcd} = \sum_{perm} (-1)^{nperm} c^{mn}_{ij} c^{op}_{kl} \tag{4.51}$$

The summation (4.51) contains all possible permutations of the indices a, b, c, and d (represented by the letters i, j, k and l in the summation) and r, s, t, u (represented by m, n, o and p). If the total number of permutations is even, the coefficient is 1, and if it is odd, it is -1. For example, the coefficient of $c^{rs}_{ac} c^{tu}_{bd}$ would be -1 and the coefficient of $c^{ru}_{ad} c^{st}_{bc}$ would be 1. There are 18 permutations in total. This relation can be used to obtain a better approximation to the many-electron wave function than the one obtained using the IEPA. The resulting CC method has the advantages of being both size extensive and invariant under unitary transformations. It is however, not variational, as is the IEPA. The original formulation of the CC method by Čižek and Paldus was CCD [231]. The CC method was extended to include single and double excitations (CCSD) by Purvis and Bartlett [232] and later expanded to include higher excitations and spin-adapted wave functions. More detailed description of CC approaches and reviews can be found in Refs. [4,233–236]. As with perturbation methods, it is possible to construct multi-reference CC methods using results from MCSCF methods as a starting point [237–240].

General CC theories can be formulated by introducing a *cluster operator* $\mathbf{T}$ [241]:

$$\mathbf{T} = \mathbf{T}_1 + \mathbf{T}_2 + \cdots + \mathbf{T}_N \tag{4.52}$$

where the operator $\mathbf{T}_i$ has the effect of generating all the ith excited determinants when acting on the reference many-electron wave function, e.g.

$$\mathbf{T}_1 \boldsymbol{\Psi}_0 = \sum_{a,r} c^r_a \boldsymbol{\Psi}^r_a \tag{4.53}$$

In the CC literature, the coefficients $c^r_a, c^{rs}_{ab}, \ldots$ are referred to as amplitudes, and usually written using the letter t instead of c. The coupled–cluster many-electron wave function is then written in terms of the cluster operator as:

$$\boldsymbol{\Phi}_{\mathrm{e,cc}} = e^{\mathbf{T}} \boldsymbol{\Psi}_0 = \left(\mathbf{I} + \mathbf{T} + \frac{1}{2}\mathbf{T}^2 + \cdots \right) \boldsymbol{\Psi}_0 \tag{4.54}$$

This expansion can be substituted into the electronic Schrödinger equation (4.4) to obtain expressions for the coefficients $c^r_a, c^{rs}_{ab}, \ldots$. Combining Eqs. (4.52) and (4.54) it is possible to see an analogy between CC and CI:

$$\boldsymbol{\Phi}_{\mathrm{e,cc}} = e^{\mathbf{T}} \boldsymbol{\Phi}_0 = \boldsymbol{\Phi}_0 + \mathbf{T}_1 \boldsymbol{\Phi}_0 + \left(\mathbf{T}_2 + \frac{1}{2}\mathbf{T}_1^2 \right) \boldsymbol{\Phi}_0 + \left(\mathbf{T}_3 + \mathbf{T}_2 \mathbf{T}_1 + \frac{1}{6}\mathbf{T}_1^3 \right) \boldsymbol{\Phi}_0 + \cdots \tag{4.55}$$

In truncated CC, only some terms of the cluster operator $\mathbf{T}$ are kept, for example in CCSD the expansion would be $\mathbf{T} = \mathbf{T}_1 + \mathbf{T}_2$. The first two terms in the expansion (4.55) are analogous to the first two terms in the CI expansion (4.33), *i.e.* the HF reference and the singly excited determinants. In the second term there is already a difference. There are two terms in the double excited part: one equal to the equivalent CI term, and another counting the "disconnected" double excitations. These additional terms make the CC method size extensive even when the cluster operator is truncated, unlike what happens in CI. Just as perturbation theory includes the contributions from all the excited-determinant corrections (single, double, etc.) up to a given order, CC includes corrections up to a given point but to infinite order [233].

It is possible to combine perturbation and CC methods to obtain accurate results with a lower computational cost [242]. An example of this is the CCSD(T) method, where the triples contribution to the energy is estimated using perturbation theory and added to the CCSD energy.

CC methods can estimate the correlation energy very accurately, and are frequently used to study chemical reactions. The lower-level methods CCD and CCSD have a cost proportional to N^6, and the more accurate CCSDT a cost of N^8, which precludes the use of the latter for any but very simple systems. CC theories are similar to CI and perturbation methods in the sense that the results can be improved both by adding more basis functions and by including more terms in the cluster expansion. In the limit of an infinite basis set with a complete (infinite) cluster expansion, the results should be exact.

Some recent representative applications involving the CC methodology are:

- A calculation of the structure, vibrational frequencies, atomization energies and standard heats of formation of hydroxylamine, ammonia, hydrogen peroxide and hyponitrous acid [243] using CCSD(T) and higher level methods. Both the structural, vibrational and energy results were found to be in good agreement with available experimental results.
- A study of the energetics, geometry and vibrational frequencies of the nitric oxide dimer using single- and multireference CC methods [244]. The NO dimer is a notoriously difficult molecule to study due to its very weak bonding.
- A study of the PES for the isomerization of the silicon hydrides Si_2H_3 and Si_2H_4 using the CCSD(T) method [245]. A total of 10 different isomers were found in this work. For these isomers, they obtained harmonic vibrational frequencies, dipole moments and infrared

intensities. In the same work, spectroscopic measurements were made and they compared very well with the *ab initio* results.

Semi-empirical Methods

An alternative approach to the electronic problem is provided by the semi-empirical methods. In these, the many-electron problem is simplified in some way, and then some parameters obtained from experiment or higher quality *ab initio* calculations are included in order to get good results. Semi-empirical methods are particularly useful for dealing with large systems (e.g. large biomolecules) where more computationally demanding methods are impossible to apply. Semi-empirical methods are not truly *ab initio* methods, because they make use of experimental information to obtain their results. Nevertheless, they play an important role in the simulation of chemical reactions, especially in complex systems.

Most semi-empirical methods can be obtained by introducing approximations into the Roothaan equations (4.28). There are several different levels of approximation that can be used to develop a semi-empirical method. As we mentioned in our discussion of the HF method, the largest computational cost comes from the evaluation of the two electron integrals appearing in Eq. (4.31):

$$(\mu\nu|\lambda\sigma) = \int\int d\mathbf{r}_1 d\mathbf{r}_2 \phi_\mu^*(\mathbf{r}_1)\phi_\nu^*(\mathbf{r}_1) \times \frac{1}{r_{12}} \phi_\lambda(\mathbf{r}_2)\phi_\sigma(\mathbf{r}_2) \tag{4.56}$$

These integrals are necessary to construct the Fock operator matrix **F**. For a basis set with K functions, there are $\sim K^4/8$ distinct two-electron integrals. For a system with many electrons (e.g. a biomolecule) the cost of calculating them can be prohibitive. A way around this problem is the *zero differential overlap* (ZDO) approximation. Within this approximation, it is assumed that the overlap between different orbitals is always zero, *i.e.*

$$\int d\mathbf{r} \phi_\mu^* \phi_\nu = 0 \quad \text{for} \quad \mu \neq \nu \tag{4.57}$$

where the integral is over *any* region of space. This is a stronger assumption than just saying that $S_{\mu v} = 0$ for $\mu \neq v$, and a direct consequence of it is that the two electron integrals defined by Eq. (4.56) are zero unless $\mu = v$ and $\lambda = \sigma$. This reduces the number of distinct integrals to calculate to $\sim K^2/2$, much less than in the HF method. There is, however, one major problem with the ZDO approximation. If all orbitals are assumed to have zero overlap over all space, two things happen: (1) The results may be dependent on the coordinate system used, because the overlap is in general not invariant to coordinate transformations, and (2) If the overlap between all pairs of orbitals in neighboring atoms is neglected, there can be no bonding.

There are several ways around the problems of the ZDO approximation. One option is used in the *complete neglect of differential overlap* (CNDO) method [246,247]. In CNDO, the two-electron integrals $(\mu\mu|\lambda\lambda)$ are assumed to be independent of the shape of the orbitals ϕ_μ and ϕ_λ. This removes the coordinate invariance problem. If the orbitals are centered on the same atom, the corresponding integrals are assigned a value representing the average electron–electron repulsion on that atom. If they are centered on different atoms, the integrals are assigned a value representative of the average electron–electron repulsion between an electron in one atom and an electron in the other atom. Note that the latter value is also dependent on the distance between the atoms. Two further assumptions are made in CNDO regarding the part of the Fock matrix that depends on the nuclei–electron interactions, which is given by:

$$H_{\mu v} = \int d\mathbf{r} \phi_\mu^* \left[-\frac{1}{2}\nabla^2 - \sum_I \frac{Z_I}{r_{iI}} \right] \phi_v \tag{4.58}$$

When ϕ_μ and ϕ_ν are on the same atom, these terms are assumed to be zero for $\mu \neq v$. For $\mu = \nu$, they are approximated using experimental ionization energies and electron affinities for the atom. Finally, when they are on different atoms, $H_{\mu\nu}$ is assumed to be proportional to the overlap integral $S_{\mu\nu}$, and the proportionality constants are parameterized in terms of empirical single-atom constants.

One defect of the CNDO method is that, since two-electron integrals are assigned the same value regardless of spin, it does not consider the "exclusion principle" energy contribution. In the *intermediate neglect of differential overlap* (INDO) method [248], these contributions are included in the form of additional contributions to the two-electron integrals that depend on the spin of the orbitals involved. This necessarily means that the differential overlap between orbitals on the same atom is not neglected anymore. In INDO, some of the two-electron integrals on the same atom are parameterized using spectroscopic data for the atom.

Aside from the CNDO and INDO methods, there are other, more sophisticated semi-empirical methods. In the *neglect of diatomic differential overlap* (NDDO) method [249], only the differential overlap between orbitals on different atoms is neglected. This means that now all the two-electron integrals $(\mu\nu|\lambda\sigma)$ when ϕ_μ, ϕ_λ are on the same atom and ϕ_λ ϕ_σ are also on the same atom have to be calculated. This causes

a major increase in the computational cost for NDDO as compared to CNDO or INDO.

Other semi-empirical methods which make more use of experimental information and are more accurate than the first-generation methods discussed above are the modified INDO (MINDO) method [250–253], the modified neglect of diatomic overlap (MNDO) method [254,255], the Austin Model 1 (AM1, a second-generation MNDO) method [256], the Parameterized Model 3 (PM3, a third-generation MNDO) method [257,258], and the Semi *Ab initio* Model 1 (SAM1) method [259], among others.

It is not easy, in general, to assess the relative accuracy of all the available semi-empirical methods, mainly because their accuracy depends on what system they are applied to. Some comparisons of the strengths and weaknesses of various empirical methods as applied to various systems can be found in Refs. [4,260–263].

As it is the case with force-field methods, there is no way to systematically improve on the results obtained with a semi-empirical method. Also similarly, their performance is limited to compounds for which experimental data is available; unlike *ab initio* methods, it is not generally good to use a semi-empirical method to predict the properties of a new or unknown compound. Most applications of semi-empirical methods involve the study of very large molecules, or molecules in complex environments. Some recent representative applications of semi-empirical methods include:

- A calculation of the permanent dipole of the enzyme α-chymotrypsin using the AM1, PM3 and PM5 methods [264]. The results from the PM5 method were the closest to the experimental values for this particular system.
- A study of the reaction path for the reduction of nitric oxide in the enzyme nitric oxide reductase from the fungus *Fusarium oxysporum* using the SAM1 method [265]. The reaction path obtained for this process consisted of a cycle of seven reaction steps, and was similar to a mechanism proposed based on previous experimental results.
- A study of the fluorination [266] and the hydrogenation and oxidation [267] of carbon nanotubes using the MNDO method. In these works the potential energy curve for the adsorption of fluorine, hydrogen and oxygen was obtained for different kinds of nanotubes.

Density Functional Theory [2–8,268–272]

As shown in the previous sections, an accurate estimation of the electronic energies for a given atom or molecule is in general a very computationally expensive task. The relatively simple approach of the HF method suffers from the correlation energy error, and improving on HF results is often very computationally demanding. Density functional theory (DFT) is an alternative approach that permits one to obtain reasonably accurate results for complex systems.

The main difference between DFT and the methods mentioned in the previous sections is that the fundamental variable is not the wave function but the electronic density $\rho(\mathbf{r})$ defined by:

$$\rho(\mathbf{r}_i) = N \int \cdots \int |\Phi_e|^2 d\mathbf{r}_1 d\mathbf{r}_2 \cdots d\mathbf{r}_{i-1} d\sigma_i d\mathbf{r}_{i+1} \cdots d\mathbf{r}_N \tag{4.59}$$

In Eq. (4.59), N is the number of electrons and σ_i is the spin coordinate of electron i. The results that make DFT possible are two theorems proved by Hohenberg and Kohn in 1964 [273,274], and later generalized by several authors. The first theorem states that, if one knows the electronic density $\rho(\mathbf{r})$ for a given system, then all the properties of the ground state can be obtained. The second theorem is a variational principle for the electronic density. It states that, for *any* electronic density ρ, which may or may not be the true density for the ground state, the relation $E[\rho] \geq E_0$ is satisfied, where E_0 is the energy of the ground state. This is analogous to the variational principle for the wave function mentioned in "The Variational Principle Section", and it also leads to a method for estimating E_0.

The energy functional $E[\rho]$ in DFT can be expressed as:

$$E[\rho] = T[\rho] + V_{en}[\rho] + V_{ee}[\rho] \tag{4.60}$$

where $T[\rho]$ accounts for the kinetic energy, $V_{en}[\rho]$ for the potential energy of the electron–nucleus interaction, and $V_{ee}[\rho]$ for the potential energy of the electron–electron interaction. The latter is further decomposed into:

$$V_{ee}[\rho] = V_{coul}[\rho] + V_{xc}[\rho] \tag{4.61}$$

where $V_{coul}[\rho]$ is the potential energy of the Coulomb interaction and $V_{xc}[\rho]$ is called the *exchange-correlation* potential energy. Comparing Eqs. (4.60) and (4.61) with Eqs. (4.24)–(4.27) shows an analogy between HF and DFT, and also the main difference: the correlation energy is included in the term $V_{xc}[\rho]$ together with the exchange potential, whereas in HF only the exchange part is accounted for. Also, the exchange energy in HF is calculated exactly, whereas in DFT it is normally approximated in some way.

If the form of the energy functional $E[\rho]$ is known, the problem of finding the ground-state electronic density and its energy is reduced to a minimization problem through use of the variational principle $E[\rho] \geq E_0$. It is possible to simplify the problem further. Since the electronic density determines

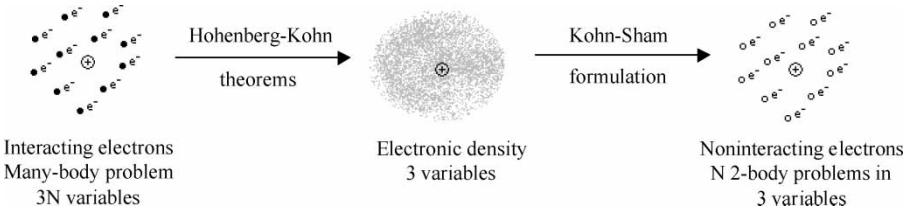

FIGURE 12 The Kohn–Sham approach.

the ground state, any system with the same electronic density as the real system will have the same ground-state properties. One may then think of a set of non-interacting electrons that give the same electronic density as the real system. In this case, the exchange-correlation energy in terms of the wave functions of these non-interacting electrons has to contain all the missing terms. In particular, it will also contain a correction to the kinetic energy. This approach, known as the *Kohn-Sham method* [275,276], is sketched in Fig. 12. Within this framework, one may write the electronic density as a sum over occupied orbitals:

$$\rho(\mathbf{r}) = \sum_{i=1}^{N_{\text{orb}}} |\psi_i(\mathbf{r})|^2 \tag{4.62}$$

and the expressions for $T[\rho]$, $V_{\text{en}}[\rho]$ and $V_{\text{coul}}[\rho]$ can be written as:

$$T(\rho) = 2\sum_{i=1}^{N_{\text{orb}}} \int \mathrm{d}\mathbf{r}\psi_i^* \left(-\frac{1}{2}\nabla^2\psi_i\right) \tag{4.63}$$

$$\begin{aligned} V_{\text{en}}[\rho] &= \sum_{i=1}^{N_{\text{orb}}} \int \mathrm{d}\mathbf{r}\psi_i^* \left(-\sum_I \frac{Z_I}{r_{iI}}\right)\psi_i \\ &= -\sum_I \int \mathrm{d}\mathbf{r}\rho(\mathbf{r})\frac{Z_I}{|\mathbf{r}-\mathbf{r}_I|} \end{aligned} \tag{4.64}$$

$$\begin{aligned} V_{\text{coul}}[\rho] &= \sum_{i=1}^{N_{\text{orb}}}\sum_{j>1}^{N_{\text{orb}}} \int\int \mathrm{d}\mathbf{r}_1\mathrm{d}\mathbf{r}_2\psi_i^*(\mathbf{r}_1)\psi_j^*(\mathbf{r}_2) \\ &\quad \times \frac{1}{r_{12}}\psi_i(\mathbf{r}_1)\psi_j(\mathbf{r}_2) \\ &= \frac{1}{2}\int\int \mathrm{d}\mathbf{r}_1\mathrm{d}\mathbf{r}_2\frac{\rho(\mathbf{r}_1)\rho(\mathbf{r}_2)}{r_{12}} \end{aligned} \tag{4.65}$$

For the exchange-correlation potential $V_{\text{xc}}[\rho]$, however, an additional theory is necessary. The simplest assumption is the *local density approximation* (LDA), which states that the exchange-correlation energy is locally that of a uniform electron gas; *i.e.* the exchange correlation energy density at a position $\mathbf{r}$ is the same as that of a uniform electron gas of density ρ, where ρ equals the local electron density at $\mathbf{r}$ in the actual system. If the exchange correlation energy $E_{\text{xc}}(\rho)$ for a uniform electron gas is known as a function of the density, ρ, then $V_{\text{xc}}[\rho]$ can be obtained from:

$$V_{\text{xc}}[\rho] = \int \mathrm{d}\mathbf{r}\rho(\mathbf{r})E_{\text{xc}}[\rho(\mathbf{r})] \tag{4.66}$$

In formulations of DFTs for open-shell systems, or systems with spin polarization, the electronic density is treated differently for spin-up and spin-down electrons. In this case one speaks of the *local spin density* (LSD) approximation, instead of the LDA.

There are more elaborate expressions for the exchange-correlation energy that give better results than the LDA. One of the most common approaches is to also include a dependence of the exchange-correlation energy on the gradient of the electronic density. This leads to the *generalized gradient approximation* (GGA) [277–282]. Among the most commonly used functionals of this kind are the Becke–Perdew (BP) functional [278,283], the Perdew–Wang 1991 [281,284–286] (PW91) functional, the Becke–Lee–Yang–Parr (BLYP) functional [278,287], and the Perdew–Burke–Ernzerhof (PBE) functional [279]. Some new GGA functionals that seem to perform very well [288–290] are the OLYP functional, a combination of the OPTX exchange functional of Handy and Cohen [291–293] and the Lee–Yang and Parr correlation functional, and the Hamprecht–Cohen–Tozer–Handy (HCTH) functionals [294–296]. Other exchange-correlation functionals in common use include a contribution from *exact exchange*, i.e. exchange energy calculated as in HF theory. A functional of this kind, which is very commonly used, is the three-parameter Becke–Lee–Yang–Parr (B3LYP) functional [297]. The main drawback of these functionals is that the calculation of the exact exchange energy is very computationally demanding, thus restricting somewhat the system sizes that can be handled.

Once the exchange-correlation functional is defined, a DFT calculation proceeds by solving the one-electron *Kohn-Sham* equations [275,276]:

$$\hat{E}_{\text{KS}}\psi_i = \varepsilon_i\psi_i \tag{4.67}$$

where $\hat{E}_{KS}$ is the one-electron *Kohn-Sham operator*:

$$\hat{E}_{KS} = -\frac{\nabla^2}{2} - \sum_m \frac{Z_m}{|\mathbf{r} - \mathbf{r}_m|} + \int d\mathbf{r}' \frac{\rho(\mathbf{r}')}{|\mathbf{r} - \mathbf{r}'|} + \frac{\delta V_{xc}}{\delta \rho} \qquad (4.68)$$

In Eq. (4.68), δ denotes functional differentiation. Once this system of equations is set up the rest of the procedure is very similar to a HF calculation, and actually less computationally demanding. Expanding now the ψ_i in terms of some basis functions as in Eq. (4.13) one can write a system of equations for the coefficients $C_{\mu i}$ and obtain the electronic density and the orbital energies.

The fact that DFT allows the calculation of energies with a much lower computational cost than other *ab initio* approaches makes this method one of the most popular. DFT allows studies of much larger and more complex systems than most other methods, and with the newer functionals its accuracy can be comparable to that of much more expensive methods.

One drawback of DFT is the fact that it is a method designed to obtain only ground-state properties. There are, however, extensions of DFT that allow the treatment of excited states, such as the *restricted open shell Kohn-Sham* (ROKS) method [298,299], which uses a mixture of symmetry-adapted Kohn-Sham all-electron wave functions, the *density functional theory/single configuration interaction* (DFT/SCI) method [300,301], which mixes the ideas of the CI method and DFT, and the *time-dependent density functional theory* (TDDFT) method [302–304], which so far seems the most promising extension of DFT to excited states. Another problem of DFT is, of course, that its accuracy is only as good as the exchange-correlation functional used. The Hohenberg–Kohn theorem guarantees that the DFT treatment is exact, unlike semiempirical approaches, because there exists an exchange-correlation functional that makes its results exact. But this functional is not known and we are forced to approximate it in some way. Other than employing a larger basis set, as with HF, there is no evident way to systematically improve on the results: one may try two different exchange-correlation functionals for the same system and there is in principle no way to tell which result is better unless results from a higher-level *ab initio* calculation are available, and this is usually not the case. Nevertheless, DFT has an excellent accuracy/computational cost ratio, and this makes it an extremely useful tool in quantum chemistry. A detailed treatment of DFT can be found in Refs. [2–4,268–271].

There are numerous applications of DFT in the literature, and their number is likely to increase as better exchange-correlation functionals are developed. DFT is used often to study large molecules, surface chemistry and properties of solids. Another common application is to do geometry optimizations that are later followed by energy calculations using more accurate methods. Some recent representative applications include:

- A study of the reaction mechanism of the cycloaddition of 1,5-cyclooctadiene with alkynes over a ruthenium catalyst, using the B3LYP functional [305]. In this work, several possible mechanisms for this complex reaction were considered, something made possible by the relatively low computational cost of DFT.
- An analysis of the stability of carbon dioxide hydrates with 20, 24 and 28 water molecules using DFT with the B3LYP functional [306]. In this study, it was found that the tetrakaidecahedral cluster with 24 molecules was the most stable of the ones considered, and good agreement with experimental results was obtained.
- A study of the vanadyl pyrophosphate (100) surface and its ability to oxidize *n*-butane to maleic anhydride using the PW91 functional [307]. In this work, the chemisorption of water onto the surface and its role on the selective oxidation of *n*-butane was analyzed.

Ab Initio Molecular Dynamics [3,10,179,308–311]

In order to simulate chemically reactive systems, one often needs to do first an *ab initio* calculation in order to find the PES. The results of this *ab initio* calculation can then be fitted to an empirical equation for the potential energy and this in turn can be used in a simulation within one of the techniques discussed in the following sections. It is also possible, in principle, to omit the fitting stage and do the *ab initio* calculations "on-the-fly" to obtain the potential energies within the simulation. There are several ways that this can be done. One may, for example, run a Molecular Dynamics (MD) simulation in which the energies at each time step are found by minimizing the electronic energy. This approach is sometimes called *Born–Oppenheimer Molecular Dynamics* [179,312] (BOMD). The major difficulty with BOMD is that it is necessary to perform an extremely accurate *ab initio* calculation at each time-step, because otherwise the error accumulates and causes an unphysical drift of the total energy of the system.

Car and Parrinello [313] proposed in 1985 an alternative way to obtain *ab initio* energies "on-the-fly", by embedding the dynamics of the electrons in the MD Lagrangian. This is called the *Car-Parrinello Molecular Dynamics* (CPMD) method. Although in principle one may formulate CPMD with any *ab initio*

method, DFT is the most commonly used because of its very good accuracy/computational cost ratio.

The idea behind CPMD is to simulate simultaneously the motion of the nuclei and of the electrons. Nevertheless, since the electrons cannot be treated classically, what is really done is to generate a *fictitious* dynamics of the one-electron orbitals ψ_i.

The first step to generate the dynamic equations for both the nuclei and the electrons in CPMD is to define a Lagrangian comprising both the electronic and nuclear dynamics as [179,308,313]:

$$L = \frac{1}{2}\sum_{i=1}^{N}\mu_i\int \mathrm{d}\mathbf{r}\left|\dot{\psi}_i(\mathbf{r})\right|^2 + \frac{1}{2}\sum_{\mathrm{I}} M_I\dot{\mathbf{R}}_I - E\left[\psi_i,\mathbf{R}_I\right] + \sum_{i=1}^{N}\sum_{j=1}^{N}\Lambda_{ij}\left(\left\langle\psi_i|\psi_j\right\rangle - \delta_{ij}\right) \quad (4.69)$$

In Eq. (4.69), the μ_i are fictitious masses assigned to the electron orbitals (typically between 400 and 2400 a.u.), M_I and $\mathbf{R}_I$ are the mass and the position of nucleus I, E is the expectation value of the Kohn–Sham Hamiltonian, δ_{ij} is the Kronecker delta and the Λ_{ij} are Lagrange multipliers associated with the orthonormality constraints [314]:

$$\langle\psi_i|\psi_j\rangle = \int \mathrm{d}r\psi_i^*\psi_j = \delta_{ij} \quad (4.70)$$

The equations of motion for the nuclei and the electronic orbitals can be obtained by writing the Euler–Lagrange equations associated with the Lagrangian (4.69):

$$\mu_i\ddot{\psi}_i = -\frac{\delta E[\psi_i,\mathbf{R}_I]}{\delta\psi_i^*} + \sum_{j=1}^{N}\Lambda_{ij}\psi_j \quad (4.71)$$

$$M_I\ddot{\mathbf{R}}_I = -\frac{\partial E[\psi_i,\mathbf{R}_I]}{\partial\mathbf{R}_I} \quad (4.72)$$

These equations can be integrated using a Verlet or velocity Verlet algorithm or a similar numerical technique [10,11,315–320]. It is important, however, to keep the electron dynamics separated from the nuclear dynamics, *i.e.* to keep the fictitious electronic kinetic energy low, in order to keep the system on the Born–Oppenheimer surface. In some cases, such as the simulation of non-conducting molecules, this can be accomplished simply by using a large enough value for the orbital masses μ_i. For conducting molecules, however, since the valence electrons are less tightly bound to the nuclei, there is a tendency for the nuclei and the electrons to achieve thermal equilibrium, hence removing the system from the Born–Oppenheimer surface. This may be avoided by using Nose–Hoover [321–323] thermostats [10,11] for the nuclei and the electrons [179,324,325].

The difficult part in the solution of the system (4.71) and (4.72) is usually the integration of Eq. (4.71), the equation of motion for the orbitals subject to the orthonormality constraints (4.70). In the standard Verlet scheme, which is the most commonly used, an unconstrained set of orbitals $\hat{\psi}_i$ at $t+\delta t$ is found from:

$$\hat{\psi}_i(t+\delta t) = 2\psi_i(t) - \psi_i(t-\delta t) - \frac{\delta t^2}{\mu}\frac{\delta E[\psi_i,\mathbf{R}_I]}{\delta\psi_i^*}\bigg|_t \quad (4.73)$$

And then these predicted orbitals are corrected by adding in the effect of the constraints:

$$\psi_i(t+\delta t) = \hat{\psi}_i(t+\delta t) + \sum_{j=1}^{N}\frac{\delta t^2}{\mu_i}\Lambda_{ij}\psi_j(t) \quad (4.74)$$

In order to find the Lagrange multipliers Λ_{ij}, Eq. (4.74) is substituted into the constraints (4.70) to get a system of equations that can be solved iteratively. Once the Λ_{ij} are known, the correct orbitals are obtained from Eq. (4.74). For a more detailed description of this kind of approach see Refs. [179,318]. Combining the Verlet algorithm with the constraints in this fashion is the method known as the SHAKE algorithm [326]. A similar method that uses the velocity Verlet method is known as the RATTLE algorithm [327].

One advantage of the CPMD approach as compared to BOMD is that it is more numerically stable. As mentioned above, BOMD requires a very accurate minimization of the electronic energy at each step to avoid energy drifts. CPMD does not have this problem, the total energy usually oscillates and its average remains constant [308,309]. On the other hand, doing a full minimization of the electronic energy at each timestep allows BOMD to use larger timesteps than CPMD (usually $\sim$10 times larger) because they only need to be of the order of the characteristic time of the nuclear motion. The extra computational effort associated with the accurate *ab initio* calculations, however, counterbalances this advantage, and at the end the choice depends more on how much of an energy drift can be accepted as payment for a faster calculation. A discussion of the relative computational efficiencies of CPMD and BOMD can be found in Ref. [179]. Recent reviews on the CPMD method can be found in Refs. [310,311].

Another advantage of CPMD is that treating the dynamics of the nuclei and the electrons simultaneously yields a very good picture of the real behavior of the system. It is not necessary to introduce empirical equations for the intermolecular potential, at least in principle, because it is obtained during the simulation. This is of course true as long

as the relevant interactions are accurately pictured by the *ab initio* method within. With DFT, for example, dispersion interactions are not well represented unless the nuclei are close to each other, limiting the application of the method in cases where dispersion is the most important interaction [328]. In a case like this, better results may be obtained by treating the interactions at longer distances with an empirical potential and using *ab initio* methods at shorter distances, as in QM/MM.

The other major issue with CPMD is its computational cost when compared to "classical" molecular simulation techniques that use empirical potentials. The time-step in a CPMD simulation has to be kept small enough to get good statistics for the motion of the electrons, typically of the order of 0.1 fs. Sometimes it is possible to increase the orbital mass μ and use slightly larger time-steps and still get good statistics. However, the total real time that can be simulated is often limited to about 10–30 ps, which allows only the study of very fast processes. In addition, the size of the system that can be studied is limited, usually of the order of 100 heavy atoms. The time scale problem can be overcome by combining CPMD with a multiple time-scale technique such as the ones described in the next section; some applications of this idea will be discussed in the "Classical Simulation Methods for Equilibrium and Rate Constants" section.

CPMD has also been adapted to efficiently explore PESs to look for different transition states in complex reactions by including history-dependent terms into the Lagrangian [329,330]. This technique seems very close to being a "black-box" method for studying reaction mechanisms. It is very useful, as there are many reactions for which the reaction mechanism is not evident *a priori*.

Although molecular dynamics is most commonly combined with DFT due to its high accuracy/computational cost ratio, it has also been combined with other *ab initio* methods. In the literature there are examples combining molecular dynamics with the HF method [331–333], the CI method [334], the CASSCF method [335,336] and others [337,338].

Applications of *ab initio* molecular dynamics have increased recently due to the availability of more efficient algorithms and faster computers. Some recent representative applications include:

- A CPMD calculation of the infrared spectrum and other properties of uracil in an aqueous solution [339], showing a remarkably good agreement with experiment. The CPMD method is often used to study water and aqueous solutions, as well as other hydrogen-bonded liquids [340]. Since the main interactions in water and aqueous solutions are hydrogen bonding and Coulomb interactions, which are strong, they can be pictured fairly well by using DFT. A recent study assessing the ability of CPMD to simulate water can be found in Ref. [341], and some other recent applications are in Refs. [342–346].
- A study of the solvent effects on the ground state and first excited singlet state of acetone in aqueous solution, using a new hybrid Car–Parrinello QM/MM technique [347]. In this work, the radial distribution function of the water atoms around the carbonyl oxygen is obtained for both the ground state and the excited state, and the absorption and fluorescence spectra of acetone in both the gas phase and the aqueous phase are calculated. The results obtained are in reasonably good agreement with experimental data for this system.
- A study of the torsions of two model arylamides, acetanilide and *o*-methylthioacetanilide, using CPMD [348]. The dynamics of these molecules are interesting because they are capable of forming intramolecular hydrogen bonds.

Quantum Mechanics/Molecular Mechanics [3,4,349–365]

As was discussed in the "Semiempirical Force Fields" section, a purely FF approach is adequate mostly for studying reactions that involve conformational changes, because force fields are classical models. Reactions that involve bond breaking or formation are much more difficult to represent, since this is inherently a quantum mechanical process. Although there are recently developed force fields targeted at the description of these reactions, such as RFF [108], AIREBO [106] and ReaxFF [60,67], it is in general preferable to use an electronic structure method to study them. The problem is that for many systems of interest an electronic structure method can have a prohibitive computational cost. It is possible to find a compromise between the two approaches by using a quantum chemistry method to handle the site(s) in the system where bond breaking or formation occurs, and a FF method to describe the other interactions. This approach is known as the *quantum mechanics/molecular mechanics* method [366,367].

The main idea in QM/MM methods is to partition space into several regions. In the simplest case, the system would be separated into a quantum mechanical (QM) region, where an electronic structure method would be used to obtain the energies [368], a molecular mechanical (MM) region, represented by a FF, and possibly a boundary region. The major difficulty in the QM/MM approach is to "match" the QM and MM potentials in a smooth way. It is also not trivial in general to decide which parts of the system would be in which region. For a system with the three regions described, the Hamiltonian of

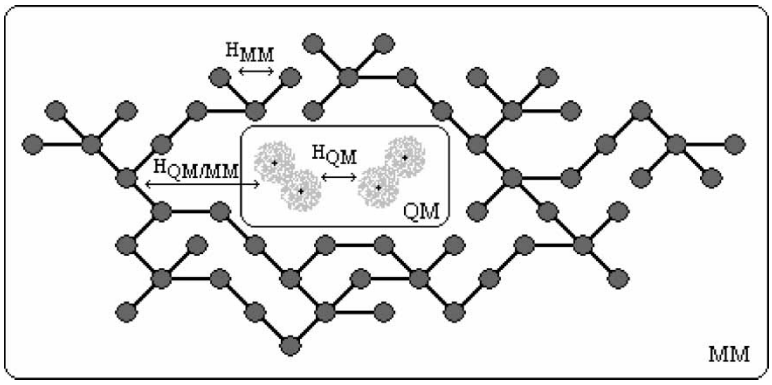

FIGURE 13 Sketch of a QM/MM system, showing the kinds of interactions that contribute to each part of the Hamiltonian in Eq. (4.75).

the system could be written as [369]:

$$H = H_{QM} + H_{MM} + H_{QM/MM} \tag{4.75}$$

As depicted in Fig. 13, the term H_{QM} includes the interactions between particles in the QM region, and H_{MM} includes the interactions between particles in the MM region. Both of these terms can be directly taken from the particular electronic structure method and FF used for each region. The $H_{QM/MM}$ term includes the interactions between particles in the QM and MM regions of the system. This is the part that is difficult to model, and its particular form will depend on the electronic structure method chosen for the QM part and the FF used for the MM part. A detailed discussion on how to build the QM/MM Hamiltonian for different methods is outside the scope of this work, more detailed descriptions and references can be found in [349–356].

It is possible to include more than one QM or MM region in a QM/MM calculation. For example, a very high-level *ab initio* method can be used in a small region, and a lower level method in the region surrounding it. Or a more complex FF can be used in an intermediate region and a simpler one in the outer region. This can be done, for example, in the *Our own N-layered Integrated mO and mM* (ONIOM) method [370,371]. A general-purpose implementation of QM/MM has been recently developed by the QUAntum Simulation in Industry (QUASI) project, a description of this can be found in Ref. [372]. Another hybrid QM/MM approach is the empirical valence bond (EVB) method [349,357,373], which is based on the valence bond representation rather than the molecular orbital representation of the wave function.

Applications of QM/MM methods are common in the study of solvation effects, reactions involving macromolecules (particularly enzymes), and surface chemistry. The QM/MM methodology seems to be an extremely efficient way of handling complex problem in chemistry. There are many examples of applications of QM/MM in the literature, and the number is likely to grow as the available computational power increases and the techniques are refined due to the high accuracy/computational cost ratio of the method. Some recent examples showing applications of the QM/MM methodology include:

- A study of the catalytic mechanism of the wild type and several mutants of the human enzyme cyclophilin A for the proline isomerization reaction [374]. In this work, the contributions of various effects to the catalytic effect of the enzyme are quantified, and transition states are found for both the wild type and the mutants.
- An analysis of the energetics of eight enol isomers of malonaldehyde in carbon tetrachloride solution [375], showing the changes in the relative energies and conformations, as well as the excitation energies of the isomers due to the interactions with the solvent.
- The original paper of the QUASI [372] program shows several applications to catalysis and enzyme chemistry, including a study of the mechanism of the synthesis of methanol over a Cu/ZnO catalyst, a study of the decomposition of nitrous oxide on a Cu-exchanged zeolite, and reactions in triosephosphate isomerase, *p*-hydroxybenzoate hydroxylase and cytochrome P450 enzymes.

CLASSICAL SIMULATION METHODS FOR EQUILIBRIUM AND RATE CONSTANTS

As we mentioned in the "Chemical Reactions" section, the goal of a simulation method for chemical reactions is usually to estimate an equilibrium constant or a reaction rate. Equilibrium constants are easier because they only require the knowledge of the thermodynamic properties of the reactants and the products. For kinetic rates the problem is more complicated. In the following sections, we will discuss some of the techniques that can be used to obtain equilibrium and rate constants once the PES is known

(or a method for obtaining it has been chosen). In the "Estimation of Equilibrium Constants" section, we will discuss an approach for the estimation of equilibrium constants, the reactive Monte Carlo method. In the remaining sections, we will discuss some of the methods that can be used for estimating reaction rates.

It is important to note that, although the methods in these sections are usually termed "classical", this does not mean that no quantum mechanical calculations are involved. *Ab initio* methods are still necessary to obtain the PES that will later be used to estimate reaction rates (unless a purely FF description is used). The term "classical" is used to distinguish the methods that are mostly based in classical statistical mechanics from those where the description of the reactive process itself is quantum mechanical (see the discussion at the end of the "Chemical Reactions" section).

Another important thing to keep in mind is that the accuracy of the results is determined by the method used to generate the PES ("Force Field Methods" section and "*Ab Initio* Methods" section). If the *ab initio* (or FF) method chosen does not give a good representation of the system, the results will be bad regardless of how good is the method chosen to determine the rate or equilibrium constant.

Estimation of Equilibrium Constants [2]

The equilibrium constant for a given chemical reaction is a thermodynamic equilibrium property, and hence it depends only on the thermodynamic properties of the reactants and the products involved, and not on the reaction mechanism. This can be restated in the terms of the "Force Field Methods" section by saying that the equilibrium constant depends only on what happens at the minima of the PES or, at a finite temperature, the minima of the FES. From classical thermodynamics, we know that the equilibrium constant can be expressed as:

$$K_{\mathrm{eq}} = \exp\left(-\Delta G^0/kT\right) = \prod_i a_i^{\nu_i} \tag{5.1}$$

where ΔG^0 is the change in the Gibbs free energy per molecule for the reaction with all the components in their standard states, the ν_i are the stoichometric coefficients and the a_i are the activities of the components involved in the reaction. These quantities can be related to the microscopic properties of the system through statistical mechanics. For example, for reacting mixture of ideal gases it is possible to write the equilibrium constant in terms of the molecular partition functions as [2,376]:

$$K_{\mathrm{eq}}^{\mathrm{id}} = \prod_i (q_i/V)^{\nu_i} \tag{5.2}$$

where the product runs over all components and the q_i are the molecular partition functions. Within the semiclassical approximation [377], it is possible to rewrite these partition functions as products of contributions from the different degrees of freedom [378]:

$$q_i = q_{i,t} q_{i,r} q_{i,v} q_{i,e} q_{i,i} \tag{5.3}$$

In Eq. (5.3), $q_{i,t} = V/\Lambda^3$ is the translational partition function (Λ being the thermal De Broglie wavelength), and the other terms are, respectively, the rotational, vibrational, electronic and internal partition function. The latter corresponds to internal degrees of freedom not considered in the remaining terms (e.g. internal rotations about a bond). Depending on the temperature, the rotational degrees of freedom may be treated classically or quantum mechanically. The vibrational and electronic partition functions must be obtained from quantum mechanics unless the system is at very high temperatures (in which case the semiclassical approximation will probably not work anyway). The electronic partition function is in many cases assumed to be constant, as we mentioned in the introduction, because for a typical system at a near-ambient temperature practically all the molecules will be in the electronic ground state. If this is not the case, it is necessary to obtain the energies for the excited electronic states. In order to obtain the vibrational partition function it is necessary to know the characteristic frequencies of oscillation for the given molecule; these can be obtained by doing a vibrational analysis using linear response theory with an *ab initio* method (see for example, Ref. [270]).

When the mixture is not ideal, it is necessary to include the effect of the intermolecular potential energy in the calculation of the equilibrium constant. Several attempts have been made to estimate equilibrium constants for chemical reactions in non-ideal systems by molecular simulation. In 1981, Coker and Watts [379,380] proposed a modification of the Grand Canonical Monte Carlo (GCMC) method [10,11,381–383] to obtain equilibrium constants. In the method, an extra Monte Carlo move was added that swapped the identity of a reactant molecule with that of a product molecule, and the transition probability was obtained by using the difference between the chemical potential of the two species. They applied their method to the reaction $Br_2 + Cl_2 \rightarrow 2BrCl$ and obtained very good agreement with experimental results. The main drawback of the method, aside from requiring the chemical potentials as an input, is the fact that it can only be used to simulate equimolecular reactions. This method was later modified and extended by Kofke and Glandt [384], who called the new method the *semigrand canonical Monte Carlo* (SGCMC) method. The SGCMC method, although more versatile than

the original modified GCMC (allowing, for example, for studying phase and chemical equilibria simultaneously), still had the limitation of being only applicable to equimolecular reactions. After this work, several other methods were proposed for the simulation of chemical equilibrium, such as the $N_{atoms}-P-T$ ensemble method of Shaw [385], the *association biased Monte Carlo* method [386,387], the *bond-biased Monte Carlo* method [388], and the *subspace sampling Monte Carlo* method [389–391]. All of these methods were successful for the systems studied, yet were difficult to generalize to any kind of reaction or ensemble, or required not readily available parameters [392].

Another method for the simulation of chemical equilibrium, the *reactive Monte Carlo* (RxMC) method, was developed independently by Smith and Triska [393] and Johnson *et al.* [394]. The RxMC method is similar to the $N_{atoms}-P-T$ ensemble method of Shaw, but is readily adapted to reactions where the number of moles is not preserved.

A simulation using RxMC includes "reactive" moves that may correspond to forward or backward reaction steps. In order to preserved detailed balance, both types of moves have to be attempted with equal probability [393,395]. In a forward reaction step, reactant molecules are removed and replaced with product molecules according to the stoichometry of the reaction. The acceptance probability of this move is obtained from:

$$P_{\text{acc}} = \min\left[1, \exp\left(-\frac{\delta U}{kT}\right)\prod_i q_i^{\nu_i}\frac{N_i!}{(N_i+\nu_i)!}\right] \quad (5.4)$$

where δU is the change in the potential energy between the initial and final configurations. For a reverse reaction step, the product molecules are removed and replaced with reactant molecules. It is important to do so in a way that preserves the microscopic reversibility. For example, when simulating a reaction of the form $A + B \rightarrow C + D$, a forward reaction step may be replacing a molecule of A with a molecule of C and a molecule of B with a molecule of D. If this is so, then in the reverse reaction step C has to be replaced with A and D with B to preserve the microscopic reversibility. The acceptance probability for a reverse reaction step is given by:

$$P_{\text{acc}} = \min\left[1, \exp\left(-\frac{\delta U}{kT}\right)\prod_i q_i^{-\nu_i}\frac{N_i!}{(N_i-\nu_i)!}\right] \quad (5.5)$$

The acceptance criteria (5.4) and (5.5) can be equivalently formulated in terms of the Gibbs free energy of reaction instead of the molecular partition functions, as in Ref. [393]. The most attractive features of the RxMC method are its versatility and the fact that the information it requires (i.e. the molecular partition functions) is readily available for most reactions. Since its inception, RxMC has been applied to a variety of reactive systems, including organic and inorganic reactions in gases, solutions, plasmas, and in nanoporous materials [394,396–408]. So far RxMC seems to be the best choice for the estimation of chemical equilibrium constants in non-ideal systems.

Transition State Theory and the Reactive Flux Method [1,2,12–14,409–411]

One of the early attempts to calculate reaction rates, and arguably the most successful, is the Transition State Theory (TST) of Eyring [412,413], sometimes also called *activated complex theory* or *absolute rate theory* [13]. Since its inception, the method has been extended and reformulated in several different ways [14,410].

The original formulation of TST is in thermodynamic terms. TST states that, for a reactive mixture in thermal equilibrium, the reaction rate may be obtained from the equilibrium constant for the conversion of reactant molecules to a transition state molecule [2,12–14]:

$$k_r^0 = \frac{kT}{h}K_{\text{eq}}^{\ddagger} = \frac{kT}{h}\exp\left(-\Delta G^{\ddagger}/kT\right) = \frac{kT}{h}\frac{a^{\ddagger}}{\prod_{\text{reac}} a_i^{-\nu_i}} \quad (5.6)$$

where the product runs over the reactants, $\Delta G^{\ddagger}$ is the *free energy of activation*, i.e. the change in the free energy of the system when reactant molecules are replaced by a transition state molecule, and k_r^0 is the standard-state reaction rate constant. TST thus reduces the dynamical problem of finding a reaction rate to an equilibrium problem that, as discussed in the previous sections, is much easier to solve. If, for example, the intermolecular potential effects are neglected, one may use Eqs. (5.2) and (5.6) to write the transition state equilibrium constant in term of molecular partition functions. In this case there is, however, an important difference. Since a transition state species corresponds to a first-order saddle point in the PES, it has one less vibrational mode than a stable molecule. The transition state does not occur at a minimum, but at a maximum free energy in the direction of the reaction coordinate. Hence, when calculating the vibrational partition function, there will be one vibrational mode missing. The term kT/h appearing in Eq. (5.6) can be interpreted as the contribution to the partition function corresponding to the non-vibrational motion along the reaction coordinate, i.e. as the term replacing the missing vibrational term [12].

It is also possible to formulate TST in dynamical terms [414,415]. This formulation requires introducing the concept of a *dividing surface*, which separates

the "reactants" and "products" regions of configurational space. In TST, the dividing surface can be defined as the plane normal to the reaction path and containing the transition state. Then the reaction rate can be defined as the net rate at which the system crosses the dividing surface in the direction of the products. For simplicity, let us consider an isomerization reaction A → B. It can be shown that its reaction rate is given by the stationary-state value of the time-correlation function $k_r(t)$ defined by [415]:

$$k_r(t) = \frac{\langle \dot{\xi}(0)\theta[\xi(t) - \xi^{\ddagger}]\delta[\xi^{\ddagger} - \xi(0)]\rangle}{\langle C_A\rangle} \tag{5.7}$$

In Eq. (5.7), C_A is the concentration of the reactant species A, $\langle C_A\rangle = \langle \theta[\xi(0) - \xi^{\ddagger}]\rangle$, $\xi(t)$ is the reaction coordinate as a function of time, $\xi^{\ddagger}$ is the value of the reaction coordinate at the dividing surface, θ is the Heaviside step function, δ the Dirac delta function, and the brackets indicate an ensemble average over equilibrium initial conditions [416]. Note that the term $\delta[\xi^{\ddagger} - \xi(0)]$ constrains the system to be initially at the dividing surface. The reaction rate is then:

$$\begin{aligned} k_r &= \lim_{t\to\infty} k_r(t) \\ &= \lim_{t\to\infty} \frac{\langle \dot{\xi}(0)\theta[\xi(t) - \xi^{\ddagger}]\delta[\xi^{\ddagger} - \xi(0)]\rangle}{\langle C_A\rangle} \end{aligned} \tag{5.8}$$

Equation (5.8) is often called the *Bennett* and *Chandler* [417–420] expression for the rate constant. In taking the limit, the time is supposed to be large compared to the characteristic time for the molecular motion, but small compared to the characteristic time for the reaction. Thus in the derivation of Eq. (5.8) it is implicitly assumed that the reaction is a rare event compared to molecular relaxation. This will be true as long as the free energy barrier for the reaction is large compared to *kT*.

It is possible to recover the TST constant by taking the limit as $t \to 0^+$ of $k_r(t)$:

$$\begin{aligned} k_{r,\mathrm{TST}} &= \lim_{t\to 0^+} \frac{\langle \dot{\xi}(0)\theta[\xi(t) - \xi^{\ddagger}]\delta[\xi^{\ddagger} - \xi(0)]\rangle}{\langle C_A\rangle} \\ &= \frac{\langle \dot{\xi}(0)\theta[\dot{\xi}(0)]\delta[\xi^{\ddagger} - \xi(0)]\rangle}{\langle C_A\rangle} \end{aligned} \tag{5.9}$$

Here, we have used the fact that $\xi(t)$ will be larger than $\xi^{\ddagger}$ as $t \to 0^+$ only if the derivative $\dot{\xi}(0)$ is positive, because only configurations starting at $\xi^{\ddagger}$ contribute to the average. It may not be directly evident that Eq. (5.9) is equivalent to Eq. (5.6); for a derivation of this see, e.g. Refs. [421,422]. Comparing Eq. (5.9) with Eq. (5.8) gives a clearer interpretation of the TST approximation: the two expressions will be equal only if, after initially crossing the dividing surface, the system does not return to the "reactants side", i.e. no recrossings of the dividing surface occur. This gives us another, more precise way of stating the quasiequilibrium assumption, which is to say that all trajectories crossing the dividing surface in the direction of the products and which do not recross it are in equilibrium with the reactants [410].

We already mentioned that, for Eq. (5.8) to be valid, it is necessary that the reaction barrier is high compared to *k*T. From the above reasoning, we see that TST will be valid when, after crossing the dividing surface, the reactive complex is able to dissipate its energy fast enough so that it cannot go back again. If this is not true, some recrossings of the dividing surface can occur and the real reaction rate will be lower than the TST rate. In order to account for this, one may define a *transmission coefficient* $\kappa \leq 1$ that corrects the TST rate constant due to the recrossings:

$$k_r = \kappa\, k_{r,TST}, \quad \kappa \leq 1 \tag{5.10}$$

Unlike the TST constant, the transmission coefficient is a dynamical quantity and cannot be obtained from an equilibrium simulation such as RxMC. The fact that $\kappa \leq 1$ implies that the TST constant is an upper bound for the true reaction rate.

There is one important remark to make about Eq. (5.10). This expression is correct even when the dividing surface is not exactly at the transition state. What is used in its derivation [415] is the separation of timescales between the reaction process and the molecular motion, and not the fact that the dividing surface contains the transition state. Now, since the $k_{r,\mathrm{TST}}$ in Eq. (5.10) is always an upper bound for the reaction rate regardless of how the dividing surface is chosen, this suggests a way to improve the TST estimate: do a TST calculation for different dividing surfaces and choose the lowest one. This is the approach used in *variational transition state theory* (VTST) [423].

One may ask why is it necessary to search for a dividing surface that does not contain the transition state. After all, it sounds reasonable to assume that the surface least likely to be recrossed is the one containing the transition state, and hence the TST reaction rate should be the lowest for that case. Nevertheless, it is important to take into account the fact that the PES does not include finite-temperature effects. Also the reactive system may be in a medium that imposes a force field on the atoms that was not taken into account during the *ab initio* calculations (e.g. an attractive surface, a solvent). Hence the true saddle point in the real FES may be quite different than the one in the PES. By using a VTST approach this can be accounted for. As an example, for

a reactive mixture of ideal gases the TST rate constant can be written, using Eqs. (5.6) and (5.2), as:

$$k_{r,TST} = \frac{kT}{h} K_{eq}^{\ddagger} = \frac{kT}{h} \frac{q^{\ddagger}/V}{\prod_{reac} (q_i/V)^{-\nu_i}} \tag{5.11}$$

In order to minimize this rate, it is necessary to choose the dividing surface such that the molecular partition function of the transition state $q^{\ddagger}$, will be minimal. Since this function contains the contributions from vibrational, rotational, etc. modes, it accounts for the finite-temperature effects not considered in the PES.

What we have given so far is a description of TST in purely classical terms. Due to the success of TST as both a theoretical and computational tool for understanding rate processes, there has been considerable effort to cast TST in quantum mechanical terms. This is a difficult problem, though, because of TST's natural formulation in terms of classical dynamical trajectories. In quantum TST (QTST), the objective is to obtain a quantum mechanical expression for the time-correlation function. Among the quantum-based versions of QTST are the short-time QTST method of Miller *et al.* [424–426] and its variational version [427], the path integral QTST methods [428–430], including the reversible action-space work QTST (RAW-QTST) method [431,432], and several others [433–439]. A discussion of QTST and related methods is beyond the scope of this paper; reviews can be found in Refs. [409,410,440,441]. One important contribution that is missing in classical TST, besides the transmission coefficient, is the quantum-tunneling correction. For some systems (e.g. reactions involving light molecules, low temperatures), it is possible for the reactants to tunnel through the activation barrier, and hence the reaction rate will be higher than that obtained by TST. A quantum mechanical treatment is necessary to obtain this correction.

Equations (5.7)–(5.10) suggest a natural way to correct a TST rate constant: obtain the transmission coefficient. In the *reactive flux method*, or *Bennett–Chandler method*, the reaction rate is obtained by using Eq. (5.7) directly, which is equivalent to finding the TST rate and the transmission coefficient. For this it is convenient to rewrite Eq. (5.7) as [10]:

$$k_f(t) = \frac{\langle \dot{\xi}(0)\theta[\xi(t) - \xi^{\ddagger}]\delta[\xi^{\ddagger} - \xi(0)]\rangle}{\langle \delta[\xi^{\ddagger} - \xi(0)]\rangle} \frac{\langle \delta[\xi^{\ddagger} - \xi]\rangle}{\langle \theta[\xi^{\ddagger} - \xi]\rangle} \tag{5.12}$$

The first term in this equation is the conditional average of the product $\dot{\xi}(0)\theta[\xi(t) - \xi^{\ddagger}]$, given that the system is initially at the dividing surface, i.e. $\xi(0) = \xi^{\ddagger}$. This term is a dynamical quantity, like the transmission coefficient. The second term is a ratio of the probability density of finding the system at the dividing surface to the probability of finding the system in the reactant side of the barrier. This term, like the TST constant, is an equilibrium quantity and can be obtained from a thermodynamic integration. In the next section, we will discuss a combined approach for finding the reaction rate from Eq. (5.12) using constrained dynamics.

One important comment about the methods discussed in this and the following sections is that studying chemical reactions is not their only application. The kinetic rate for any process that involves crossing an energy barrier can be obtained within the formalism. This includes, for example, nucleation [442] and diffusion on solid surfaces [443,444]. Finally, an improved reactive flux method allowing the estimation of rate constants with a lower computational effort has been recently proposed by Drozdov and Tucker [445].

Constrained Reaction Dynamics: "Blue Moon" Method [476]

As discussed in the previous section, it is possible to find good estimates of kinetic rate constants by separately evaluating the two factors in Eq. (5.12). The first term is a conditional average over trajectories starting at the dividing surface, and it can be evaluated from Molecular Dynamics (MD) simulations with the system initially at the top of the barrier. In this case, it is necessary to correct the statistics using bias factors to get the right averages. The second factor in Eq. (5.12) can be obtained also from constrained dynamics, and hence it is possible to use a unified two-step MD approach to calculate the reaction rate. This is the so-called "Blue Moon" approach for finding reaction rates [10,446–450].

In the Blue Moon method, a constrained MD run with the reaction coordinate held fixed at the constant value $\xi = \xi^{\ddagger}$ is used to generate configurations at the top of the barrier *and* also to estimate the second term in Eq. (5.12) using the constraint force. Then these configurations can be used in a second set of MD runs where the constraint is relaxed and the atoms are assigned initial velocities from a Maxwell–Boltzmann distribution for the given temperature. These runs are used to accumulate statistics on the number of pathways with $\dot{\xi}(0) > 0$ that reach the "products" region of space, thus allowing the estimation of the first term in Eq. (5.12).

In order to derive expressions for the proper averages when the Blue Moon technique is used, let us start from the canonical ensemble probability distribution for states with a pre-specified value of the reaction coordinate, $\xi = \xi^{\ddagger}$ [446]:

$$P_{\mathrm{I}}(\mathbf{r}^N, \mathbf{p}^N)\delta(\xi - \xi^{\ddagger})\mathrm{d}\mathbf{r}^N\mathrm{d}\mathbf{p}^N = \frac{1}{Q_{\mathrm{I}}} \exp\left(-\frac{H}{kT}\right)\delta(\xi - \xi^{\ddagger})\mathrm{d}\mathbf{r}^N\mathrm{d}\mathbf{p}^N \tag{5.13}$$

We will call this ensemble I. In this equation, H is the system Hamiltonian, Q_{I} is the partition function

and δ is the Dirac delta function. Note that in ensemble I the reaction coordinate is restricted to the value $\xi = \xi^{\ddagger}$, but is not constrained, i.e. its time derivative $\dot{\xi}$ is not restricted to be zero. The phase–space points generated in this ensemble could be used as starting points for an MD simulation, and would generate reacting trajectories frequently. The probability distribution Eq. (5.13) can be factored as:

$$P_{\mathrm{I}}(\mathbf{r}^N, \mathbf{p}^N)\delta(\xi - \xi^{\ddagger})\mathrm{d}\mathbf{r}^N\mathrm{d}\mathbf{p}^N = P_{c,\mathrm{I}}(\mathbf{r}^N)P_{m,\mathrm{I}}(\mathbf{p}^N|\mathbf{r}^N)\delta(\xi - \xi^{\ddagger})\mathrm{d}\mathbf{r}^N\mathrm{d}\mathbf{p}^N \quad (5.14)$$

where $P_{c,\mathrm{I}}(\mathbf{r}^N)$ is the configurational probability density $P_{m,I}(\mathbf{P}^N|\mathbf{r}^N)$ and is the conditional probability density of the momenta given the configuration. Only the latter will be of interest to us. It can be expressed as:

$$P_{m,\mathrm{I}}(\mathbf{p}^N|\mathbf{r}^N)\mathrm{d}\mathbf{p}^N = \exp\left(-\frac{K}{kT}\right)\mathrm{d}\mathbf{p}^N \quad (5.15)$$

where K is the kinetic energy:

$$K = \sum_{j=1}^{N} \frac{\mathbf{p}_j \cdot \mathbf{p}_j}{2m_j} \quad (5.16)$$

The probability density (5.15) is a product of Maxwell distributions for individual atoms, and it is fairly straightforward to sample from it. Now we will introduce an ensemble II where the reaction coordinate is not only restricted to the value $\xi = \xi^{\ddagger}$, but also constrained to it (i.e. where $\dot{\xi} = 0$). The configurational part of the probability distribution for this ensemble II will be:

$$P_{c,\mathrm{II}}(\mathbf{r}^N)\mathrm{d}\mathbf{r}^N = \frac{1}{Q_{\mathrm{II}}}|\mathbf{Z}|^{1/2}\exp\left(-\frac{U}{kT}\right)\delta(\xi - \xi^{\ddagger})\mathrm{d}\mathbf{r}^N \quad (5.17)$$

where $U = U(\mathbf{r}^N)$ is the potential energy and is the partition function for this ensemble. The term $|\mathbf{Z}|^{1/2}$ is a bias factor arising from the constraint imposed on the reaction coordinate. For the case being discussed (where only the reaction coordinate is constrained), it can be obtained from:

$$|\mathbf{Z}| = \sum_{j=1}^{N} \frac{1}{m_j}\left(\frac{\partial \xi}{\partial \mathbf{r}_j}\right)^2 \quad (5.18)$$

The derivation for the more general case when other constraints are imposed on the system is discussed in Refs. [446,448].

At this stage, we recognize that both ensembles I and II are difficult to sample in a MD run. In ensemble I, since there is no restriction on the derivative of the reaction coordinate, it is fairly easy to sample from the momentum distribution, but it is difficult to generate the configurations. We would need to keep $\xi = \xi^{\ddagger}$ as time goes on, but without having $\dot{\xi} = 0$(!). In ensemble II, on the other hand, we can easily generate configurations because $\dot{\xi} = 0$. The problem, however, is that we cannot use the states from ensemble II to get statistics on how the system crosses the energy barrier because of the constraint. This reasoning suggests defining a new ensemble, the *Blue Moon Ensemble* [446], with the configurational probability density of ensemble II and the conditional momenta probability density of ensemble I, i.e.

$$P_{\mathrm{BM}}(\mathbf{r}^N, \mathbf{p}^N)\mathrm{d}\mathbf{r}^N\mathrm{d}\mathbf{p}^N = P_{c,\mathrm{II}}(\mathbf{r}^N)P_{m,\mathrm{I}}(\mathbf{p}^N|\mathbf{r}^N)\mathrm{d}\mathbf{r}^N\mathrm{d}\mathbf{p}^N = \frac{1}{Q_{\mathrm{II}}}|\mathbf{Z}|^{1/2}\exp\left(-\frac{H}{kT}\right)\delta(\xi - \xi^{\ddagger})\mathrm{d}\mathbf{r}^N\mathrm{d}\mathbf{p}^N \quad (5.19)$$

We now have an ensemble that is easier to sample. We need to generate configurations with a constrained value of the reaction coordinate, and velocities from a Maxwell distribution. This procedure will generate a set of configurations that, if used as starting points for a MD, will produce barrier crossings frequently. The true dynamic trajectories, however, are the ones of ensemble I, where $\dot{\xi}$ is not restricted, and therefore we need to include a bias factor when averaging over the blue moon ensemble.

If we want to obtain the average of the observable $A(\mathbf{r}^N, \mathbf{p}^N)$ over ensemble I, we need to calculate:

$$\langle A \rangle = \frac{\left\langle A(\mathbf{r}^N, \mathbf{p}^N)\delta(\xi - \xi^{\ddagger})\right\rangle_{\mathrm{I}}}{\left\langle \delta(\xi - \xi^{\ddagger})\right\rangle_{\mathrm{I}}} \quad (5.20)$$

Comparing the probability distribution of ensemble I, Eq. (5.13), with the probability distribution of the Blue Moon ensemble, Eq. (5.19), we see that this is equivalent to:

$$\langle A \rangle = \frac{\left\langle |\mathbf{Z}|^{-1/2} A(\mathbf{r}^N, \mathbf{p}^N)\right\rangle_{\mathrm{BM}}}{\left\langle |\mathbf{Z}|^{-1/2}\right\rangle_{\mathrm{BM}}} \quad (5.21)$$

Thus the factor $|\mathbf{Z}|^{-1/2}$ is what we need to correct the bias caused by the constraint $\dot{\xi} = 0$ in the configurational distribution. The averages in Eq. (5.21) are now taken in the Blue Moon ensemble.

The derivation above pertains to the case where only the reaction coordinate is being constrained. Sometimes it is convenient to include additional constraints in the simulation, for example fixed bond lengths in a molecule. For the general case when L additional holonomic [451] constraints of the form $\sigma_i(\mathbf{r}^N) = 0, i = 1, \cdots, L$, are included, Eq. (5.21) has to be modified. The corresponding equations can be found in Refs. [446,448].

We may now turn to the problem of calculating reaction constants in the Blue Moon ensemble. For this we need to rewrite the averages in

Eq. (5.12) as averages in the blue moon ensemble. For the first factor in Eq. (5.12), we can directly use the result Eq. (5.21):

$$\frac{\left\langle \dot{\xi}(0)\theta[\xi(t)-\xi^*]\delta[\xi^*-\xi(0)]\right\rangle}{\langle\delta[\xi^*-\xi(t)]\rangle} = \frac{\left\langle |\mathbf{Z}|^{-1/2}\dot{\xi}(0)\theta[\xi(t)-\xi^*]\right\rangle_{\mathrm{BM}}}{\left\langle |\mathbf{Z}|^{-1/2}\right\rangle_{\mathrm{BM}}} \quad (5.22)$$

The second factor in Eq. (5.12), as we mentioned earlier, is the probability density of finding the system at the top of the barrier, divided by the probability that the system is on the "reactants" side of the dividing surface. This can also be obtained from the constrained MD in the Blue Moon simulation. We will define the probability of finding the system at any value of the reaction coordinate $\xi = \xi'$ (not necessarily at the top of the energy barrier) as:

$$P(\xi') = \frac{\int \mathrm{d}\mathbf{r}^N \exp(-U/kT)\delta(\xi'-\xi)}{\int \mathrm{d}\mathbf{r}^N \exp(-U/kT)\theta(\xi^\ddagger-\xi)} \quad (5.23)$$

Differentiating the logarithm of $P(\xi')$ with respect to ξ', we obtain:

$$\frac{\partial \ln P(\xi')}{\partial \xi'} = \frac{\int \mathrm{d}\mathbf{r}^N \exp(-U/kT)\partial\delta(\xi'-\xi)/\partial\xi'}{\int \mathrm{d}\mathbf{r}^N \exp(-U/kT)\delta(\xi^\ddagger-\xi)} \quad (5.24)$$

The negative of this quantity (times kT) is the *mean force* associated with the reaction coordinate constraint. In order to remove the derivative of the Dirac delta in Eq. (5.24), we need to integrate by parts. However, the dependence of ξ on the configuration in Eq. (5.24) is implicit. It is convenient to define a new set of generalized coordinates $(\mathbf{q}^{N-1}, \xi)$ where ξ appears explicitly. In terms of these coordinates, Eq. (5.24) is:

$$\frac{\partial \ln P(\xi')}{\partial \xi'} = \frac{\int \mathrm{d}\mathbf{q}^{N-1}\mathrm{d}\xi|\mathbf{J}|\exp(-U/kT)\partial\delta(\xi'-\xi)/\partial\xi'}{\int \mathrm{d}r^N \exp(-U/kT)\delta(\xi^\ddagger-\xi)} \quad (5.25)$$

where $|\mathbf{J}|$ is the Jacobian of the transformation $\mathbf{r}^N \rightarrow (\mathbf{q}^{N-1}, \xi)$. The exact form of this transformation will depend on the functional form of the reaction coordinate. Integrating the numerator of Eq. (5.25) by parts, we find:

$$\begin{aligned}\frac{\partial \ln P(\xi')}{\partial \xi'} &= \frac{\int \mathrm{d}\mathbf{q}^{N-1}\mathrm{d}\xi\delta(\xi'-\xi)\partial[|\mathbf{J}|\exp(-U/kT)]/\partial\xi}{\int \mathrm{d}\mathbf{r}^N \exp(-U/kT)\delta(\xi^\ddagger-\xi)} \\ &= \frac{\int \mathrm{d}\mathbf{q}^{N-1}\mathrm{d}\xi\delta(\xi'-\xi)\exp(-U/kT)\partial\{\ln[|\mathbf{J}|-U/kT]\}/\partial\xi}{\int \mathrm{d}\mathbf{r}^N \exp(-U/kT)\delta(\xi^\ddagger-\xi)}\end{aligned} \quad (5.26)$$

The latter expression can be expressed in terms of averages in the Blue Moon ensemble by using Eq. (5.21):

$$\frac{\partial \ln P(\xi')}{\partial \xi'} = \frac{\left\langle |\mathbf{Z}|^{-1/2}\partial[|\mathbf{J}|\exp(-U/kT)]/\partial\xi\right\rangle_{\mathrm{BM}}}{\left\langle |\mathbf{Z}|^{-1/2}\right\rangle_{\mathrm{BM}}} \quad (5.27)$$

If we now want the second factor in Eq. (5.12), we need to integrate this expression from $\xi' = 0$ (the reactant side) to $\xi' = \xi^\ddagger$. The expression will therefore be:

$$\frac{\langle\delta[\xi^\ddagger-\xi(t)]\rangle}{\langle\theta[\xi^\ddagger-\xi(t)]\rangle} = \int_0^{\xi^\ddagger} \mathrm{d}\xi \frac{\left\langle |\mathbf{Z}|^{-1/2}\partial[|\mathbf{J}|\exp(-U/kT)]/\partial\xi\right\rangle_{\mathrm{BM}}}{\left\langle |\mathbf{Z}|^{-1/2}\right\rangle_{\mathrm{BM}}} \quad (5.28)$$

This expression has to be calculated numerically from runs in the Blue Moon ensemble. It is possible [446,449] to relate the integral on the right-hand side to the Lagrangian multiplier associated with the constraint $\xi = \xi^\ddagger$, which is obtained during the constrained MD run using an algorithm such as SHAKE [326]. Therefore, the second term in Eq. (5.12) can be obtained from quantities that are already calculated during the constrained MD run. Summing up all the information we have, we may write the procedure for obtaining rate constants from blue moon MD:

(1) Specify a value for the reaction coordinate, $\xi^\ddagger$, at the dividing surface.
(2) Generate phase–space trajectories where the reaction coordinate is constrained to $\xi = \xi^\ddagger$. These can be obtained from a constrained MD algorithm such as SHAKE.
(3) Choose a set of configurations generated in step 2. For each of these:
  (3.1) Assign velocities to the particles from a Maxwell–Boltzmann distribution
  (3.2) Using the configuration from 2 and the velocities from 3.1, run an MD simulation for a time long enough for the system to reach the reactants or products basin
  (3.3) Record the final state of the system. Accumulate the number of configurations with $\dot{\xi} > 0$ that reach the products basin.
(4) Using the results from step 3, compute the first term in Eq. (5.12) using Eq. (5.22).
(5) Obtain the second term in Eq. (5.12) by numerically integrating the mean constraint force at values ξ from 0 to $\xi^\ddagger$, i.e. using Eq. (5.28).
(6) Finally, use Eq. (5.12) to obtain the reaction rate.

A schematic of this is shown in Fig. 14. An advantage of the Blue Moon MD approach is that it can in principle handle systems as large as a standard MD simulation [452]. The time interval spanned in each MD run in step 3 may also be chosen

FIGURE 14 Sampling in the Blue Moon method. The thick line represents the phase space trajectory with the reaction coordinate constrained, which is used to obtain the second factor in Eq. (5.12). The thin lines are unconstrained trajectories starting at configurations from the constrained simulation; these are used to obtain the first factor in Eq. (5.12). From Ref. [447].

to be the same as in a standard MD simulation [452], but the "real-time" interval spanned in the blue moon ensemble is much longer. The reason for this is that Blue Moon MD "jumps" from one reaction event to another, not simulating in detail over the long time intervals between two events [446].

One disadvantage of Blue Moon MD is that the reaction must be simple enough to have a clearly defined energy barrier and reaction coordinate. Recently, however, the method has been extended to handle more complex systems [448]. Another problem is that it is necessary to impose a definition of the reaction coordinate beforehand. If this reaction coordinate is too far from the intrinsic reaction coordinate, the results will not be good. It is important to verify that the reaction coordinate chosen is a good one. A way to do this that is amenable to the Blue Moon MD method is to repeat the calculation of mean forces with a reversed reaction path. If a large hysteresis loop appears, the reaction coordinate is not adequate [453,454] and it is necessary to choose another one (see Fig. 4).

The most recent applications of the blue moon MD methodology are in combination with *ab initio* molecular dynamics, due to the ability of the latter to generate dynamic trajectories while taking the electronic degrees of freedom into account explicitly. Some of these applications include:

- A study of the intramolecular solvation effects on the reaction of a chloride anion with several cyano-chloroalkanes [455]. In this work, the blue moon methodology in conjunction with CPMD was used to find the thermal effects on the PES for the reactions considered.
- An *ab initio* MD study of the reaction of the fluoride ion with chloromethane [456] and chloroethane [457]. In this work, as in the previous one, the blue moon MD methodology is used to incorporate the thermal effects on the PES in combination with the CPMD method.
- A calculation of the pK_a for the axial and equatorial hydroxyl groups in aqueous $P(OH)_5$ using constrained *ab initio* molecular dynamics [458]. The calculated values in this work show good agreement with experimental results for a related system (aqueous tetracyclohexyloxy-hydroxyphosphorane).

Transition Path Sampling

As mentioned in the previous sections, when a system has a PES that depends on a small number of degrees of freedom, it is not too difficult to find the relevant transition state(s) and reaction coordinate(s). For more complex systems with high-dimensional PES, however, there are usually many local minima and saddle points and it becomes much harder to determine the relevant reaction paths. This is illustrated in Fig. 15. The *Transition Path Sampling* (TPS) method [459–465] offers a way to determine reaction rates for such systems.

There is no single way to deal with the problem of the separation of timescales between reactions and molecular relaxation. In the Blue Moon MD method, for example, this problem is overcome by creating

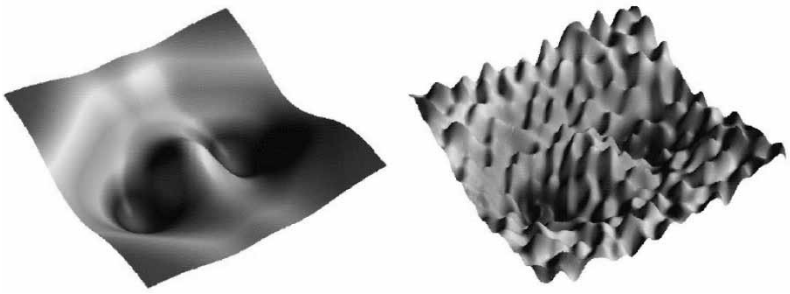

FIGURE 15 For simple reactions that do not involve many degrees of freedom it is usually easy to determine the reaction mechanism by locating the energy minima and saddle points (left). In complex reactions where many degrees of freedom are involved there may be many saddle-points and local minima, and hence many possible reaction pathways (right). From Ref. [465]. Copyright (c) 2002 Wiley. Reprinted with permission from John Wiley & Sons, Inc.

an ensemble of initial states close to the top of the energy barrier, running simulations starting from these states, and then obtaining reaction rates from ensemble averages over the results of these runs. Nevertheless, if the energy landscape is complicated, one does not know where the top of the barrier is to begin with, and it is even possible that several different paths contribute to the reaction rate. In TPS, as in Blue Moon MD, we generate an ensemble of dynamic trajectories and find the reaction rate from averages on this ensemble. The trajectories, however, are not restricted to start from the top of any barrier.

The basic idea behind TPS is to construct reactive trajectories that go from the reactants basin (A) to the products basin (B) in the PES, and then sample over these trajectories [459]. The *transition path ensemble* is defined as the collection of all trajectories starting at A and ending at B after a given time t_F. The trajectories are defined as a set of points in phase–space $\{\Gamma(0), \Gamma(\delta t), \Gamma(2\delta t), \cdots, \Gamma(M\delta t)\}$, where δt is the time-step and $M\delta t = t_F$. These trajectories can be chosen to be Verlet [10,11,315,316] trajectories, although other definitions are possible [465]. It is clear from this definition that, in order to run a TPS simulation, we need to identify beforehand the reactant and products basins, and choose a time t_F. It is also necessary to find a reactive trajectory to start the simulation. These points are discussed below.

In order to find a reactive trajectory, one possibility is to run a MD simulation at conditions for which the reaction is no longer a rare event, such as a higher temperature, and then anneal the system to obtain a reactive trajectory at a lower temperature. This procedure, however, is very laborious. An alternative is to use an action-based method, i.e. find a dynamic path connecting a reactant and a product state that corresponds to a stationary point of the classical action. A procedure for doing this in the context of CPMD has been proposed in Ref. [466]. Other alternatives for finding an initial trajectory are discussed in Ref. [465].

Since the molecular equations of motion are non-linear, the trajectories generated from them are chaotic and hence sensitively dependent on the initial conditions. Therefore, a small change in a position or momentum in one time slice of a given trajectory will cause it to diverge from the original one after some time. Once this happens, the trajectory becomes uncorrelated with the original one and depends solely on the PES. The total path time t_F has, thus, to be larger than the time required for the trajectory to diverge after a small change to get a correct sampling of the true dynamics. The simplest way to do this is to take the initial reactive path, change the momentum of one time-slice in the smallest possible value representable on the computer, and integrate the dynamic equations forward and backwards in time. The time after which the trajectories have diverged from the original one, multiplied by some factor (usually around 10), is taken as t_F.

Defining the basins of reactants and products is one of the crucial points in TPS. If the reactants and/or products basin is defined as a too narrow region of phase–space, it is likely that many reactive trajectories are not sampled, yielding a wrong value of the reaction constant. On the other hand, if they are too large, there is a chance that non-reactive trajectories are counted as reactive. In most cases, defining the basins of attraction is a trial-and-error procedure, as described in Ref. [465].

Once the parameters of the simulation are set and an initial reacting trajectory is known, the simulation proceeds by generating new trajectories and checking if they are still reactive, i.e. if they still connect regions A and B. The new trajectories may be generated in several different ways, the two most common being shooting and shifting moves. Shooting moves are the simplest possible. In this case a time slice from the original trajectory is selected at random and the momenta of the particles are randomly changed by a small amount δp. Then the equations of motion are integrated either forward in time to t_F, or backwards in time to $t = 0$. If the new trajectory still connects regions A and B, it is accepted. In a shifting move, an additional number of time slices l is added to either the beginning of the trajectory (by integrating backwards in time from $t = 0$ to $t = -l\delta t$) or its end (by integrating forward in time from $t = t_F$ to $t = t_F + l\delta t$). When the shift is done at the beginning of the trajectory, the last l slices are discarded and when it is done at the end, the first l slices are discarded. This is done to keep the total number of time-steps fixed. If the new trajectory still connects regions A and B, it is accepted.

Once the set of trajectories is generated, the reaction rate can be obtained through expressions similar to the ones used in the reactive flux method. First, the θ (**x**) functions are defined as:

$$\theta_{\mathrm{A,B}}(\mathbf{x}) = \begin{cases} 1 & \text{for} \quad \mathbf{x} \in \mathrm{A,B} \\ 0 & \text{for} \quad \mathbf{x} \notin \mathrm{A,B} \end{cases} \tag{5.29}$$

These are the equivalent of the step function in Blue Moon MD. The θ_{A} function is one for configurations in the reactants basin, and zero outside, and the θ_{B} function is one for configurations in the products basin, and zero outside. In terms of these functions, the forward reaction rate will be the stationary value of:

$$k_f(t) = \frac{\left\langle \theta_{\mathrm{A}}(\mathbf{x}(0))\dot{\theta}_{\mathrm{B}}(\mathbf{x}(t)) \right\rangle}{\left\langle \theta_{\mathrm{A}}(\mathbf{x}(0)) \right\rangle} \tag{5.30}$$

This is analogous to Eq. (5.7) for the reactive flux method. It expresses that the reaction rate is

proportional to the time derivative of the probability that the system is in region B at time t, provided that it started from region A at time 0. This equation is often rewritten as:

$$k_f(\tau\delta t) = \frac{\langle \theta_A(\mathbf{x}_0)\dot{\theta}_B(\mathbf{x}_\tau)\rangle}{\langle \theta_A(\mathbf{x}_0)\theta_B(\mathbf{x}_M)\rangle}\frac{\langle \theta_A(\mathbf{x}_0)\theta_B(\mathbf{x}_M)\rangle}{\langle \theta_A(\mathbf{x}_0)\rangle} = \langle \dot{\theta}_B(\mathbf{x}_\tau)\rangle_{AB}\frac{\langle \theta_A(\mathbf{x}_0)\theta_B(\mathbf{x}_M)\rangle}{\langle \theta_A(\mathbf{x}_0)\rangle} \quad (5.31)$$

where $\tau \equiv t/\delta t$ is a dimensionless time. This equation is also analogous to Eq. (5.12). The first factor can be obtained directly from the TPS simulation, but the second factor requires additional work. The first term is the time derivative of the probability that, in a trajectory connecting A and B, region B is reached after τ time steps. For k_f to attain a stationary value it is necessary that this first factor also attain a stationary value within the time frame studied. This can be used as a test to check if the transition path is long enough: if the stationary value is not frequently attained, it is necessary to use a larger number of time slices, M.

The second factor in Eq. (5.31) is the probability that a system starting in region A reaches region B in M time steps. This cannot be obtained directly from TPS, because all trajectories in the TPS ensemble are assumed to start at A and end in B. It cannot be obtained either from a standard simulation because the reaction is a rare event (otherwise we would have used a standard simulation to begin with). One way around this problem is very similar to the thermodynamic integration used to find the second factor of Eq. (5.12) in the Blue Moon MD method. We define a quantity $W(M)$ as:

$$W(M) = -\ln\frac{\langle \theta_A(\mathbf{x}_0)\theta_B(\mathbf{x}_M)\rangle}{\langle \theta_A(\mathbf{x}_0)\rangle} \quad (5.32)$$

This can be regarded as the reversible work needed to make the trajectory end in region B at $t = M\delta t$. We can find it through thermodynamic integration. First we define a succession of regions B_λ, where λ is a parameter, with B_λ at $\lambda = 0$ spanning the whole of phase–space, and with $B_\lambda = B$ for $\lambda = 1$. The quantity $W(M)$ will then be:

$$W(M) = -\int_0^1 \frac{d}{d\lambda}\ln\langle \theta_A(\mathbf{x}_0)\theta_{B_\lambda}(\mathbf{x}_M)\rangle d\lambda \quad (5.33)$$

This quantity can be obtained by running MD simulations for several different values of λ, and then numerically evaluating Eq. (5.33). It is also possible to obtain it by using constrained dynamics, as in the Blue Moon method.

Putting everything together, we can write the procedure for finding a reaction rate using TPS as:

1. Obtain an initial reacting trajectory, for example, by running a standard MD simulation at a much higher temperature or using an action-based method. Define the length of the path t_F and the number of slices M, and the reactant and product regions A and B.
2. Generate new paths by slightly modifying the previous path. This may be done using the shooting and shifting moves described earlier.
3. For each of these paths, obtain the quantity $\langle \dot{\theta}_B(\mathbf{x}_\tau)\rangle_{AB}$. If this function does not attain a stationary value, restart the simulation using a longer path length.
4. Run a set of MD simulations for different end regions B_λ, and numerically obtain the integrand in Eq. (5.33). Then integrate Eq. (5.33) numerically to obtain the reversible work $W(M)$.
5. Using the results from steps 3 and 4, obtain the reaction rate from Eq. (5.31).

A detailed and very clear description of how to find reaction rates using TPS can be found in Ref. [465]. A description of a new modified method to evaluate reaction rates, *transition interface sampling*, can be found in Ref. [467]. The major advantages of the TPS methodology are the fact that it can generate real dynamic trajectories, which can be used to compute time correlation functions, and the fact that it does not require defining a reaction coordinate, or identifying an energy barrier for the reaction. The TPS trajectories are not biased by imposing an artificial restriction on the initial conditions, and thus better represent the real behavior of the system. This, however, has to be balanced against the increased computational cost of TPS [468].

The trajectories generated with TPS can be used to find the transition state regions of configurational space, and to determine proper reaction coordinates for the system. In order to determine the transition state region, one may take TPS trajectories and, starting from a given time slice, generate several dynamic trajectories by assigning initial velocities from a Maxwell–Boltzmann probability distribution. If the time slice selected corresponds to the transition state region, the probability of ending in either basin of attraction should be close to 1/2. Further descriptions of how to define transition states and reaction coordinates using TPS results can be found in Refs. [465,469–471].

The TPS methodology is relatively new, and hence there are not as many applications in the literature. Some recent representative applications of TPS are:

- A study of the reaction mechanism for the autoionization of liquid water using TPS in

combination with CPMD [472]. This simple reaction, which is key to the understanding of acid-base chemistry, has actually a complicated mechanism involving the hydrogen-bonded network of liquid water.

- A study of the reaction between the ferrous ion and hydrogen peroxide in aqueous solution using TPS in combination with CPMD [473]. In this work, TPS is used to elucidate the reaction mechanism, which involves complex solvent effects.
- An analysis of the folding pathways of β-hairpin folding of aqueous G-B1 protein, using TPS together with the CHARMM force field [474]. In this work, the proper order parameters to define the stable states are found for this system, and the rates for the transitions involved in the folding are estimated.
- A study of the kinetic pathways for single base-pair binding/unbinding in DNA, using the CHARMM force field [475]. In this work, the FES for a model DNA sequence in aqueous solution at 300 K, and proper reaction coordinates and the transition state region are found for the base pairing/unpairing.

CONCLUDING REMARKS

In recent years, many methods have been developed for the study of the dynamics of different chemical reactions. To this date, there are several approaches available for the computation of rate constants, depending on the complexity of the reaction studied, how well its mechanism is understood, and how long is the characteristic time associated with it. From the basic principles of quantum chemistry, we have the *ab initio* methods, which make it possible for us to understand how a reaction proceeds without much previous knowledge. The CPMD method even provides a way of looking at the dynamics of a reaction from first principles. The computational cost of such methods, however, makes them prohibitive for the study of complex systems where a large number of atoms has to be considered.

We have also reviewed methods that allow us to handle the separation of time scales typical of reaction processes, for both the cases when the mechanism is well understood (TST, Reactive Flux Method, Blue Moon MD) and the cases where it is not (TPS). Although these methods are relatively new, they promise to be very useful. They allow us to bridge the gap between the extremely detailed, short-time description of CPMD and the much longer-time description required for studying activated processes. In several recent applications, the CPMD method has been successfully combined with the Blue Moon MD and TPS techniques to obtain accurate pictures of reactive processes.

There are still major limitations to the types of systems that can be handled using current state-of-the-art techniques. Many chemical reactions of interest to both scientists and engineers (e.g. polymerizations, biological reactions) are not simple enough to be treated with a method like CPMD, and can be expected to be still too complex for many years. Force field methods offer a way around this, but they cannot be used as predictive tools as *ab initio* methods can. The intermediate approach of QM/MM is the most likely to be successful as a predictive tool for such complex systems.

There is a definite need to develop methods that simplify the problem of finding potential energies. The CPMD method is a big step in this direction, but still has serious limitations. It is also necessary to refine the methods for handling differing time scales, so they can be applied to larger systems without prohibitive computational costs. Nevertheless, we have seen a big increase in the complexity of the systems that can be studied in the recent past, an increase due more to the development of better simulation techniques than to the development of better computers. If this trend continues, we can expect to have much better tools in the near future.

Acknowledgements

We are grateful to B. Trout for very helpful suggestions and discussions, and to L. Mitas, F. Hung, B. Coasne and M. Kostov for reading the manuscript and providing valuable suggestions. This work was supported, in part, by NSF grant CTS-0211792 and DOE grant DE-FG02-98ER14847.

References

[1] Truhlar, D. (1981) *Potential Energy Surfaces and Dynamics Calculations for Chemical Reactions and Molecular Energy Transfer* (Plenum Press, New York).
[2] Simons, J. (2003) *An Introduction to Theoretical Chemistry* (Cambridge University Press, Cambridge).
[3] Leach, A.R. (2001) *Molecular Modeling. Principles and Applications*, 2nd ed. (Prentice Hall, Harlow).
[4] Jensen, F. (1999) *Introduction to Computational Chemistry* (John Wiley and Sons, Chichester).
[5] Hirst, D.M. (1985) *Potential Energy Surfaces: Molecular Structure and Reaction Dynamics* (Taylor and Francis, London).
[6] Szabo, A. and Ostlund, N. (1996) *Modern Quantum Chemistry: Introduction to Advanced Electronic Structure Theory* (Dover, New York).
[7] McQuarrie, D.A., Simon, J.D. and Choi, J. (1997) *Physical Chemistry: A Molecular Approach* (University Science Books, Sausalito).
[8] Simons, J. (1991) "An experimental chemist's guide to *ab initio* quantum chemistry", *J. Phys. Chem.* **95**, 1017.
[9] Thijssen, J.M. (1999) *Computational Physics* (Cambridge University Press, Cambridge).

[10] Frenkel, D. and Smit, B. (2002) *Understanding Molecular Simulation: From Algorithms to Applications*, 2nd ed. (Academic Press, London).

[11] Allen, M.P. and Tildesley, D.J. (1987) *Computer Simulation of Liquids* (Clarendon Press, Oxford).

[12] Connors, K.A. (1990) *Chemical Kinetics: The Study of Reaction Rates in Solution* (VCH Publishers, New York).

[13] Laidler, K.J. (1969) *Theories of Chemical Reaction Rates* (McGraw-Hill, New York).

[14] Glasstone, S., Laidler, K.J. and Eyring, H. (1941) *The Theory of Rate Processes* (McGraw-Hill, New York).

[15] For several examples of this kind of system, see Ref. [5], chapter 3.

[16] Sprik, M. (2000) "Computation of the pK of liquid water using coordination constraints", *Chem. Phys.* **258**, 139.

[17] Sprik, M. (1998) "Coordination numbers as reaction coordinates in constrained molecular dynamics", *Faraday Discuss.* **110**, 437.

[18] Gertner, B.J. and Hynes, J.T. (1998) "Model molecular dynamics simulation of hydrochloric acid ionization at the surface of stratospheric ice", *Faraday Discuss.* **110**, 301.

[19] Geissler, P.L., Dellago, C. and Chandler, D. (1999) "Kinetic pathways of ion pair dissociation in water", *J. Phys. Chem. B* **103**, 3706.

[20] See "*Ab Initio* Molecular Dynamics" section, also see Refs. [329,330].

[21] Fukui, K. (1970) "A formulation of reaction coordinate", *J. Phys. Chem.* **74**, 4161.

[22] Fukui, K., Kato, S. and Fujimoto, H. (1975) "Constituent analysis of the potential gradient along a reaction coordinate. Method and an application to $CH_4 + T$ reaction", *J. Am. Chem. Soc.* **97**, 1.

[23] Fukui, K. (1981) "The path of chemical reactions—The IRC approach", *Acc. Chem. Res.* **14**, 363.

[24] The Hessian is the matrix of second derivatives of the energy with respect to the configurational variables. It is also often called the *dynamical matrix*.

[25] For a system with N degrees of freedom, there are $N(N+1)/2$ distinct elements in the Hessian matrix. The numerical estimation of each derivative would require at least two single-point calculations using, for example, an *ab initio* method. This can be prohibitive for all but the simplest systems.

[26] Schinke, R. and Lester, W.A., Jr. (1979) "Trajectory study of $O + H_2$ reactions fitted *ab initio* surfaces I: triplet case", *J. Chem. Phys.* **70**, 4893.

[27] An exception to this is transition path sampling, which does not require a previous knowledge of the transition state. This method is discussed in "Classical Simulation Methods for Equilibrium and Rate Constants" section.

[28] Fletcher, R. (1987) *Practical Methods of Optimization*, 2nd ed. (Wiley, New York).

[29] Gill, P.E., Murray, W. and Wright, M.H. (1981) *Practical Optimization* (Academic Press, New York).

[30] Schlegel, H.B. (2003) "Exploring potential energy surfaces for chemical reactions: an overview of some practical methods", *J. Comput. Chem.* **24**, 1514.

[31] Broyden, C.G. (1970) "The convergence of a class of double-rank minimization algorithms 1. General considerations", *J. Inst. Math. Appl.* **6**, 76.

[32] Broyden, C.G. (1970) "The convergence of a class of double-rank minimization algorithms 2. The new algorithm", *J. Inst. Math. Appl.* **6**, 222.

[33] Fletcher, R. (1970) "A new approach to variable metric algorithms", *Comput. J.* **13**, 317.

[34] Goldfarb, D. (1970) "A family of variable-metric methods derived by variational means", *Math. Comput.* **24**, 23.

[35] Shanno, D.F. (1970) "Conditioning of quasi-Newton methods for function minimization", *Math. Comput.* **24**, 647.

[36] Banerjee, A., Adams, N., Simons, J. and Shepard, R. (1985) "Search for stationary points on surfaces", *J. Phys. Chem.* **89**, 52.

[37] Liu, D.C. and Nocedal, J. (1989) "On the limited memory BFGS method for large-scale optimization", *Math. Prog.* **45**, 503.

[38] Nocedal, J. (1980) "Updating quasi-Newton matrices with limited storage", *Math. Comput.* **35**, 773.

[39] Murrell, J.N., Carter, S., Farantos, S.C., Huxley, P. and Varandas, A.J.C. (1984) *Molecular Potential Energy Functions* (Wiley, New York).

[40] Jasien, P.G. and Shepard, R. (1988) "A general polyatomic potential energy surface fitting method", *Int. J. Quantum Chem. Quantum Chem. Symp.* **22**, 183.

[41] Downing, J.W. and Michi, J. (1981) "Interpolation of multidimensional potential surfaces by polynomial roots", In: Truhlar, D., ed., *Potential Energy Surfaces and Dynamics Calculations for Chemical Reactions and Molecular Energy Transfer* (Plenum Press, New York).

[42] Hollebeek, T., Ho, T.S. and Rabitz, H. (1999) "Constructing multidimensional molecular potential energy surfaces from *ab initio* data", *Annu. Rev. Phys. Chem.* **50**, 537.

[43] Ischtwan, J. and Collins, M.A. (1994) "Molecular potential energy surfaces by interpolation", *J. Chem. Phys.* **100**, 8080.

[44] Jordan, M.J.T., Thompson, K.C. and Collins, M.A. (1995) "Convergence of molecular potential energy surfaces by interpolation: application to the $OH + H_2 \rightarrow H_2O + H$ reaction", *J. Chem. Phys.* **102**, 5647.

[45] Jordan, M.J.T., Thompson, K.C. and Collins, M.A. (1995) "The utility of higher order derivatives in constructing molecular potential energy surfaces by interpolation", *J. Chem. Phys.* **103**, 9669.

[46] Thompson, K.C., Jordan, M.J.T. and Collins, M.A. (1998) "Molecular potential energy surfaces by interpolation in Cartesian coordinates", *J. Chem. Phys.* **108**, 564.

[47] Thompson, K.C., Jordan, M.J.T. and Collins, M.A. (1998) "Polyatomic molecular potential energy surfaces by interpolation in local internal coordinates", *J. Chem. Phys.* **108**, 8302.

[48] Bettens, R.P.A. and Collins, M.A. (1999) "Learning to interpolate molecular potential energy surfaces with confidence: a Bayesian approach", *J. Chem. Phys.* **111**, 816.

[49] Wu, T. and Manthe, I. (2003) "A potential energy surface construction scheme for accurate reaction rate calculations: general approach and a test for the $H + CH_4 \rightarrow H_2 + CH_3$", *J. Chem. Phys.* **119**, 14.

[50] Ayala, P.Y. and Schlegel, H.B. (1997) "A combined method for determining reaction paths, minima, and transition state geometries", *J. Chem. Phys.* **107**, 375.

[51] Elber, R. and Karplus, M. (1987) "A method for determining reaction paths in large molecules: application to myoglobin", *Chem. Phys. Lett.* **139**, 375.

[52] Czerminski, R. and Elber, R. (1990) "Reaction path study of conformational transitions in flexible systems: applications to peptides", *J. Chem. Phys.* **92**, 5580.

[53] Jónsson, H., Mills, G. and Jacobsen, K.W. (1998) "Nudged elastic band method for finding minimum energy paths of transitions", In: Berne, B.J., Ciccotti, G. and Coker, D.F., eds, *Computer Simulation of Rare Events and Dynamics of Classical and Quantum Condensed-Phase Systems—Classical and Quantum Dynamics in Condensed Phase Simulations* (World Scientific, Singapore), see references therein for related methods.

[54] Ponder, J.W. and Case, D.A. (2003) "Force fields for protein simulations", *Adv. Prot. Chem.* **66**, 27.

[55] Hünenberger, P.H. and van Gunsteren, W.F. (1997) "Empirical classical force fields for molecular systems", In: van Gunsteren, W.F., Weiner, P.K. and Wilkinson, A.J., eds, *Computer Simulations of Biomolecular Systems* (Kluwer Academic Publishers, Dordrecht, Netherlands).

[56] MacKerell, A.D., Jr. (2001) "Atomistic models and force fields", In: Becker, O., MacKerell, A.D., Jr., Roux, B. and Watanabe, M., eds, *Computational Biochemistry and Biophysics* (Marcel Dekker Inc., New York).

[57] Orozco, M., Pérez, A., Noy, A. and Luque, F.J. (2003) "Theoretical methods for the simulation of nucleic acids", *Chem. Soc. Rev.* **32**, 350.

[58] Note that this also requires a way to determine which atoms are bonded. This can be an input to the method or it can be calculated using some empirical equations.

[59] Morse, P.M. (1929) "Diatomic molecules according to the wave mechanics. II. Vibrational levels", *Phys. Rev.* **34**, 57.

[60] van Duin, A.C.T., Dasgupta, S., Lorant, F. and Goddard, W.A., III (2001) "ReaxFF: a reactive force field for hydrocarbons", *J. Phys. Chem. A* **105**, 9396.

[61] This is also true for the stretching and valence angle terms. Sometimes the energy penalty due to the out-of-plane bending of an sp^2-hibridized molecule is added separately to the energy expansion.

[62] London, F. (1930) "Zur theorie und systematik der molekularkräfte", *Z. Phys.* **63**, 245.

[63] London, F. (1930) "Über einige eigenschaften und anwendungen der molekularkräfte", *Z. Phys. Chem. B* **11**, 222.

[64] London, F. (1937) "The general theory of molecular forces", *Trans. Faraday Soc.* **33**, 8.

[65] Stone, A.J. (1996) *The Theory of Intermolecular Forces* (Clarendon Press, Oxford).

[66] Morley, S.D., Abraham, R.J., Haworth, I.S., Jackson, D.E., Saunders, M.R. and Vinter, J.G. (1991) "COSMIC(90)—An improved molecular mechanics treatment of hydrocarbons and conjugated systems", *J. Comput.-Aid. Mol. Des.* **5**, 475.

[67] van Duin, A.C.T., Strachan, A., Stewman, S., Zhang, Q., Xu, X. and Goddard, W.A., III (2003) "$ReaxFF_{SiO}$ reactive force field for silicon and silicon oxide systems", *J. Phys. Chem. A* **107**, 3803.

[68] Rappé, A.K. and Goddard, W.A. (1991) "Charge equilibration for molecular dynamics simulations", *J. Phys. Chem.* **95**, 3358.

[69] Mortier, W.J., Ghosh, S.K. and Shankar, S. (1986) "Electronegativity equalization method for the calculation of atomic charges in molecules", *J. Am. Chem. Soc.* **108**, 4315.

[70] Janssens, G.O.A., Baekelandt, B.G., Toufar, H., Mortier, W.J. and Schoonheydt, R.A. (1995) "Comparison of cluster and infinite crystal calculations on zeolites with the electronegativity equalization method (EEM)", *J. Phys. Chem.* **99**, 3251.

[71] This list is by no means complete. For more comprehensive lists of FFs see, for example, Refs. [3,4,54].

[72] Allinger, N.L. (1977) "Conformational analysis. 130. MM2. A hydrocarbon force field utilizing V_1 and V_2 torsional terms", *J. Am. Chem. Soc.* **99**, 8127.

[73] Allinger, N.L., Zhou, X.F. and Bergsma, J. (1994) "Molecular mechanics parameters", *J. Mol. Struct. Theochem.* **118**, 69.

[74] Allinger, N.L., Yuh, Y.H. and Lii, J.H. (1989) "Molecular mechanics. The MM3 force field for hydrocarbons. 1", *J. Am. Chem. Soc.* **111**, 8551.

[75] Lii, J.H. and Allinger, N.L. (1989) "Molecular mechanics. The MM3 force field for hydrocarbons. 2. Vibrational frequencies and thermodynamics", *J. Am. Chem. Soc.* **111**, 8566.

[76] Lii, J.H. and Allinger, N.L. (1989) "Molecular mechanics. The MM3 force field for hydrocarbons. 3. The van der Waals' potentials and crystal data for aliphatic and aromatic hydrocarbons", *J. Am. Chem. Soc.* **111**, 8576.

[77] Allinger, N.L., Chen, K. and Lii, J.H. (1996) "An improved force field (MM4) for saturated hydrocarbons", *J. Comput. Chem.* **17**, 642.

[78] Nevins, N., Chen, K. and Allinger, N.L. (1996) "Molecular mechanics (MM4) calculations on alkenes", *J. Comput. Chem.* **17**, 669.

[79] Nevins, N., Lii, J.H. and Allinger, N.L. (1996) "Molecular mechanics (MM4) calculations on conjugated hydrocarbons", *J. Comput. Chem.* **17**, 695.

[80] Nevins, N. and Allinger, N.L. (1996) "Molecular mechanics (MM4) vibrational frequency calculations for alkenes and conjugated hydrocarbons", *J. Comput. Chem.* **17**, 730.

[81] Allinger, N.L., Chen, K., Katzenellenbogen, J.A., Wilson, S.R. and Anstead, G.M. (1996) "Hyper conjugative effects on carbon-carbon bond lengths in molecular mechanics (MM4)", *J. Comput. Chem.* **17**, 747.

[82] Halgren, T.A. (1996) "Merck molecular force field. 1. Basis, form, scope, parameterization, and performance of MMFF94", *J. Comput. Chem.* **17**, 490.

[83] Halgren, T.A. (1996) "Merck molecular force field. 2. MMFF94 van der Waals and electrostatic parameters for intermolecular interactions", *J. Comput. Chem.* **17**, 520.

[84] Halgren, T.A. (1996) "Merck molecular force field. 3. Molecular geometries and vibrational frequencies for MMFF94", *J. Comput. Chem.* **17**, 553.

[85] Halgren, T.A. (1996) "Merck molecular force field. 4. Conformational energies and geometries for MMFF94", *J. Comput. Chem.* **17**, 587.

[86] Halgren, T.A. (1996) "Merck molecular force field. 5. Extension of MMFF94 using experimental data, additional computational data, and empirical rules", *J. Comput. Chem.* **17**, 616.

[87] Weiner, P.K. and Kollman, P.A. (1981) "AMBER: assisted model building with energy refinement. A general program for modeling molecules and their interactions", *J. Comput. Chem.* **2**, 287.

[88] Cornell, W.D., Cieplak, P., Bayly, C.I., Gould, I.R., Merz, K.M., Jr., Ferguson, D.M., Spellmeyer, D.C., Fox, T., Caldwell, J.W. and Kollman, P.A. (1995) "A second generation force field for the simulation of proteins, nucleic acids, and organic molecules", *J. Am. Chem. Soc.* **117**, 5179.

[89] For a history of the development of the AMBER, OPLS and CHARMM force fields, as well as a more complete list of references, see Ref. [54].

[90] Damm, W., Frontera, A., Tirado-Rives, J. and Jorgensen, W.L. (1997) "OPLS all-atom force field for carbohydrates", *J. Comput. Chem.* **18**, 1955.

[91] Jorgensen, W.L. (1998) "OPLS Force Fields", In: von Rague Schleyer, P., Allinger, N.L., Clark, T., Gasteiger, J., Kollman, P.A., Schaefer, H.F., III and Schreiner, P.R., eds, *Encyclopedia of Computational Chemistry* (John Wiley and Sons, Chichester).

[92] Brooks, R., Bruccoleri, R.E., Olafson, B.D., States, D.J., Swaminathan, S. and Karplus, M. (1983) "CHARMM: a program for macromolecular energy, minimization, and dynamics calculations", *J. Comput. Chem.* **4**, 187.

[93] MacKerell, A.D., Jr., Brooks, B., Brooks, C.L., III, Nilsson, L., Roux, B., Won, Y. and Karplus, M. (1998) "CHARMM: the energy function and its parameterization with an overview of the program", In: von Rague Schleyer, P., Allinger, N.L., Clark, T., Gasteiger, J., Kollman, P.A., Schaefer, H.F., III and Schreiner, P.R., eds, *Encyclopedia of Computational Chemistry* (John Wiley and Sons, Chichester).

[94] van Gunsteren, W.F. and Berendsen, H.J.C. (1987) *Groningen Molecular Simulation (GROMOS) Library Manual* (University of Groningen, Netherlands).

[95] van Gunsteren, W.F., Daura, X. and Mark, A.E. (1998) "The GROMOS Force Field", In: von Rague Schleyer, P., Allinger, N.L., Clark, T., Gasteiger, J., Kollman, P.A., Schaefer, H.F., III and Schreiner, P.R., eds, *Encyclopedia of Computational Chemistry* (John Wiley and Sons, Chichester).

[96] Scott, W.R.P., Hünenberger, P.H., Tironi, I.G., Mark, A.E., Billeter, S.R., Fennen, J., Torda, A.E., Huber, T., Krüger, P. and van Gunsteren, W.F. (1999) "The GROMOS biomolecular simulation program package", *J. Phys. Chem. A* **103**, 3596.

[97] Némethy, G., Pottle, M.S. and Scheraga, H.A. (1983) "Energy parameters in polypeptides. 9. Updating of geometrical parameters, nonbonded interactions, and hydrogen bond interactions for the naturally occurring amino acids", *J. Phys. Chem.* **87**, 1883.

[98] Némethy, G., Gibson, K.D., Palmer, K.A., Yoon, C.N., Paterlini, G., Zagari, A., Rumsey, S. and Scheraga, H.A. (1992) "Energy parameters in polypeptides. 10. Improved geometrical parameters and nonbonded interactions for use in the ECEPP/3 algorithm, with application to proline-containing peptides", *J. Phys. Chem.* **96**, 6472.

[99] Ripoll, D.R. and Scheraga, H.A. (1998) "ECEPP: empirical conformational energy program for peptides", In: von Rague Schleyer, P., Allinger, N.L., Clark, T., Gasteiger, J., Kollman, P.A., Schaefer, H.F., III and Schreiner, P.R., eds, *Encyclopedia of Computational Chemistry* (John Wiley and Sons, Chichester).

[100] Mayo, S.L., Olafson, B.D. and Goddard, W.A., III (1990) "DREIDING: a generic force field for molecular simulations", *J. Phys. Chem.* **94**, 8897.

[101] Comba, P. and Hambley, T.W. (2001) *Molecular Modeling of Inorganic Compounds* (Wiley-VCH, Weinheim).

[102] Allured, V.S., Kelly, C.M. and Landis, C.R. (1991) "SHAPES empirical force field: new treatment of angular potentials and its application to square-planar transition-metal complexes", *J. Am. Chem. Soc.* **113**, 1.

[103] Dillen, J.L.M. (1995) "An empirical force field. 1. Alkanes", *J. Comput. Chem.* **16**, 595.

[104] Dillen, J.L.M. (1995) "An empirical force field. 2. Crystalline alkanes", *J. Comput. Chem.* **16**, 610.

[105] Brenner, D.W. (1990) "Empirical potential for hydrocarbons for use in simulating the chemical vapor deposition of diamond films", *Phys. Rev. B* **42**, 9458.
[106] Stuart, S.J., Tutein, A.B. and Harrison, J.A. (2000) "A reactive potential for hydrocarbons with intermolecular interaction", *J. Chem. Phys.* **112**, 6472.
[107] Rappé, A.K., Casewit, C.J., Colwell, K.S., Goddard, W.A., III and Skiff, W.M. (1992) "UFF, a full periodic table force field for molecular mechanics and molecular dynamics simulations", *J. Am. Chem. Soc.* **114**, 10024.
[108] Rappé, A.K., Pietsch, M.A., Wiser, D.C., Hart, J.R., Bormann, L.M. and Skiff, W.M. (1997) "RFF, conceptual development of a full periodic table force field for studying reaction potential surfaces", *J. Mol. Eng.* **7**, 385.
[109] Eksterowicz, J.E. and Houk, K.N. (1993) "Transition-state modeling with empirical force fields", *Chem. Rev.* **93**, 2439.
[110] Jensen, F. (2003) "Using force field methods for locating transition structures", *J. Chem. Phys.* **119**, 8804.
[111] Jensen, F. and Norrby, P.O. (2003) "Transition states from empirical force fields", *Theor. Chem. Acc.* **109**, 1.
[112] Jensen, F. (1994) "Transition structure modeling by intersecting potential energy surfaces", *J. Comput. Chem.* **15**, 1199.
[113] Jensen, F. (1992) "Locating minima on seams of intersecting potential energy surfaces. An application to transition structure modeling", *J. Am. Chem. Soc.* **114**, 1596.
[114] Kim, Y., Corchado, J.C., Villà, J., Xing, J. and Truhlar, D.G. (2000) "Multiconfiguration molecular mechanics algorithm for potential energy surfaces of chemical reactions", *J. Chem. Phys.* **112**, 2718.
[115] Albu, T.V., Corchado, J.C. and Truhlar, D.G. (2001) "Molecular mechanics for chemical reactions: a standard strategy for using multiconfiguration molecular mechanics for variational transition state theory with optimized multidimensional tunneling", *J. Phys. Chem. A* **105**, 8465.
[116] Norrby, P.O. (2000) "Selectivity in asymmetric synthesis from QM-guided molecular mechanics", *J. Mol. Struct. Theochem.* **506**, 9.
[117] Bernardi, F., Olivucci, M. and Robb, M.A. (1992) "Simulation of MC-SCF results on covalent organic multi-bond reactions: molecular mechanics with valence bond (MM-VB)", *J. Am. Chem. Soc.* **114**, 1606.
[118] Bearpark, M.J. and Robb, M.A. (1994) "Molecular mechanics valence-bond methods for large active spaces: application to conjugated polycyclic hydrocarbons", *Chem. Phys. Lett.* **217**, 513.
[119] Mo, Y. and Gao, J. (2000) "An *ab initio* molecular orbital—valence bond (MOVB) method for simulating chemical reactions in solution", *J. Phys. Chem. A* **104**, 3012.
[120] Mo, Y. and Gao, J. (2000) "*Ab initio* QM/MM simulations with a molecular orbital—valence bond (MOVB) method: application to an S_N2 reaction in water", *J. Comput. Chem.* **21**, 1458.
[121] Gundertofte, K., Palm, J., Pettersson, I. and Stamvik, A. (1991) "A comparison of conformational energies calculated by molecular mechanics (MM2(85), SYBYL-5.1, SYBYL-5.21 and CHEMX) and semiempirical (AM1 and PM3) methods", *J. Comput. Chem.* **12**, 200.
[122] Roterman, I.K., Gibson, K.D. and Scheraga, H.A. (1989) "A comparison of the CHARMM, AMBER and ECEPP potentials for peptides. 1. Conformational predictions of the tandemly repeated peptide $(ASN\text{-}ALA\text{-}ASN\text{-}PRO)_9$", *J. Biomol. Struct. Dyn.* **7**, 391.
[123] Roterman, I.K., Lambert, M.H., Gibson, K.D. and Scheraga, H.A. (1989) "A comparison of the CHARMM, AMBER and ECEPP potentials for peptides. 2. Phi-psi maps for n-acetyl alanine n′-methyl amide: comparisons, contrasts and simple experimental tests", *J. Biomol. Struct. Dyn.* **7**, 421.
[124] Teeter, M.M. and Case, D.A. (1990) "Harmonic and quasiharmonic descriptions of crambin", *J. Phys. Chem.* **94**, 8091.
[125] Kini, R.M. and Evans, H.J. (1992) "Comparison of protein models minimized by the all-atom and united-atom models in the AMBER force field: correlation of RMS deviation with the crystallographic R factor and size", *J. Biomol. Struct. Dyn.* **10**, 265.
[126] Kaminski, G. and Jorgensen, W.L. (1996) "Performance of the AMBER94, MMFF94, and OPLS-AA force fields for modeling organic liquids", *J. Phys. Chem.* **100**, 18010.
[127] Gundertofte, K., Liljefors, T., Norrby, P.O. and Pettersson, I. (1996) "A comparison of the conformational energies calculated by several molecular mechanics methods", *J. Comput. Chem.* **17**, 429.
[128] Hobza, P., Kabeláč, M., Šponer, J., Mejzlík, P. and Vondrášek, J. (1997) "Performance of empirical potentials (AMBER, CFF95, CVFF, CHARMM, OPLS, POLTEV), semiempirical quantum chemical methods (AM1, MNDO/M, PM3), and *ab initio* Hartree–Fock method for interaction of DNA bases: comparison with nonempirical beyond Hartree-Fock results", *J. Comput. Chem.* **18**, 1136.
[129] Ceccarelli, M. and Marchi, M. (1997) "Simulation of a protein crystal at constant pressure", *J. Phys. Chem. B* **101**, 2105.
[130] Pérez, S., Imberty, A., Engelsen, S.B., Gruza, J., Mazeau, K., Jimenez-Barbero, J., Poveda, A., Espinosa, J.-F., van Eyck, B.P., Johnson, G., French, A.D., Kouwijzer, M.L.C.E., Grootenuis, P.D.J., Bernardi, A., Raimondi, L., Senderowitz, H., Durier, V., Vergoten, G. and Rasmussen, K. (1998) "A comparison and chemometric analysis of several molecular mechanics force fields and parameter sets applied to carbohydrates", *Carbohyd. Res.* **314**, 141.
[131] Price, D.J. and Brooks, C.L., III (2002) "Modern protein force fields behave comparably in molecular dynamics simulations", *J. Comput. Chem.* **23**, 1045.
[132] Reddy, S.Y., Leclerc, F. and Karplus, M. (2003) "DNA polymorphism: a comparison of force fields for nucleic acids", *Biophys. J.* **84**, 1421.
[133] Hu, H., Elstner, M. and Hermans, J. (2003) "Comparison of a QM/MM force field and molecular mechanics force fields in simulations of alanine and glycine dipeptides (Ace-Ala-Nme and Ace-Gly-Nme) in water in relation to the problem of modeling the unfolded peptide backbone in solution", *Proteins* **50**, 451.
[134] Zhou, R.H. (2003) "Free energy landscape of protein folding in water: explicit vs. implicit solvent", *Proteins* **53**, 148.
[135] Patra M. and Karttunen, M. (2004) "Systematic comparison of force fields for microscopic simulations of NaCl in aqueous solutions: diffusion and structural properties", *J. Comput. Chem.* **25**, 678.
[136] Ford, M.G., Weimar, T., Köhli, T. and Woods, R.J. (2003) "Molecular dynamics simulations of galectin-1-oligosaccharide complexes reveal the molecular basis for ligand diversity", *Proteins* **53**, 229.
[137] Bingham, N.C., Smith, N.E.C., Cross, T.A. and Busath, D.D. (2003) "Molecular dynamics simulations of Trp side-chain conformational flexibility in the gramicidin A channel", *Biopolymers* **71**, 593.
[138] Clément, M.J., Imberty, A., Phalipon, A., Pérez, S., Simenel, C., Mulard, L.A. and Delepierre, M. (2003) "Conformational studies of the O-species polysaccharide of Shigella flexneri 5a and of four related synthetic pentasaccharide fragments using NMR and molecular modeling", *J. Biol. Chem.* **278**, 47928.
[139] Sarzynska, J., Nilsson, L. and Kulinski, T. (2003) "Effects of base substitutions in an RNA hairpin from molecular dynamics and free energy simulations", *Biophys. J.* **85**, 3445.
[140] Schaefer, H.F. III, ed. (1977) *Modern Theoretical Chemistry* (Plenum Press, New York), Vols. III and IV.
[141] Lawley, K.P., ed. (1987) *Advances in Chemical Physics* (Wiley, New York), Vols. LXVII and LXIX.
[142] Makri, N. (1999) "Time-dependent quantum methods for large systems", *Annu. Rev. Phys. Chem.* **50**, 167.
[143] Althorpe, S.C. and Clary, D.C. (2003) "Quantum scattering calculations on chemical reactions", *Annu. Rev. Phys. Chem.* **54**, 493.
[144] Lester, W.A. Jr. and Hammond, B.L. (1990) "Quantum Monte Carlo for the electronic structure of atoms and molecules", *Annu. Rev. Phys. Chem.* **41**, 283.
[145] Foulkes, W.M.C., Mitas, L., Needs, R.J. and Rajagopal, G. (2001) "Quantum Monte Carlo simulations of solids", *Rev. Mod. Phys.* **73**, 33.
[146] Born, M. and Oppenheimer, R. (1927) "Zur Quantentheorie der Molekeln", *Ann. Phys.* **84**, 457.

[147] Tully, J.C. (2000) "Perspective on Zur Quantentheorie der Molekeln:", *Theor. Chem. Acc.* **103**, 173, Born, M., Oppenheimer, R. (1927) Ann. Phys. 84:457.

[148] Sutcliffe, B.T. (1975) "Fundamentals of computational quantum chemistry", In: Diercksen, G.H.F., Sutcliffe, B.T. and Veillard, A., eds, *Computational Techniques in Quantum Chemistry* (Reidel, Boston).

[149] The term "adiabatic" in this context makes reference to the absence of thermal coupling between the electrons and the nuclei, which is equivalent to the statement that the electronic states do not depend on the momenta of the nuclei. Strictly speaking, the adiabatic approximation is not exactly the same as the BO approximation, although the terms are often confused. For a detailed explanation of this point, see Ref. [5], chapter 1, and Ref. [4], chapter 3.

[150] Preston, R.K. and Tully, J.C. (1971) "Effects of surface crossing in chemical reactions: the H_3^+ system", *J. Chem. Phys.* **54**, 4297.

[151] Tully, J.C. and Preston, R.K. (1971) "Trajectory surface hopping approach to nonadiabatic molecular collisions: the reaction of H^+ with D_2", *J. Chem. Phys.* **55**, 562.

[152] Tully, J.C. (1990) "Molecular dynamics with electronic transitions", *J. Chem. Phys.* **93**, 1061.

[153] Drukker, K. (1999) "Basics of surface hopping in mixed quantum/classical simulations", *J. Comput. Phys.* **153**, 225.

[154] Butler, L.J. (1998) "Chemical reaction dynamics beyond the Born–Oppenheimer approximation", *Annu. Rev. Phys. Chem.* **49**, 125.

[155] A Hermitian operator is one that is equal to its adjoint.

[156] Poirier, R., Kari, R. and Csizmadia, I.G. (1985) *Handbook of Gaussian Basis Sets: A Compendium for Ab-Initio Molecular Orbital Calculations* (Elsevier, New York).

[157] Dunning, T.H. and Hay, P.J. Gaussian Basis Sets for Molecular Calculations, in Ref. [140], Vol. 3.

[158] Slater, J.C. (1930) "Atomic shielding constants", *Phys. Rev.* **36**, 57.

[159] Collins, J.B., Schleyer, P.R., Binkley, J.S. and Pople, J.A. (1976) "Self-consistent molecular orbital methods. XVII. Geometries and binding energies of second-row molecules. A comparison of three basis sets", *J. Chem. Phys.* **64**, 5142 and references therein.

[160] Binkley, J.S., Pople, J.A. and Hehre, W.J. (1980) "Self-consistent molecular orbital methods. 21. Small split-valence basis sets for first-row elements", *J. Am. Chem. Soc.* **102**, 939.

[161] Gordon, M.S., Binkley, J.S., Pople, J.A., Pietro, W.J. and Hehre, W.J. (1982) "Self-consistent molecular orbital methods. 22. Small split-valence basis sets for second-row elements", *J. Am. Chem. Soc.* **104**, 2797.

[162] Pietro, W.J., Francl, M.M., Hehre, W.J., Defrees, D.J., Pople, J.A. and Binkley, J.S. (1982) "Self-consistent molecular orbital methods. 24. Supplemented small split-valence basis sets for second-row elements", *J. Am. Chem. Soc.* **104**, 5039.

[163] Ditchfield, R., Hehre, W.J. and Pople, J.A. (1971) "Self-consistent molecular orbital methods. IX. An extended Gaussian-type basis for molecular-orbital studies of organic molecules", *J. Chem. Phys.* **54**, 724.

[164] Hehre, W.J., Ditchfield, R. and Pople, J.A. (1972) "Self-consistent molecular orbital methods. XII. Further extensions of Gaussian-type basis sets for use in molecular orbital studies of organic molecules", *J. Chem. Phys.* **56**, 2257.

[165] Hariharan, P.C. and Pople, J.A. (1974) "Accuracy of AH equilibrium geometries by single determinant molecular-orbital theory", *Mol. Phys.* **27**, 209.

[166] Krishnan, R., Binkley, J.S., Seeger, R. and Pople, J.A. (1980) "Self-consistent molecular orbital methods. XX. A basis set for correlated wave functions", *J. Chem. Phys.* **72**, 650.

[167] McLean, A.D. and Chandler, G.S. (1980) "Contracted Gaussian basis sets for molecular calculations. I. Second row atoms, $Z = 11–18$", *J. Chem. Phys.* **72**, 5639.

[168] Blaudeau, J.P., McGrath, M.P., Curtiss, L.A. and Radom, L. (1997) "Extension of Gaussian-2 (G2) theory to molecules containing third-row atoms K and Ca", *J. Chem. Phys.* **107**, 5016.

[169] Curtiss, L.A., McGrath, M.P., Blaudeau, J.-P., Davis, N.E., Binning, R.C. Jr. and Radom, L. (1995) "Extension of Gaussian-2 theory to molecules containing third-row atoms Ga-Kr", *J. Chem. Phys.* **103**, 6104.

[170] Francl, M.M., Pietro, W.J., Hehre, W.J., Binkley, J.S., Gordon, M.S., DeFrees, D.J. and Pople, J.A. (1982) "Self-consistent molecular orbital methods. XXIII. A polarization-type basis set for second-row elements", *J. Chem. Phys.* **77**, 3654.

[171] Rassolov, V.A., Pople, J.A., Ratner, M.A. and Windus, T.L. (1998) "6-31G* basis set for atoms K through Zn", *J. Chem. Phys.* **109**, 1223.

[172] Rassolov, V.A., Ratner, M.A., Pople, J.A., Redfern, P.C. and Curtiss, L.A. (2001) "6-31G* basis set for third-row atoms", *J. Comput. Chem.* **22**, 976.

[173] Petersson, G.A., Bennett, A., Tensfeldt, T.G., Al-Laham, M.A. and Shirley, W.A. (1988) "A complete basis set model chemistry. I. The total energies of closed-shell atoms and hydrides of the first-row elements", *J. Chem. Phys.* **89**, 2193.

[174] A *Rydberg orbital* is a diffuse function that describes the region of space that would be occupied by an electron in the presence of a closed-shell molecular cation. An example of a Rydberg state is that of the NH_4 molecule.

[175] Dunning, T.H., Jr. (1989) "Gaussian basis sets for use in correlated molecular calculations. I. The atoms boron through neon and hydrogen", *J. Chem. Phys.* **90**, 1007.

[176] Kendall, R.A., Dunning, T.H., Jr. and Harrison, R.J. (1992) "Electron affinities of the first-row atoms revisited. Systematic basis sets and wave functions", *J. Chem. Phys.* **96**, 6796.

[177] Woon, D.E. and Dunning, T.H., Jr. (1993) "Gaussian basis sets for use in correlated molecular calculations. III. The atoms aluminum through argon", *J. Chem. Phys.* **98**, 1358.

[178] This is also known as the *basis set superposition error*. The term *Pulay forces* is more commonly used in the context of *ab initio* molecular dynamics, where plane wave basis sets are most commonly used.

[179] Marx, D. and Hutter, J. (2000) "*Ab Initio* molecular dynamics: theory and implementation", In: Grotendorst, J., ed., *Modern Methods and Algorithms of Quantum Chemistry Proceedings* (Forschungszentrum Jülich, Vol. 1.

[180] Hartree, D.R. (1928) "The wave mechanics of an atom with a non-Coulomb central field. Part I. Theory and methods", *Proc. Camb. Philos. Soc.* **24**, 89.

[181] Hartree, D.R. (1928) "The wave mechanics of an atom with a non-Coulomb central field. Part II. Some results and discussion", *Proc. Camb. Philos. Soc.* **24**, 111.

[182] Fock, V. (1930) "Näherungsmethode zur Lösung der quantenmechanischen Mehrkörperproblems", *Z. Physik.* **61**, 126.

[183] Slater, J.C. (1929) "The theory of complex spectra", *Phys. Rev.* **34**, 1293.

[184] In RHF calculations for open-shell systems (which are not recommendable in general), UHF calculations, and in calculations involving excited determinants, there is an additional complication because states appear that are not eigenfunctions of the electronic spin operator. This problem can be solved by using spin-adapted configurations. Discussions of this topic can be found in Refs. [4,6].

[185] Roothaan, C.C.J. (1951) "New developments in molecular orbital theory", *Rev. Mod. Phys.* **23**, 69.

[186] Zerner, M.C. (2000) "Perspective on 'New developments in molecular orbital theory':", *Theor. Chem. Acc.* **103**, 217, Roothaan, C.C.J. (1951) Rev. Mod. Phys. 23:69–89.

[187] Hall, G.G. (1951) "The molecular orbital theory of chemical valency. 8. A method of calculating ionization potentials", *Proc. Roy. Soc. Lond. Ser. A* **205**, 541.

[188] This is the *Mulliken*, or *chemist's* notation for the two-electron integrals.

[189] There is, in fact, some correlation between the electrons included in the HF method due to the presence of the exchange energy. In the HF picture, electrons with the same spin avoid being in the same region, and a *Fermi hole* is said to exist around each electron. The term correlation energy refers to the energy that is not included in the HF method.

[190] Prencipe, M., Tribaudino, M. and Nestola, F. (2003) "Charge-density analysis of spodumene ($LiAlSi_2O_6$), from *ab initio* Hartree–Fock calculations", *Phys. Chem. Miner.* **30**, 606.

[191] Csontos, J., Kálmán, M. and Tasi, G. (2003) "Conformational analysis of melatonin at Hartree–Fock *ab initio* level", *J. Mol. Struct. Theochem.* **640**, 69.

[192] Zhang, D.W., Xiang, Y. and Zhang, J.Z.H. (2003) "New advance in computational chemistry: full quantum mechanical *ab initio* computation of Streptavidin–Biotin interaction energy", *J. Phys. Chem. B* **107**, 12039.
[193] Schütz, M., Hetzer, G. and Werner, H.J. (1999) "Low-order scaling local electron correlation methods. I. Linear scaling local MP2", *J. Chem. Phys.* **111**, 5691.
[194] Scuseria, G.E. and Ayala, P.Y. (1999) "Linear scaling coupled cluster and perturbation theories in the atomic orbital basis", *J. Chem. Phys.* **111**, 8330.
[195] Koopmans, T. (1933) "Ordering of wave functions and eigenenergies to the individual electrons of an atom", *Physica* **1**, 104.
[196] and also the energies of the occupied orbitals to the ionization potentials. For a discussion of Koopmans' theorem see, for example, Refs. [2,4,6].
[197] Pople, J.A., Binkley, J.S. and Seeger, R. (1976) "Theoretical models incorporating electron correlation", *Int. J. Quantum Chem.* **Y-10**, 1.
[198] Pople, J.A., Head-Gordon, M. and Raghavachari, K. (1987) "Quadratic configuration interaction. A general technique for determining electron correlation energies", *J. Chem. Phys.* **87**, 5968.
[199] Ross, B.O., Taylor, P.R. and Siegbahn, P.E.M. (1980) "A complete active space SCF method (CASSCF) using a density matrix formulated super-CI approach", *Chem. Phys.* **48**, 157; see also Refs. [44,141].
[200] In the case of transition metals, also the *d* states from the next-to-last layer will likely need to be included.
[201] Goddard, W.A., III, Dunning, T.H., Jr., Hunt, W.J. and Hay, P.J. (1973) "Generalized valence bond description of bonding in low-lying states of molecules", *Acc. Chem. Res.* **6**, 368 and references therein.
[202] Goddard, W.A., III and Harding, L.B. (1978) "The description of chemical bonding from *ab initio* calculations", *Ann. Rev. Phys. Chem.* **29**, 363.
[203] Heitler, W. and London, F. (1927) "Wechselwirkung neutraler atome und homöopolare bindung nach der quantenmechanik", *Z. Phys.* **44**, 455.
[204] Frenking, G. (2000) "Perspecitve on Wechselwirkung neutraler atome und homöopolare bindung nach der quantenmechanik:", *Theor. Chem. Acc.* **103**, 177, Heitler, W., London, F. (1927) Z. Phys. 44:455–472.
[205] Gallup, G.A. (2002) *Valence Bond Methods: Theory and Applications* (Cambridge University Press, Cambridge).
[206] Cooper, D.L., ed. (2002) *Valence Bond Theory* (Elsevier, Amsterdam).
[207] Gerratt, J., Cooper, D.L., Karadakov, P.B. and Raimondi, M. (1997) "Modern valence bond theory", *Chem. Soc. Rev.* **26**, 87.
[208] Hiberty, P.C. and Shaik, S. (2002) "Two new symmetry-adapted perturbation theories for the calculation of intermolecular interaction energies", *Theor. Chem. Acc.* **108**, 255.
[209] Thorsteinsson, T., Cooper, D.L., Gerratt, J., Karadakov, P.B. and Raimondi, M. (1996) "Modern valence bond representations of CASSCF wavefunctions", *Theor. Chem. Acc.* **93**, 343.
[210] Sakai, S. (2003) "Theoretical analysis of concerted and stepwise mechanisms of the hetero-Diels-Alder reaction of butadiene with formaldehyde and thioformaldehyde", *J. Mol. Struct. Theochem.* **630**, 177.
[211] Wirtz, L., Burgdörfer, J., Dallos, M., Müller, T. and Lischka, H. (2003) "Potential-energy surfaces for charge exchange between singly charged ions and a LiF surface", *Phys. Rev. A* **68**, #032902.
[212] Chattopadhyaya, S. and Das, K.K. (2003) "Electronic states of SiSe: a configuration interaction study", *Chem. Phys. Lett.* **382**, 249.
[213] Møller, C. and Plesset, M.S. (1934) "Note on an approximation treatment for many-electron systems", *Phys. Rev.* **46**, 618.
[214] Pople, J.A., Krishnan, R., Schlegel, H.B. and Binkley, J.S. (1978) "Electron correlation theories and their application to study of simple reaction potential surfaces", *Int. J. Quantum Chem.* **14**, 545.
[215] Bartlett, R.J. and Silver, D.M. (1975) "Many-body perturbation theory applied to electron pair correlation energies. I. Closed-shell first-row diatomic hydrides", *J. Chem. Phys.* **62**, 3258.
[216] Head-Gordon, M., Pople, J.A. and Frisch, M.J. (1988) "MP2 energy evaluation by direct methods", *Chem. Phys. Lett.* **153**, 503.
[217] Frisch, M.J., Head-Gordon, M. and Pople, J.A. (1990) "A direct MP2 gradient method", *Chem. Phys. Lett.* **166**, 275.
[218] Frisch, M.J., Head-Gordon, M. and Pople, J.A. (1990) "Semi-direct algorithm for the MP2 energy and gradient", *Chem. Phys. Lett.* **166**, 281.
[219] Krishnan, R. and Pople, J.A. (1978) "Approximate 4th-order perturbation theory of electron correlation energy", *Int. J. Quantum Chem.* **14**, 91.
[220] Andersson, K., Malmqvist, P.-Å. and Ross, B.O. (1992) "Second-order perturbation theory with a complete active space self-consistent field reference function", *J. Chem. Phys.* **96**, 1218.
[221] Ignatov, S.K., Sennikov, P.G., Razuvaev, A.G., Chuprov, L.A., Schrems, O. and Ault, B.S. (2003) "Theoretical study of the reaction mechanism and role of water clusters in the gas-phase hydrolysis of $SiCl_4$", *J. Phys. Chem. A* **107**, 8705.
[222] Enchev, V., Ivanova, G. and Stoyanov, N. (2003) "Tautomeric and conformational equilibrium of 2-nitrosophenol and 9,10-phenanthrenequinonemonooxime: *ab initio* and NMR study", *J. Mol. Struct. Theochem.* **640**, 149.
[223] Khuong, K.S. and Houk, K.N. (2003) "One-bond, two-bond, and three-bond mechanisms in thermal diazetizations of 2,3-Diazabicyclo[2.2.2]oct-2-enes, *trans*-Azomethane, and 2,3-Diazabicyclo[2.2.1]hept-2-ene", *J. Am. Chem. Soc.* **125**, 14867.
[224] Sinanoğlu, O. (1964) "Many-electron theory of atoms, molecules and their interactions", *Adv. Chem. Phys.* **6**, 315.
[225] Nesbet, R.K. (1965) "Electronic correlation in atoms and molecules", *Adv. Chem. Phys.* **9**, 321.
[226] Rigorously speaking, the pair function should also contain the contributions from the single excitations of electrons *a* and *b*. We include only the double excitations in this discussion, which eventually leads to the CCD method.
[227] A unitary transformation is defined in terms of an operator whose inverse is equal to its adjoint. It is the complex equivalent of a rotation operator.
[228] Also triplets, quintuples, etc., which would lead to full CI. As mentioned in note [226], we consider only the even excitation contributions.
[229] Čižek, J. (1966) "Correlation problem in atomic and molecular systems. Calculation of wave function components in Ursell-type expansion using quantum-field theoretical methods", *J. Chem. Phys.* **45**, 4256.
[230] Čižek, J. (1969) "Use of the cluster expansion and the technique of diagrams in calculations of correlation effects in atoms and molecules", *Adv. Chem, Phys.* **14**, 35.
[231] The equations for CCD were derived in Čižek, J. and Paldus, J. (1971) "Correlation problems in atomic and molecular systems. III. Rederivation of the coupled-pair many-electron theory using the traditional quantum chemical methods", *Int. J. Quantum. Chem.* **5**, 359.
[232] Purvis, G.D., III, and Bartlett, R.J. (1982) "A full coupled-cluster singles and doubles model: the inclusion of disconnected triples", *J. Chem. Phys.* **76**, 1910.
[233] Bartlett, R.J. (1989) "Coupled-cluster approach to molecular structure and spectra: a step toward predictive quantum chemistry", *J. Phys. Chem.* **93**, 1697.
[234] Bartlett, R.J. (1981) "Many-body perturbation theory and coupled cluster theory for electron correlation in molecules", *Annu. Rev. Phys. Chem.* **32**, 359.
[235] Lee, T.J. and Scuseria, G.E. (1995) "Achieving chemical accuracy with coupled-cluster theory", In: Langhoff, S.R., ed., *Quantum Mechanical Structure Calculations with Chemical Accuracy* (Kluwer Academic, Boston).
[236] Bartlett, R.J., ed. (1997) *Recent Advances in Coupled-Cluster Methods* (World Scientific, New Jersey).
[237] Oliphant, N. and Adamowicz, L. (1993) "Multireference coupled-cluster method for electronic structure of molecules", *Int. Rev. Phys. Chem.* **12**, 339.
[238] Mahapatra, U.S., Datta, B. and Mukherjee, D. (1999) "A size-consistent state-specific multireference coupled cluster theory: formal developments and molecular applications", *J. Chem. Phys.* **110**, 6171.

[239] Kowalski, K. and Piecuch, P. (2000) "Complete set of solutions of multireference coupled-cluster equations: the state-universal formalism", *Phys. Rev. A* **61**, #052506.

[240] Chattopadhyay, S., Mahapatra, U.S. and Mukherjee, D. (1999) "Property calculations using perturbed orbitals via state-specific multireference coupled-cluster and perturbation theories", *J. Chem. Phys.* **111**, 3820.

[241] See, e.g. Ref. [4].

[242] Scuseria, G.E. and Lee, T.J. (1990) "Comparison of coupled-cluster methods which include the effects of connected triple excitations", *J. Chem. Phys.* **93**, 5851.

[243] Feller, D. and Dixon, D.A. (2003) "A nonparametrized *ab initio* determination of the heat of formation of hydroxylamine, NH_2OH", *J. Phys. Chem. A* **107**, 10419.

[244] Tobita, M., Perera, S.A., Musial, M., Bartlett, R.J., Nooijen, M. and Lee, J.S. (2003) "Critical comparison of single-reference and multireference coupled-cluster methods: geometry, harmonic frequencies, and excitation energies of N_2O_2", *J. Chem. Phys.* **119**, 10713.

[245] Sari, L., McCarthy, M.C., Schaefer, H.F., III and Thaddeus, P. (2003) "Mono- and dibridged isomers of Si_2H_3 and Si_2H_4: the true ground state global minima. Theory and experiment in concert", *J. Am. Chem. Soc.* **125**, 11409.

[246] Pople, J.A. and Segal, G.A. (1965) "Approximate self-consistent molecular orbital theory. 2. Calculations with complete neglect of differential overlap", *J. Chem. Phys.* **43**, S136.

[247] Pople, J.A. and Segal, G.A. (1966) "Approximate self-consistent molecular orbital theory. 3. CNDO results for AB_2 and AB_3 systems", *J. Chem. Phys.* **44**, 3289.

[248] Pople, J.A., Beveridge, D.L. and Dobosh, P.A. (1967) "Approximate self-consistent molecular orbital theory. 5. Intermediate neglect of differential overlap", *J. Chem. Phys.* **47**, 2026.

[249] Pople, J.A., Santry, D.P. and Segal, G.A. (1965) "Approximate self-consistent molecular orbital theory. I. Invariant procedures", *J. Chem. Phys.* **43**, S129.

[250] Bingham, R.C., Dewar, M.J.S. and Lo, D.H. (1975) "Ground states of molecules. XXV. MINDO/3. Improved version of the MINDO semiempirical SCF-MO method", *J. Am. Chem. Soc.* **97**, 1285.

[251] Bingham, R.C., Dewar, M.J.S. and Lo, D.H. (1975) "Ground states of molecules. XXVI. MINDO/3 calculations for hydrocarbons", *J. Am. Chem. Soc.* **97**, 1294.

[252] Bingham, R.C., Dewar, M.J.S. and Lo, D.H. (1975) "Ground states of molecules. XXVII. MINDO/3 calculations for carbon, hydrogen, oxygen and nitrogen species", *J. Am. Chem. Soc.* **97**, 1302.

[253] Bingham, R.C., Dewar, M.J.S. and Lo, D.H. (1975) "Ground states of molecules. XXVIII. MINDO/3 calculations for compounds containing carbon, hydrogen, fluorine, and chlorine", *J. Am. Chem. Soc.* **97**, 1307.

[254] Dewar, M.J.S. and Thiel, W. (1977) "Ground states of molecules. 38. The MNDO method. Approximations and parameters", *J. Am. Chem. Soc.* **99**, 4899.

[255] Dewar, M.J.S. and Thiel, W. (1977) "Ground states of molecules. 39. MNDO results for molecules containing hydrogen, carbon, nitrogen and oxygen", *J. Am. Chem. Soc.* **99**, 4907.

[256] Dewar, M.J.S., Zoebisch, E.G., Healy, E.F. and Stewart, J.J.P. (1985) "Development and use of quantum mechanical molecular models. 76. AM1: a new general purpose quantum mechanical molecular model", *J. Am. Chem. Soc.* **107**, 3902.

[257] Stewart, J.J.P. (1989) "Optimization of parameters for semiempirical methods. 1. Method", *J. Comput. Chem.* **10**, 209.

[258] Stewart, J.J.P. (1989) "Optimization of parameters for semiempirical methods. 2. Applications", *J. Comput. Chem.* **10**, 221.

[259] Dewar, M.J.S., Jie, C. and Yu, J. (1993) "SAM1: the first of a new series of general purpose quantum mechanical molecular models", *Tetrahedron* **49**, 5003.

[260] Winget, P., Selçuki, C., Horn, A.H.C., Martin, B. and Clark, T. (2003) "Towards a next generation neglect of diatomic differential overlap based semiempirical molecular orbital technique", *Theor. Chem. Acc.* **110**, 254.

[261] Linnanto, J. and Korppi-Tommola, K. (2004) "Semiempirical PM5 molecular orbital study on chlorophylls and bacteriochlorophylls: comparison of semiempirical, *ab initio*, and density functional results", *J. Comput. Chem.* **25**, 123.

[262] Tubert-Brohman, I., Guimarães, C.R.W., Repasky, M.P. and Jorgensen, W.L. (2004) "Extension of the PDDG/PM3 and PDDG/MNDO semiempirical molecular orbital methods to the halogens", *J. Comput. Chem.* **25**, 138.

[263] Bräuer, M., Kunert, M., Dinjus, E., Kluβmann, M., Döring, M., Görls, H. and Anders, E. (2000) "Evaluation of the accuracy of PM3, AM1 and MNDO/d as applied to zinc compounds", *J. Mol. Struct. Theochem.* **505**, 289.

[264] Pichierri, F. (2003) "Computation of the permanent dipole moment of α-chymotrypsin from linear scaling semiempirical quantum mechanical methods", *J. Mol. Struct. Theochem.* **664–665**, 197.

[265] Tsukamoto, K., Nakamura, S. and Shimizu, K. (2003) "SAM1 semiempirical calculations on the catalytic cycle of nitric oxide reductase from *Fusarium oxysporum*", *J. Mol. Struct. Theochem.* **624**, 309.

[266] Lebedev, N.G., Zaporotskova, I.V. and Chernozatonskii, L.A. (2004) "Fluorination of carbon nanotubes: Quantum chemical investigation within MNDO approximation", *Int. J. Quant. Chem.* **96**, 142.

[267] Zaporotskova, I.V., Lebedev, N.G. and Chernozatonskii, L.A. (2004) "Single and regular hydrogenation and oxidation of carbon nanotubes: MNDO calculations", *Int. J. Quant. Chem.* **96**, 149.

[268] Parr, R.G. and Yang, W. (1989) *Density-Functional Theory of Atoms and Molecules* (Oxford University Press, Oxford).

[269] Lundqvist, S. and March, N.H. (1983) *Theory of the Inhomogeneous Electron Gas* (Plenum Press, New York).

[270] Gross, E.K.U. and Dreizler, R.M. (1995) *Density Functional Theory* (Plenum Press, New York).

[271] Koch, W. and Holthausen, M.C. (2000) *A Chemist's Guide to Density Functional Theory* (Wiley-VCH, Weinheim).

[272] Baerends, E.J. and Gritsenko, O.V. (1997) "A quantum chemical view of density functional theory", *J. Phys. Chem. A* **101**, 5383.

[273] Hohenberg, P. and Kohn, W. (1964) "Inhomogeneous electron gas", *Phys. Rev.* **136**, B864.

[274] Ernzerhof, M. and Scuseria, G.E. (2000) "Perspective on 'Inhomogeneous electron gas':", *Theor. Chem. Acc.* **103**, 259, Hohenberg, P. and Kohn, W. (1964) Phys. Rev. 136:B846.

[275] Kohn, W. and Sham, L.J. (1965) "Self-consistent equations including exchange and correlation effects", *Phys. Rev.* **140**, A1133.

[276] Baerends, E.J. (2000) "Perspective on 'Self-consistent equations including exchange and correlation effects'", *Theor. Chem. Acc.* **103**, 265, Kohn, W. and Sham, L.J. (1965) Phys. Rev. A, 140:133–1138.

[277] Langreth, D.C. and Mehl, M.J. (1983) "Beyond the local-density approximation in calculations of ground-state electronic properties", *Phys. Rev. B* **28**, 1809.

[278] Becke, A.D. (1988) "Density-functional exchange-energy approximation with correct asymptotic behavior", *Phys. Rev. A* **38**, 3098.

[279] Perdew, J.P., Burke, K. and Ernzerhof, M. (1996) "Generalized gradient approximation made simple", *Phys. Rev. Lett.* **77**, 3865.

[280] Perdew, J.P., Burke, K. and Ernzerhof, M. (1997) "Generalized gradient approximation made simple [Phys. Rev. Lett., 77, 3865 (1996)]", *Phys. Rev. Lett.* **78**, 1396.

[281] Perdew, J.P., Chevary, J.A., Vosko, S.H., Jackson, K.A., Pederson, M.R., Singh, D.J. and Fiolhais, C. (1992) "Atoms, molecules, solids and surfaces: applications of the generalized gradient approximation for exchange and correlation", *Phys. Rev. B* **46**, 6671.

[282] Perdew, J.P., Chevary, J.A., Vosko, S.H., Jackson, K.A., Pederson, M.R., Singh, D.J. and Fiolhais, C. (1993) "Erratum: atoms, molecules, solids and surfaces: applications of the generalized gradient approximation for exchange and correlation", *Phys. Rev. B* **48**, 4978.

[283] Perdew, J.P. (1986) "Density-functional approximation for the correlation energy of the inhomogeneous electron gas", *Phys. Rev. B* **33**, 8822.

[284] Wang, Y. and Perdew, J.P. (1991) "Correlation hole of the spin-polarized electron gas, with exact small-wave-vector and high-density scaling", *Phys. Rev. B* **44**, 13298.
[285] Perdew, J.P. and Wang, Y. (1992) "Accurate and simple analytical representation of the electron-gas correlation energy", *Phys. Rev. B* **45**, 13244.
[286] Perdew, J.P., Burke, K. and Wang, Y. (1996) "Generalized gradient approximation for the exchange-correlation hole of a many-electron system", *Phys. Rev. B* **54**, 16533.
[287] Lee, C., Yang, W. and Parr, R.G. (1988) "Development of the Colle–Salvetti correlation-energy formula into a functional of the electron density", *Phys. Rev. B* **37**, 785.
[288] Baker, J. and Pulay, P. (2002) "Assessment of the Handy–Cohen optimized exchange density functional for organic reactions", *J. Chem. Phys.* **117**, 1441.
[289] Baker, J. and Pulay, P. (2003) "Assessment of the OLYP and O3LYP density functionals for first-row transition metals", *J. Comput. Chem.* **24**, 1184.
[290] Altmann, J.A. and Handy, N.C. (1999) "Evaluation of the performance of the HCTH exchange-correlation functional using a benchmark of sulfur compounds", *Phys. Chem. Chem. Phys.* **1**, 5529.
[291] Handy, N.C. and Cohen, A.J. (2001) "Left-right correlation energy", *Mol. Phys.* **99**, 403.
[292] Hoe, W.M., Cohen, A.J. and Handy, N.C. (2001) "Assessment of a new local exchange functional OPTX", *Chem. Phys. Lett.* **341**, 319.
[293] Handy, N.C. and Cohen, A.J. (2002) "A dynamical correlation functional", *J. Chem. Phys.* **116**, 5411.
[294] Hamprecht, F.A., Cohen, A.J., Tozer, D.J. and Handy, N.C. (1998) "Development and assessment of new exchange-correlation functionals", *J. Chem. Phys.* **109**, 6264.
[295] Boese, A.D., Doltsinis, N.L., Handy, N.C. and Sprik, M. (2000) "New generalized gradient approximation functionals", *J. Chem. Phys.* **112**, 1670.
[296] Boese, A.D. and Handy, N.C. (2001) "A new parametrization of exchange-correlation generalized gradient approximation functionals", *J. Chem. Phys.* **114**, 5497.
[297] Becke, A.D. (1993) "Density-functional thermochemistry. III. The role of exact exchange", *J. Chem. Phys.* **98**, 5648.
[298] Filatov, M. and Shaik, S. (1998) "Spin-restricted density functional approach to the open-shell problem", *Chem. Phys. Lett.* **288**, 689.
[299] Filatov, M. and Shaik, S. (1999) "Application of spin-restricted open-shell Kohn–Sham method to atomic and molecular multiplet states", *J. Chem. Phys.* **110**, 116.
[300] Grimme, S. (1996) "Density functional calculations with configuration interaction for the excited states of molecules", *Chem. Phys. Lett.* **259**, 128.
[301] See also Grimme, S. and Waletzke, M.(1999) "A combination of Kohn-Sham density functional theory and multi-reference configuration interaction methods", *J. Chem. Phys.* **111**, 5645 for an extension to multireference CI.
[302] Casida, M.E. (1995) "Time dependent density functional response theory for molecules", In: Chong, D.P., ed., *Recent Advances in Density Functional Methods, Part I* (World Scientific, Singapore).
[303] Burke, K. and Gross, E.K.U. (1998) "A guided tour of time-dependent density functional theory", In: Joubert, D., ed., *Density Functionals: Theory and Applications, Lecture Notes in Physics* (Springer, Heidelberg), Vol. 500.
[304] Petersilka, M., Gossmann, U.J. and Gross, E.K.U. (1998) "Time dependent optimized effective potential in the linear response regime", In: Dobson, J.F., Vignale, G. and Das, M.P., eds, *Electronic Density Functional Theory, Recent Progress and New Directions* (Plenum Press, New York).
[305] Huang, X. and Lin, Z. (2003) "Density functional theory studies of ruthenium-catalyzed bis-Diels-Alder cycloaddition of 1,5-cyclooctadiene with alkynes", *Organometallics* **22**, 5478.
[306] Khan, A. (2003) "Theoretical studies of $CO_2(H_2O)_{20,24,28}$ clusters: stabilization of cages in hydrates by CO_2 guest molecules", *J. Mol. Struct. Theochem.* **237**, 664–665.
[307] Thompson, D.J., Ciobîcă, I.M., Hodnett, B.K., van Santen, R.A. and Fanning, M.O. (2003) "A DFT periodic study of the vanadyl pyrophosphate (100) surface", *Surf. Sci.* **547**, 438.
[308] Pastore, G., Smargiassi, E. and Buda, F. (1991) "Theory of *ab initio* molecular-dynamics calculations", *Phys. Rev. A* **44**, 6334.
[309] Remler, D.K. and Madden, P.A. (1990) "Molecular dynamics without effective potentials via the Car–Parrinello approach", *Mol. Phys.* **70**, 921.
[310] Parrinello, M. (1997) "From silicon to RNA: the coming of age of *ab initio* molecular dynamics", *Solid State Commun.* **102**, 107.
[311] Tse, J.S. (2002) "*Ab initio* molecular dynamics with density functional theory", *Annu. Rev. Phys. Chem.* **53**, 249.
[312] Bolton, K., Hase, W.L. and Peslherbe, G.H. (1998) "Mapping multidimensional intramolecular dynamics using frequency analysis", In: Thompson, D.L., ed., *Modern Methods for Multidimensional Dynamics Computations in Chemistry* (World Scientific, Singapore).
[313] Car, R. and Parrinello, M. (1985) "Unified approach for molecular dynamics and density-functional theory", *Phys. Rev. Lett.* **55**, 2471.
[314] There may be additional constraints imposed on the system, such as a fixed volume, pressure, etc. In this case there would be additional terms in the Lagrangian. Here we consider the simplest case, i.e. when only orthonormality constraints are imposed. For a more general treatment, see Ref. [179], and also Laasonen, K., Pasquarello, A., Car, R., Lee, C. and Vanderbilt, D. (1993) "Car-Parrinello molecular dynamics with Vanderbilt ultrasoft pseudopotentials", *Phys. Rev. B* **47**, 10142.
[315] Verlet, L. (1967) "Computer 'experiments' on classical fluids. I. Thermodynamical properties of Lennard–Jones molecules", *Phys. Rev.* **159**, 98.
[316] Swope, W.C., Andersen, H.C., Berens, P.H. and Wilson, K.R. (1982) "A computer simulation method for the calculation of equilibrium constants for the formation of physical clusters of molecules: application to small water clusters", *J. Chem. Phys.* **76**, 637.
[317] Tuckerman, M., Berne, B.J. and Martyna, G.J. (1992) "Reversible multiple time scale molecular dynamics", *J. Chem. Phys.* **97**, 1990.
[318] Tuckerman, M.E. and Parrinello, M. (1994) "Integrating the Car–Parrinello equations. I. Basic integration techniques", *J. Chem. Phys.* **101**, 1302.
[319] Tuckerman, M.E. and Parrinello, M. (1994) "Integrating the Car–Parrinello equations. II. Multiple time scale techniques", *J. Chem. Phys.* **101**, 1316.
[320] Hutter, J., Tuckerman, M.E. and Parrinello, M. (1995) "Integrating the Car–Parrinello equations. III. Techniques for ultrasoft pseudopotentials", *J. Chem. Phys.* **102**, 859.
[321] Nose, S. (1984) "A molecular dynamics method for simulations in the canonical ensemble", *Mol. Phys.* **2**, 255.
[322] Nose, S. (1984) "A unified formulation of the constant temperature molecular dynamics methods", *J. Chem. Phys.* **81**, 511.
[323] Hoover, W.G. (1985) "Canonical dynamics: equilibrium phase-space distributions", *Phys. Rev. A* **31**, 1695.
[324] Blöchl, P.E. and Parrinello, M. (1992) "Adiabaticity in first-principles molecular dynamics", *Phys. Rev. B* **45**, 9413 (1992).
[325] Pasquarello, A., Laasonen, K., Car, R., Lee, Ch. and Vanderbilt, D. (1992) "*Ab initio* molecular dynamics for *d*-electron systems: liquid copper at 1500 K", *Phys. Rev. Lett.* **69**, 1982.
[326] Ryckaert, J.P., Ciccotti, G. and Berendsen, H.J.C. (1977) "Numerical integration of Cartesian equations of motion of a system with constraints: molecular dynamics of n-alkanes", *J. Comput. Phys.* **23**, 237.
[327] Andersen, H.C. (1983) "RATTLE: a velocity version of the SHAKE algorithm for molecular dynamics calculations", *J. Comput. Phys.* **52**, 24.
[328] See, for example, Giannozzi, P., Car, R. and Scoles, G.(2003) "Oxygen adsorption on graphite and nanotubes", *J. Chem. Phys.* **118**, 1003.
[329] Laio, A. and Parrinello, M. (2002) "Escaping free-energy minima", *Proc. Natl Acad. Sci. USA* **99**, 12562.
[330] Iannuzzi, M., Laio, A. and Parrinello, M. (2003) "Efficient exploration of reactive potential energy surfaces using Car–Parrinello molecular dynamics", *Phys. Rev. Lett.* **90**, #238302.

[331] Leforestier, V. (1978) "Classical trajectories using the full *ab initio* potential energy surface $H^- + CH_4 \rightarrow CH_4 + H^-$", *J. Chem. Phys.* **68**, 4406.
[332] Field, M.J. (1991) "Constrained optimization of *ab initio* and semiempirical Hartree–Fock wave functions using direct minimization or simulated annealing", *J. Phys. Chem.* **95**, 5104.
[333] Jellinek, J., Bonačić-Koutecký, V., Fantucci, P. and Wiechert, M. (1994) "*Ab initio* Hartree–Fock self-consistent-field molecular dynamics study of structure and dynamics of Li_8", *J. Chem. Phys.* **101**, 10092.
[334] Liu, Z., Carter, L.E. and Carter, E.A. (1995) "Full configuration interaction molecular dynamics of Na_2 and Na_3", *J. Phys. Chem.* **99**, 4355.
[335] Senda, Y., Shimojo, F. and Hoshino, K. (1999) "The origin of the first sharp diffraction peak in liquid Na-Pb alloys: *ab initio* molecular-dynamics simulations", *J. Phys. Condens. Matter.* **11**, 2199.
[336] Senda, Y., Shimojo, F. and Hoshino, K. (1999) "Composition dependence of the structure and the electronic states of liquid K-Pb alloys: *ab initio* molecular-dynamics simulations", *J. Phys. Condens. Matter.* **11**, 5387.
[337] Ortega, J., Lewis, J.P. and Sankey, O.F. (1994) "Simplified electronic-structure model for hydrogen-bonded systems: water", *Phys. Rev. B* **50**, 10516.
[338] Ortega, J., Lewis, J.P. and Sankey, O.F. (1997) "First principles simulations of fluid water: the radial distribution functions", *J. Chem. Phys.* **106**, 3696.
[339] Gaigeot, M.P. and Sprik, M. (2003) "*Ab initio* molecular dynamics computation of the infrared spectrum of aqueous uracil", *J. Phys. Chem. B* **107**, 10344.
[340] For a recent application to methanol, for example, see Pagliai, M., Cardini, G., Righini, R. and Schettino, V. (2003) "Hydrogen bond dynamics in liquid methanol", *J. Chem. Phys.* **119**, 6655.
[341] Grossman, J.C., Schwegler, E., Draeger, E.W., Gygi, F. and Galli, G. (2004) "Towards an assessment of the accuracy of density functional theory for first principles simulations of water", *J. Chem. Phys.* **120**, 300.
[342] Trout, B.L. and Parrinello, M. (1998) "The dissociation mechanism of H_2O in water studied by first-principles molecular dynamics", *Chem. Phys. Lett.* **288**, 343.
[343] Trout, B.L. and Parrinello, M. (1999) "Analysis of the dissociation of H_2O in water using first-principles molecular dynamics", *J. Phys. Chem. B* **103**, 7340.
[344] Izvekov, S. and Voth, G.A. (2002) "Car–Parrinello molecular dynamics simulation of liquid water: new results", *J. Chem. Phys.* **116**, 10372.
[345] Buhl, M. (2002) "Structure, dynamics, and magnetic shieldings of permanganate ion in aqueous solution. A density functional study", *J. Phys. Chem. A* **106**, 10505.
[346] Sillanpaa, A.J., Simon, C., Klein, M.L. and Laasonen, K. (2002) "Structural and spectral properties of aqueous hydrogen fluoride studied using *ab initio* molecular dynamics", *J. Phys. Chem. B* **106**, 11315.
[347] Röhrig, U.F., Frank, I., Hutter, J., Laio, A., VandeVondele, J. and Rothlisberger, U. (2003) "QM/MM Car–Parrinello molecular dynamics study of the solvent effects on the ground state and on the first excited states of acetone in water", *Chemphyschem.* **4**, 1177.
[348] Doerksen, R.J., Chen, B. and Klein, M.L. (2003) "Intramolecular hydrogen bonds: *ab initio* Car–Parrinello simulations of arylamide torsions", *Chem. Phys. Lett.* **380**, 150.
[349] Åqvist, J. and Warshel, A. (1993) "Simulation of enzyme reactions using valence bond force fields and other hybrid quantum/classical approaches", *Chem. Rev.* **93**, 2523.
[350] Gao, J. (1996) "Hybrid quantum and molecular mechanical simulations: an alternative avenue to solvent effects in organic chemistry", *Acc. Chem. Res.* **29**, 298.
[351] Monard, G. and Merz, K.M., Jr. (1999) "Combined quantum mechanical/molecular mechanical methodologies applied to biomolecular systems", *Acc. Chem. Res.* **32**, 904.
[352] Amara, P. and Field, M.J. (1998) "Combined quantum mechanical and molecular mechanical potentials", In: von Rague Schleyer, P., Allinger, N.L., Clark, T., Gasteiger, J., Kollman, P.A., Schaefer, H.F., III and Schreiner, P.R., eds, *Encyclopedia of Computational Chemistry* (John Wiley and Sons, Chichester).
[353] Ruiz-Lopez, M.F. and Rivail, J.L. (1998) "Combined quantum mechanics and molecular mechanics approaches to chemical and biochemical reactivity", In: von Rague Schleyer, P., Allinger, N.L., Clark, T., Gasteiger, J., Kollman, P.A., Schaefer, H.F., III and Schreiner, P.R., eds, *Encyclopedia of Computational Chemistry* (John Wiley and Sons, Chichester).
[354] Merz, K.M., Jr. and Stanton, R.V. (1998) "Quantum mechanical/molecular mechanical (QM/MM) coupled Potentials", In: von Rague Schleyer, P., Allinger, N.L., Clark, T., Gasteiger, J., Kollman, P.A., Schaefer, H.F., III and Schreiner, P.R., eds, *Encyclopedia of Computational Chemistry* (John Wiley and Sons, Chichester).
[355] Tomasi, J. and Pomelli, C.S. (1998) "Quantum mechanics/molecular mechanics", In: von Rague Schleyer, P., Allinger, N.L., Clark, T., Gasteiger, J., Kollman, P.A., Schaefer, H.F., III and Schreiner, P.R., eds, *Encyclopedia of Computational Chemistry* (John Wiley and Sons, Chichester).
[356] Sauer, J. and Sierka, M. (2000) "Combining quantum mechanics and interatomic potential functions in *ab initio* studies of extended systems", *J. Comput. Chem.* **21**, 1470.
[357] Warshel, A. (1997) *Computer Modeling of Chemical Reactions in Enzymes and Solutions* (Wiley, New York).
[358] Clementi, E. (1980) *Computational Aspects for Large Chemical Systems* (Springer-Verlag, Berlin).
[359] Gao, J. and Thompson, M.A., eds (1998) *Combined Quantum Mechanical and Molecular Mechanical Methods* (American Chemical Society, Washington).
[360] Tomasi, J. and Persico, M. (1994) "Molecular interactions in solution: an overview of methods based on continuous distributions of the solvent", *Chem. Rev.* **94**, 2027.
[361] Hwang, J.-K., King, G., Creighton, S. and Warshel, A. (1988) "Simulation of the free energy relationships and dynamics of S_N2 reactions in aqueous solution", *J. Am. Chem. Soc.* **110**, 5297.
[362] Wesolowski, T.A. and Warshel, A. (1993) "Frozen density functional approach for *ab initio* calculations of solvated molecules", *J. Phys. Chem.* **97**, 8050.
[363] Stanton, R.V., Hartsough, D.S. and Merz, K.M., Jr. (1993) "Calculation of solvation free energies using a density functional/molecular dynamics coupled potential", *J. Phys. Chem.* **97**, 11868.
[364] Gao, J. and Truhlar, D.G. (2002) "Quantum mechanical methods for enzyme kinetics", *Annu. Rev. Phys. Chem.* **53**, 467.
[365] Truhlar, D.G., Gao, J.L., Alhambra, C., García-Viloca, M., Corchado, J., Sanchez, M.L. and Villa, J. (2002) "The incorporation of quantum effects in enzyme kinetics modeling", *Acc. Chem. Res.* **35**, 341.
[366] Warshel, A. and Levitt, M. (1976) "Theoretical studies of enzymic reactions: dielectric, electrostatic and steric stabilization of carbonium ion in reaction of lysozyme", *J. Mol. Biol.* **103**, 227.
[367] Field, M.J., Bash, P.A. and Karplus, M. (1990) "A combined quantum mechanical and molecular mechanical potential for molecular dynamics simulations", *J. Comput. Chem.* **11**, 700.
[368] Very often the method of choice for the quantum mechanical part is DFT due to its good accuracy/cost ratio.
[369] An additional term including the contribution from the boundary region, $H_{boundary}$ can also be included.
[370] Svensson, M., Humbel, S., Froese, R.D.J., Matsubara, T., Sieber, S. and Morokuma, K. (1996) "ONIOM: a multilayered integrated MO + MM method for geometry optimizations and single point energy predictions. A test for Diels-Alder reactions and $Pt(P(t\text{-}Bu)_3)_2 + H_2$ oxidative addition", *J. Phys. Chem.* **100**, 19357.
[371] Froese, R.D.J. and Morokuma, K. (1998) "The ONIOM method. Integration of different levels of molecular orbital methods and/or molecular mechanics methods for large molecular systems and its applications to structures, energies and chemical reactions", In: von Rague Schleyer, P., Allinger, N.L., Clark, T., Gasteiger, J., Kollman, P.A., Schaefer, H.F., III and Schreiner, P.R., eds, *Encyclopedia of Computational Chemistry* (John Wiley and Sons, Chichester).

[372] Sherwood, P., de Vries, A.H., Guest, M.F., Schreckenbach, G., Catlow, C.R.A., French, S.A., Sokol, A.A., Bromley, S.T., Thiel, W., Turner, A.J., Billeter, S., Terstegen, F., Thiel, S., Kendrick, J., Rogers, S.C., Casci, J., Watson, M., King, F., Karlsen, E., Sjøvoll, M., Fahmi, A., Schäfer, A. and Lennartz, C. (2003) "QUASI: a general purpose implementation of the QM/MM approach and its application to problems in catalysis", *J. Mol. Struct. Theochem.* **632**, 1.
[373] Warshel, A. and Weiss, R.M. (1980) "An empirical valence bond approach for comparing reactions in solutions and in enzymes", *J. Am. Chem. Soc.* **102**, 6218.
[374] Li, G. and Cui, Q. (2003) "What is so special about Arg 55 in the catalysis of Cyclophilin A? Insights from hybrid QM/MM simulations", *J. Am. Chem. Soc.* **125**, 15028.
[375] Shigeta, Y. (2004) "Hybrid QM/MM studies on energetics of malonaldehyde in condensed phase", *Int. J. Quant. Chem.* **96**, 32.
[376] Hill, T.L. (1960) *An Introduction to Statistical Thermodynamics* (Dover, New York).
[377] Gray, C.C. and Gubbins, K.E. (1984) *Theory of Molecular Fluids* (Clarendon Press, Oxford).
[378] This is not the only possibility. In particular, when simulating a chemical reaction at very high temperatures, there is a coupling of the internal degrees of freedom of the molecule and the molecular partition function cannot be factored as in Eq. (5.3). We will not concern ourselves with such complications here.
[379] Coker, D.F. and Watts, R.O. (1981) "Computer simulation of reactive liquids in chemical equilibrium", *Chem. Phys. Lett.* **78**, 333.
[380] Coker, D.F. and Watts, R.O. (1981) "Chemical equilibria in mixtures of bromine and chlorine", *Mol. Phys.* **44**, 1303.
[381] Norman, G.E. and Filinov, V.S. (1969) "Investigations of phase transitions by a Monte Carlo method", *High Temp.* **7**, 216.
[382] Adams, D.J. (1974) "Chemical potential of hard-sphere fluids by Monte Carlo methods", *Mol. Phys.* **28**, 1241.
[383] Adams, D.J. (1975) "Grand canonical ensemble Monte Carlo for a Lennard–Jones fluid", *Mol. Phys.* **29**, 307.
[384] Kofke, D.A. and Glandt, E.D. (1988) "Monte Carlo simulation of multicomponent equilibria in a semigrand canonical ensemble", *Mol. Phys.* **64**, 1105.
[385] Shaw, M.S. (1991) "Monte Carlo simulation of equilibrium chemical composition of molecular fluid mixtures in the $N_{atoms}PT$ ensemble", *J. Chem. Phys.* **94**, 7550.
[386] Busch, N.A., Wertheim, W.S., Chiew, Y.C. and Yarmush, M.L. (1994) "A Monte Carlo method for simulating associating fluids", *J. Chem. Phys.* **101**, 3147.
[387] Busch, N.A., Wertheim, M.S. and Yarmush, M.L. (1996) "Monte Carlo simulation of *n*-member associating fluids: application to antigen-antibody systems", *J. Chem. Phys.* **104**, 3962.
[388] Tsangaris, D.M. and de Pablo, J.J. (1994) "Bond-bias simulation of phase equilibria for strongly associated fluids", *J. Chem. Phys.* **101**, 1477.
[389] Shew, C.-Y. and Mills, P. (1993) "A Monte Carlo method to simulate systems with barriers: subspace sampling", *J. Phys. Chem.* **97**, 13824.
[390] Shew, C.Y. and Mills, P. (1995) "The subspace sampling method: a Monte Carlo approach for simulating the single-particle density function and the equilibrium constant for systems described by multiple Hamiltonians", *J. Phys. Chem.* **99**, 12980.
[391] Shew, C.Y. and Mills, P. (1995) "Monte Carlo simulations of the pair correlation function and the equilibrium association constant of the sticky electrolyte model using the subspace sampling method", *J. Phys. Chem.* **99**, 12988.
[392] Turner, C.H. (2002) PhD Thesis, (North Carolina State University, Raleigh).
[393] Smith, W.R. and Triska, B. (1994) "The reaction ensemble method for the computer simulation of chemical and phase equilibria. I. Theory and basic examples", *J. Chem. Phys.* **100**, 3019.
[394] Johnson, J.K., Panagiotopoulos, A.Z. and Gubbins, K.E. (1994) "Reactive canonical Monte Carlo: a new simulation technique for reacting or associating fluids", *Mol. Phys.* **81**, 717.
[395] Johnson, J.K. (1991) "Reactive canonical Monte Carlo", *Adv. Chem. Phys.* **105**, 461.
[396] Turner, C.H., Johnson, J.K. and Gubbins, K.E. (2001) "Effect of confinement on chemical reaction equilibria: the reactions $2NO \leftrightarrow (NO)_2$ and $N_2 + 3H_2 \leftrightarrow 2NH_3$ in carbon micropores", *J. Chem. Phys.* **114**, 1851.
[397] Turner, C.H., Pikunic, J. and Gubbins, K.E. (2001) "Influence of chemical and physical surface heterogeneity on chemical reaction equilibria in carbon micropores", *Mol. Phys.* **99**, 1991.
[398] Turner, C.H., Brennan, J.K., Johnson, J.K. and Gubbins, K.E. (2002) "Effect of confinement by porous materials on chemical reaction kinetics", *J. Chem. Phys.* **116**, 2138.
[399] Turner, C.H., Brennan, J.K. and Pikunic, J. (2002) "Simulation of chemical reaction equilibria and kinetics in heterogeneous carbon micropores", *Appl. Surf. Sci.* **196**, 366.
[400] Turner, C.H. and Gubbins, K.E. (2003) "Effects of supercritical clustering and selective confinement on reaction equilibrium: a molecular simulation study of the esterification reaction", *J. Chem. Phys.* **119**, 6057.
[401] Lisal, M., Nezbeda, I. and Smith, W.R. (1999) "The reaction ensemble method for the computer simulation of chemical and phase equilibria. II. The $Br_2 + Cl_2 + BrCl$ system", *J. Chem. Phys.* **110**, 8597.
[402] Smith, W.R. and Lisal, M. (2002) "Direct Monte Carlo simulation methods for nonreacting and reacting systems at fixed total internal energy or enthalpy", *Phys. Rev. E* **66**, #011104.
[403] Lisal, M., Smith, W.R. and Nezbeda, I. (2000) "Computer simulation of the thermodynamic properties of high-temperature chemically-reacting plasmas", *J. Chem. Phys.* **113**, 4885.
[404] Lisal, M., Smith, W.R. and Nezbeda, I. (1999) "Accurate computer simulation of phase equilibrium for complex fluid mixtures. Application to binaries involving isobutene, methanol, methyl *tert*-butyl ether, and *n*-butane", *J. Phys. Chem. B* **103**, 10496.
[405] Lisal, M., Smith, W.R. and Nezbeda, I. (2000) "Accurate vapour–liquid equilibrium calculations for complex systems using the reaction Gibbs ensemble Monte Carlo simulation method", *Fluid Phase Equil.* **181**, 127.
[406] de Souza, L.E.S. and Deiters, U.K. (1999) "Non-ideality of the system NH_3-H_2-N_2. Comparison of equation of state and simulation predictions with experimental data", *Phys. Chem. Chem. Phys.* **1**, 4069.
[407] Borówko, M. and Zagórski, R. (2001) "Chemical equilibria in slitlike pores", *J. Chem. Phys.* **114**, 5397.
[408] Brennan, J.K. and Rice, B.M. (2002) "Molecular simulation of shocked materials using the reactive Monte Carlo method", *Phys. Rev. E* **66**, #021105.
[409] Truhlar, D.G., Hase, W.L. and Hynes, J.T. (1983) "Current status of transition-state theory", *J. Phys. Chem.* **87**, 2664.
[410] Truhlar, D.G., Garrett, B.C. and Klippenstein, S.J. (1996) "Current status of transition-state theory", *J. Phys. Chem.* **100**, 12771.
[411] Garrett, B.C. and Truhlar, D.G. (1998) "Transition state theory", In: Schleyer, P.V.R., Allinger, N.L., Clark, T., Gasteiger, J., Kollman, P.A. and Schaefer, H.F., III, eds, *Encyclopedia of Computational Chemistry* (John Wiley, Chichester).
[412] Eyring, H. (1935) "Activated complex in chemical reactions", *J. Chem. Phys.* **3**, 107.
[413] Petersson, G.A. (2000) "Perspective on 'The activated complex in chemical reactions'", *Theor. Chem. Acc.* **103**, 190, Eyring, H. (1935) J. Chem. Phys. 3:107.
[414] Yamamoto, T. (1960) "Quantum statistical mechanical theory of the rate of exchange chemical reactions in the gas phase", *J. Chem. Phys.* **33**, 281.
[415] See, for example, Refs. [10,418].
[416] This expression is ensemble-independent, see, e.g. Ref. [418].
[417] Bennett, C.H. (1977) "Algorithms for chemical computations", In: Christofferson, R.E., ed., *ACS Symposium Series* (American Chemical Society, Washington), Vol. 46.
[418] Chandler, D. (1978) "Statistical mechanics of isomerization dynamics in liquids and the transition state approximation", *J. Chem. Phys.* **68**, 2959.

[419] Chandler, D. (1987) *Introduction to Modern Statistical Mechanics* (Oxford University Press, Oxford).

[420] Chandler, D. (1998) "Barrier crossings: classical theory of rare but important events", In: Berne, B.J., Ciccotti, G. and Coker, D.F., eds, *Computer Simulation of Rare Events and Dynamics of Classical and Quantum Condensed-Phase Systems–Classical and Quantum Dynamics in Condensed Phase Simulations* (World Scientific, Singapore).

[421] Mahan, B.H. (1974) "Activated complex theory of bimolecular reactions", *J. Chem. Educ.* **51**, 709.

[422] Miller, W.H. (1976) "Importance of nonseparability in quantum mechanical transition-state theory", *Acc. Chem. Res.* **9**, 306.

[423] Truhlar, D.G. and Garrett, B.C. (1980) "Variational transition-state theory", *Acc. Chem. Res.* **13**, 440.

[424] Miller, W.H., Schwartz, S.D. and Tromp, J.W. (1983) "Quantum mechanical rate constants for bimolecular reactions", *J. Chem. Phys.* **79**, 4889.

[425] Tromp, J.W. and Miller, W.H. (1986) "New approach to quantum mechanical transition-state theory", *J. Phys. Chem.* **90**, 3482.

[426] Tromp, J.W. and Miller, W.H. (1987) "The reactive flux correlation function for collinear reactions $H + H_2$, $Cl + HCl$ and $F + H_2$", *Faraday Discuss. Chem. Soc.* **84**, 441.

[427] Day, P.N. and Truhlar, D.G. (1991) "Calculation of thermal rate coefficients from the quantum flux autocorrelation function: converged results and variational quantum transition state theory for $O + HD \leftrightarrow OD + H$ and $O + HD \leftrightarrow OH + D$", *J. Chem. Phys.* **95**, 5097.

[428] Voth, G.A., Chandler, D. and Miller, W.H. (1989) "Rigorous formulation of quantum transition state theory and its dynamical corrections", *J. Chem. Phys.* **91**, 7749.

[429] Voth, G.A. (1993) "Feynman path integral formulation of quantum mechanical transition-state theory", *J. Phys. Chem.* **97**, 8365.

[430] Stuchebrukhov, A.A. (1991) "Green's functions in quantum transition state theory", *J. Chem. Phys.* **95**, 4258.

[431] Mills, G., Schenter, G.K., Makarov, D.E. and Jónsson, H. (1998) "RAW quantum transition state theory", In: Berne, B.J., Ciccotti, G. and Coker, D.F., eds, *Computer Simulation of Rare Events and Dynamics of Classical and Quantum Condensed-Phase Systems—Classical and Quantum Dynamics in Condensed Phase Simulations* (World Scientific, Singapore).

[432] Mills, G., Schenter, G.K., Makarov, D. and Jónsson, H. (1997) "Generalized path integral based quantum transition state theory", *Chem. Phys. Lett.* **278**, 91.

[433] Hansen, N.F. and Anderson, H.C. (1994) "A new formulation of quantum transition state theory for adiabatic rate constants", *J. Chem. Phys.* **101**, 6032.

[434] Cheney, B.G. and Andersen, H.C. (2003) "Dynamical corrections to quantum transition state theory", *J. Chem. Phys.* **118**, 9542.

[435] Park, T.J. and Light, J.C. (1986) "Unitary quantum time evolution by iterative Lanczos reduction", *J. Chem. Phys.* **85**, 5870.

[436] Miller, W.H. (1993) "Beyond transition-state theory: a rigorous quantum theory of chemical reaction rates", *Acc. Chem. Res.* **26**, 174.

[437] Manthe, U., Seideman, T. and Miller, W.H. (1993) "Full-dimensional quantum mechanical calculation of the rate constant for the $H_2 + OH \rightarrow H_2O + H$ reaction", *J. Chem. Phys.* **99**, 10078.

[438] Barik, D., Banik, S.K. and Ray, D.S. (2003) "Quantum phase-space function formulation of reactive flux theory", *J. Chem. Phys.* **119**, 680.

[439] For a reactive-flux formulation for mixed quantum/classical dynamics, see Sergi, A. and Kapral, R.(2003) "Quantum-classical dynamics of nonadiabatic chemical reactions", *J. Chem. Phys.* **118**, 8566 and references therein.

[440] Miller, W.H. (1998) "Direct and correct calculation of canonical and microcanonical rate constants for chemical reactions", *J. Phys. Chem. A* **102**, 793.

[441] Miller, W.H. (1998) "Spiers memorial lecture quantum and semiclassical theory of chemical reaction rates", *Faraday Discuss.* **110**, 1.

[442] See, for example, Schenter, G.K., Kathmann, S.M. and Garrett, B.C.(1999) "Variational transition state theory of vapor phase nucleation", *J. Chem. Phys.* **110**, 7951.

[443] See, for example, Bader, J.S., Berne, B.J. and Pollak, E.(1995) "Activated rate processes: the reactive flux method for one-dimensional surface diffusion", *J. Chem. Phys.* **102**, 4037.

[444] See, for example, Voter, A.F.(1997) "A method for accelerating the molecular dynamics simulation of infrequent events", *J. Chem. Phys.* **106**, 4665.

[445] Drozdov, A.N. and Tucker, S.C. (2001) "An improved reactive flux method for evaluation of rate constants in dissipative systems", *J. Chem. Phys.* **115**, 9675.

[446] Carter, E.A., Ciccotti, G., Hynes, J.T. and Kapral, R. (1989) "Constrained reaction coordinate dynamics for the simulation of rare events", *Chem. Phys. Lett.* **156**, 472.

[447] Ciccotti, G. and Ferrario, M. (2000) "Rare events by constrained molecular dynamics", *J. Mol. Liquids* **89**, 1.

[448] Coluzza, I., Sprik, M. and Ciccotti, G. (2003) "Constrained reaction coordinate dynamics for systems with constraints", *Mol. Phys.* **101**, 2885.

[449] Sprik, M. and Ciccotti, G. (1998) "Free energy from constrained molecular dynamics", *J. Chem. Phys.* **109**, 7737.

[450] Paci, E., Ciccotti, G., Ferrario, M. and Kapral, R. (1991) "Activation energies by molecular dynamics with constraints", *Chem. Phys. Lett.* **176**, 581.

[451] A *holonomic constraint* is a constraint that involves only configurational variables, not momenta.

[452] This, of course, assumes that there is a way to obtain atom-atom interactions that is not too computationally costly, such as a reactive force field. If the potentials are obtained from 'on-the-fly' *ab initio* calculations, as in CPMD, the system sizes that can be handled by the method are much smaller.

[453] Meijer, E.J. and Sprik, M. (1998) "*Ab initio* molecular dynamics study of the reaction of water with formaldehyde in sulfuric acid solution", *J. Am. Chem. Soc.* **120**, 6345.

[454] Ensing, B., Meijer, E.J., Blöchl, B.E. and Baerends, E.J. (2001) "Solvation effects on the S_N2 reaction between CH_3Cl and Cl^- in water", *J. Phys. Chem. A* **105**, 3300.

[455] Pagliai, M., Raugei, S., Cardini, G. and Schettino, V. (2003) "Intramolecular solvation effects in the S_N2 reaction $Cl^- + Cl(CH_2)_nCN$", *J. Chem. Phys.* **119**, 9063.

[456] Mugnai, M., Cardini, G. and Schettino, V. (2003) "An *ab initio* molecular dynamics study of the S_N2 reaction $F^- + CH_3Cl \rightarrow CH_3F + Cl^-$", *J. Chem. Phys.* **118**, 2767.

[457] Mugnai, M., Cardini, G. and Schettino, V. (2003) "Substitution and elimination reaction of F^- with C_2H_5Cl: an *ab initio* molecular dynamics study", *J. Phys. Chem. A* **107**, 2540.

[458] Doltsinis, N. and Sprik, M. (2003) "Theoretical pK_a estimates for solvated $P(OH)_5$ from coordination constrained Car–Parrinello molecular dynamics", *Phys. Chem. Chem. Phys.* **5**, 2612.

[459] Dellago, C., Bolhuis, P.G., Csajka, F.S. and Chandler, D. (1998) "Transition path sampling and the calculation of rate constants", *J. Chem. Phys.* **108**, 1964.

[460] Dellago, C., Bolhuis, P.G. and Chandler, D. (1999) "On the calculation of reaction rate constants in the transition path ensemble", *J. Chem. Phys.* **110**, 6617.

[461] Dellago, C., Bolhuis, P.G. and Chandler, D. (1998) "Efficient transition path sampling: application to Lennard–Jones cluster rearrangements", *J. Chem. Phys.* **108**, 9236.

[462] Bolhuis, P.G., Dellago, C. and Chandler, D. (1998) "Sampling ensembles of deterministic transition pathways", *Faraday Discuss. Chem. Soc.* **110**, 421.

[463] Bolhuis, P.G., Chandler, D., Dellago, C. and Geissler, P.L. (2002) "Transition path sampling: throwing ropes over rough mountain passes, in the dark", *Annu. Rev. Phys. Chem.* **53**, 291.

[464] Chandler, D. (1998) "Finding transition pathways: throwing ropes over rough mountain passes, in the dark", In: Berne, B.J., Ciccotti, G. and Coker, D.F., eds, *Computer Simulation of Rare Events and Dynamics of Classical and Quantum Condensed-Phase Systems—Classical and Quantum Dynamics in Condensed Phase Simulations* (World Scientific, Singapore).

[465] Dellago, C., Bolhuis, P.G. and Geissler, P.L. (2002) "Transition path sampling", *Adv. Chem. Phys.* **123**, 1.
[466] Passerone, D. and Parrinello, M. (2001) "Action-derived molecular dynamics in the study of rare events", *Phys. Rev. Lett.* **87**, #108302.
[467] van Erp, T.S., Moroni, D. and Bolhuis, P.G. (2003) "A novel path sampling method for the calculation of rate constants", *J. Chem. Phys.* **118**, 7762.
[468] Ramírez, J. and Laso, M. (2001) "Conformational kinetics in liquid *n*-butane by transition path sampling", *J. Chem. Phys.* **115**, 7285.
[469] Bolhuis, P.G., Dellago, C. and Chandler, D. (2000) "Reaction coordinates of biomolecular isomerization", *Proc. Natl Acad. Sci. USA* **97**, 5877.
[470] Bolhuis, P.G. and Chandler, D. (2000) "Transition path sampling of cavitation between molecular scale solvophobic surfaces", *J. Chem. Phys.* **113**, 8154.
[471] Geissler, P.L., Dellago, C. and Chandler, D. (1999) "Kinetic pathways of ion pair dissociation in water", *J. Phys. Chem. B* **103**, 3706.
[472] Geissler, P.L., Dellago, C., Chandler, D., Hutter, J. and Parrinello, M. (2001) "Autoionization in liquid water", *Science* **291**, 2121.
[473] Ensing, B. and Baerends, E.J. (2002) "Reaction path sampling of the reaction between iron(II) and hydrogen peroxide in aqueous solution", *J. Phys. Chem. A* **106**, 7902.
[474] Bolhuis, P.G. (2003) "Transition path sampling of β-hairpin folding", *Proc. Natl Acad. Sci. USA* **100**, 12129.
[475] Hagan, M.F., Dinner, A.R., Chandler, D. and Chakraborty, A.K. (2003) "Atomistic understanding of kinetic pathways for single base-pair binding and unbinding in DNA", *Proc. Natl Acad. Sci. USA* **100**, 13922.
[476] Occasionally, a full moon occurs twice in a given calendar month. The second occurred is referred to as a "Blue Moon".